NATIONAL ADVISORY COMMITTEE
FOR AERONAUTICS

TECHNICAL NOTE 3677

INVESTIGATION OF LATERAL CONTROL NEAR THE STALL

ANALYSIS FOR REQUIRED LONGITUDINAL TRIM

CHARACTERISTICS AND DISCUSSION

OF DESIGN VARIABLES

By Fred E. Weick and H. Norman Abramson

Agricultural and Mechanical College of Texas

NACA

Washington

June 1956

P

NATIONAL ADVISORY COMMITTEE FOR AERONAUTICS

TECHNICAL NOTE 3677

INVESTIGATION OF LATERAL CONTROL NEAR THE STALL

ANALYSIS FOR REQUIRED LONGITUDINAL TRIM

CHARACTERISTICS AND DISCUSSION

OF DESIGN VARIABLES

By Fred E. Weick and H. Norman Abramson

SUMMARY

It has been recognized for some time, and shown quantitatively by the results of flight tests, that low-speed lateral control of airplanes may be insured by a simple limitation of the maximum elevator deflection so that the maximum angle of attack maintainable is that which will still allow satisfactory lateral control characteristics. However, this procedure places severe requirements on the longitudinal trim characteristics of the airplane, inasmuch as this maximum elevator deflection must be adequate for the range of power settings and center-of-gravity locations encountered in flight. The purpose of this report is to provide the analytical means by which designers may estimate the elevator deflection required to trim in steady longitudinal flight and to demonstrate in a quantitative manner the effects on longitudinal trim of changes in some of the more important design parameters.

Simplified methods and semiempirical data have been summarized from existing literature and employed to provide analytical procedures that are simple to apply but yet are accurate enough for use in preliminary design. Two light aircraft are analyzed quantitatively by the procedures given, for both power-on and power-off conditions, in order to demonstrate the use of the analytical methods and to provide a comparison with flight-test results. Computed and flight-test values of elevator deflection are in good agreement. Calculated values of elevator deflection are also presented for both aircraft to demonstrate the quantitative effects of changes in some of the more important variables, as well as the effects of power. Applications to design are discussed.

It is concluded that these procedures can result in a design in which the maximum up-elevator deflection may be maintained within the highest value that will result in satisfactory damping in roll and reliable lateral control under all flight conditions, while, at the same time, adequate longitudinal control is available.

INTRODUCTION

This report is the third and final one in a series dealing with the
problem of lateral control of airplanes near the stall. Previous work
has been reported in references 1 and 2.

The major objective of this program has been to provide the designer
with quantitative design information from which the proper combination of
variables may be selected to insure satisfactory control near the stall.

In general, there are two methods by which reliable low-speed lat-
eral control characteristics may be obtained. One of these is to increase
the angle of attack for the stall of the wing, or at least the outboard
portions of the wing, to a point beyond the highest angle that is required
in steady flight or in landing, thus maintaining effective damping-in-roll
characteristics. This method utilizes aerodynamic devices such as
leading-edge slots and wing washout. In reference 1 results were pre-
sented of flight tests employing this method; the results showed that
effective and reliable low-speed lateral control could be attained with
the airplane configuration tested but only for power-off flight and a
narrow range of center-of-gravity positions.

The second method consists of simply limiting the elevator deflec-
tion so that the maximum angle of attack maintainable is that which will
still allow satisfactory lateral control characteristics. It was shown
in reference 2 that satisfactory lateral control was obtained, for all
airplanes tested, up to a "critical" angle of attack that was within 2°
of the angle of attack at which the airplane stalled; the reduction in
minimum speed was almost negligible. However, this approach is a diffi-
cult one because the elevator deflections required for longitudinal trim
usually vary greatly with center-of-gravity location and power setting;
the elevator deflection required to land causes further scatter of the
range of required elevator deflections. Nevertheless, the designer does
have a certain degree of control over longitudinal trim characteristics
by means of a number of design variables. Flight tests on several air-
planes, conducted to obtain quantitative information regarding the range
of elevator deflections encountered, are reported in reference 2. There
are also included the results of flight tests on one airplane utilizing
different horizontal tail configurations which were proportioned so as
to minimize the change in horizontal trim caused by application of power.

The results of the flight investigations showed that it is feasible
to have airplane configurations for which application of power makes a
very slight change in the angle of attack at which the airplane trims
with a given elevator setting. The results also showed that for moderate
ranges of center-of-gravity travel a single maximum elevator deflection
gave acceptable low-speed performance (the maximum up-elevator deflection

that would produce the critical angle of attack with the rearward center-of-gravity condition would produce an acceptable minimum speed in the forward center-of-gravity condition). With airplanes having tail-wheel-type landing gears, however, it appears to be extremely difficult to cover the three-point-landing situation satisfactorily. Because of the ground effect a greater elevator deflection is required to attain a given angle of attack while the airplane is landing than when it is flying well above the ground. On this account, it is unlikely (but not impossible) that a single maximum elevator deflection can be found that will not produce an angle of attack above the critical value for satisfactory lateral control in the most rearward center-of-gravity condition with power full on and that will also produce a three-point landing without power in the most forward center-of-gravity condition.

With airplanes having tricycle gears, however, the three-point landing is not a consideration, and all of the conditions can be met satisfactorily without great difficulty. With both of the tails tested on the one airplane fitted with a tricycle gear, satisfactory maximum elevator deflection was found which allowed good lateral control at minimum speed, with power off and power on, and provided satisfactory landing and take-off performance, throughout the entire center-of-gravity range for the various possible conditions of loading. The tests thus showed the system to be entirely usable for airplanes having tricycle landing gears and a moderate range of center-of-gravity locations.

It is the purpose of the present report to provide designers with detailed procedures for analyzing the effects of changes in design parameters on longitudinal trim characteristics for airplanes of various configurations. This is accomplished by (1) presenting a summary of pertinent data and formulas which may be used to evaluate longitudinal trim characteristics analytically, (2) presenting detailed numerical examples which illustrate the analytical procedures, and (3) presenting the results of numerical studies which are intended to demonstrate the effects of changes in some of the more important design variables. In addition, the results of the numerical examples are correlated with the results of flight tests from references 1 and 2. It is hoped that these results will be of assistance to designers in determining the relationships between the various factors involved so that satisfactory control characteristics can be provided for the particular configuration in question.

Simplicity and ease of computation have been the keynote throughout the preparation of this report. Data have been presented in curve form wherever possible and empirical or semiempirical factors and formulas have been used freely; correction factors which experience has shown are usually small (as, for example, the effect of the wake on downwash angle and the actual value of the thrust coefficient in the windmilling propeller condition), at least for light aircraft, have sometimes been omitted. Nevertheless, it is believed that the procedures described herein are sufficiently accurate for preliminary design purposes.

When comparisons with flight-test results are attempted later in
this report, it should be kept in mind that (1) the simplified procedures
utilized will result in computed values which might be improved somewhat
by the use of more exact methods; (2) the flight-test results should be
considered in the light of the limited accuracy of experimental measure-
ment; and (3) measurements made by flight test more often than not reflect
pilot technique in some measure. In view of these comments, it will be
considered satisfactory if computed values of control-surface deflection
are within about $\pm 4^\circ$ of the corresponding experimental values. In a
previous unrelated study (ref. 3), a correlation of about 3° was con-
sidered acceptable; however, in that investigation, the computed results
were obtained by employing data obtained directly from flight tests,
wherever feasible. The philosophy of the present report is to present
methods which may be used in the preliminary design stage where accurate
or even adequate data are often not available; therefore, it is not
unrealistic to accept differences of somewhat more than 3°. It is empha-
sized once again that the guiding principle of this report is the pre-
sentation of methods which may be used to predict the effects of changes
in design variables.

It might be mentioned that the methods of analysis presented herein
will also yield information concerning the longitudinal static stability.
Calculations may be made for the pitching moment about the center of
gravity (zero elevator deflection) for several values of lift coefficient.
The customary plot of pitching moment versus lift coefficient will show
the static stability characteristic by the slope of the resulting curve.

The authors wish to thank Mr. James D. Barnard for his assistance
in performing computations and in preparing the figures. This work was
conducted at the Aircraft Research Center of the Texas Engineering
Experiment Station, Texas Agricultural and Mechanical College System,
under the sponsorship and with the financial assistance of the National
Advisory Committee for Aeronautics.

ANALYSIS

Power Off

Basic analysis.- The equilibrium equation for steady longitudinal
flight may be written from a consideration of the forces and moments
acting in the plane of symmetry. Assuming that

(1) There are no power effects (direct or indirect)
(2) The aircraft is not in close proximity to the ground
(3) Moments contributed by the drag forces, except wing drag, are
negligible

(4) The only lifting elements are the wing and horizontal tail

the equilibrium equation is

$$\left[C_{L_W} \cos\left(\alpha_W - i_W\right) + C_{D_W} \sin\left(\alpha_W - i_W\right)\right]\frac{x_{ac}}{\bar{c}_W} + \left[C_{D_W} \cos\left(\alpha_W - i_W\right) - \right.$$

$$\left. C_{L_W} \sin\left(\alpha_W - i_W\right)\right]\frac{z_{ac}}{\bar{c}_W} + C_{m_{fu}} - a_t\left(\alpha_W - \epsilon - i_W + i_t + \tau\delta_e\right)\frac{S_t}{S_W}\frac{l_t}{\bar{c}_W}\eta_t = 0$$

$$(1)$$

The meaning of each symbol in this equation may be found in the list of symbols given in the appendix. (See fig. 1 also.)

The moment contributed by the fuselage may be estimated by the simple formula (ref. 3)

$$C_{m_{fu}} = \frac{K_{fu}w_{fu}^2 L_{fu}}{S_W\bar{c}_W a_W}C_{L_W} \qquad (2)$$

The factor K_{fu}, which depends on the wing location on the body, may be determined from figure 2.

The horizontal tail lift-curve slope may be obtained from figure 3 as a function of tail aspect ratio (ref. 4). In the absence of more reliable data, the upper curves in figure 3 may be utilized for estimating the wing lift-curve slope, depending on the section lift-curve slope a_0.

The downwash angle ϵ is a very important quantity; however, its accurate determination requires exceedingly complex procedures. For most analyses, it will be adequate to determine ϵ by means of convenient design charts (ref. 5). These charts, which are reproduced here in figures 4 to 13, give downwash angles for plain and flapped untwisted wings. The wings considered include both elliptical and tapered plan forms (taper ratios of 1, 2, 3, and 5) with aspect ratios of 6 and 9 and flaps covering 40 and 70 percent of the wing span.

The following procedures govern the use of these charts:

Plain wings: The procedure for plain wings is as follows: (1) Find the longitudinal distance x of the elevator hinge axis from the quarter-chord point of the root section and the vertical distance m (with respect to the airplane reference line) of the hinge axis from the wing trailing edge (negative down). (2) Find the contribution h_W of the plain wing to the downward displacement of the wake center line at the distance x

from the quarter-chord point by multiplying the value at the distance x
on the corresponding displacement chart by the lift coefficient. (3) Locate
the point $(x, |m + h_w|)$ on the downwash contour chart and multiply the cor-
responding downwash angle by the lift coefficient and by the correction
factor obtained from figure 14 which accounts for the variation of down-
wash angle across the span of the horizontal tail (ref. 5).

Flapped wings: For flapped wings the procedure is as follows:
(1) Find the longitudinal distance x of the elevator hinge axis from
the quarter-chord point of the root section and the vertical distance m
of the hinge axis from a point (the wake origin) lying at a distance h_o
below the trailing edge of the wing, where

$$h_o = \frac{\left(\frac{c_f}{2}\right) \sin \delta_f + k\bar{c}_w}{b/2} \tag{3}$$

and k is given in figure 15. (2) Find the contribution h_w of the
plain wing to the downward displacement of the wake center line at dis-
tance x from the quarter-chord point by multiplying the value on the
corresponding displacement chart (plain wing), at the distance x, by
C_{L_w}. (3) Find the contribution h_f of the flap to the downward dis-
placement by multiplying the value on the corresponding chart (flap), at
the distance x, by C_{L_f}. (4) Locate the point $(x, |m + h_w + h_f|)$ on
the contour charts for the plain wing and for the flap; multiply the cor-
responding downwash angles, respectively, by C_{L_w} and C_{L_f} and by the
correction factor from figure 14 and add in order to obtain the downwash
angle.

A slight correction is often added to the downwash angles obtained
by the procedures just described which accounts for the effect of the
wake on the downwash angle. The effect is to increase the downwash above
the wake center line (located by $m + h_w$ or, in the case of a flapped
wing, by $m + h_w + h_f$) and to decrease the downwash below it. The cor-
rection is usually negligible for plain wings; for flapped wings with
small flap deflections a correction of 1.5° within the wake to 1° at the
wake edge should be adequate, while for large flap deflections those
values should be doubled. The location of the horizontal tail with respect
to the wake may be determined from figures 16 and 17. For a more accurate
determination of the magnitude of the wake correction, reference 5 should
be consulted.

For wings or flap spans other than those included in these charts,
linear interpolation or extrapolation is usually quite sufficient. For
wings which possess considerable twist, the downwash due to twist must be
calculated from the spanwise load distribution at the zero-lift condition,

and this is used as an increment of downwash to be added to the downwash found by the procedures outlined on the preceding page.[1]

The contribution of flaps to the wing lift, drag, and moment may also be accounted for conveniently by means of certain design charts (refs. 5 and 6). The increase in section lift coefficient, corresponding to a given flap deflection, may be obtained from figure 18(a); the increase in total wing lift coefficient may then be obtained from figure 18(b). The increments in wing section moment coefficient and total wing drag may be found from figure 19. These design charts should only be used in the absence of more reliable aerodynamic data pertaining to the particular design.

Deflection of the elevator serves to change the effective angle of attack of the horizontal tail. The change of α_t with elevator deflection thus constitutes an important parameter τ, known as the elevator effectiveness factor. An empirically derived curve for τ (ref. 6), as a function of S_e/S_t, is shown in figure 20.

The dynamic pressure in the vicinity of the horizontal tail is often quite different from the free-stream dynamic pressure; the ratio $q_t/q = \eta_t$ is called the tail efficiency factor. For power-off flight, τ is less than unity because of the unavoidable loss of energy as the air flows past the aircraft ahead of the tail plane. The value of η_t may be estimated, for plain wings and wings with split flaps, from figure 21 (ref. 7); however, these values may be revised upward slightly depending upon the aerodynamic cleanness of the wing-fuselage combination.

The data just discussed, together with the aerodynamic and geometric data established for the proposed design, will enable the analyst to evaluate the elevator deflection required for longitudinal trim from equation (1).

Effect of windmilling propeller and ground proximity.- The effects of running propellers are very pronounced and some account should be taken of them in any stability or equilibrium analysis. Even in the case of a windmilling propeller the normal force (i.e., normal to the thrust line) may be a rather significant quantity. Therefore, although a detailed analysis of the effects of application of power will be given in a later section of this report, a simple analysis will now be presented for the effect of the windmilling propeller, assuming that the axial thrust is zero.

---

[1]In many cases it will be sufficient to employ a weighted incidence angle and treat the wing as though it were untwisted. The applicability of this procedure will generally depend upon the distribution of the twist, since, for example, if the wing is mostly twisted near the tips the influence on the downwash in the vicinity of the horizontal tail will be small.

The moment contributed by the propeller normal force may be written as (ref. 6, p. 241)

$$\left[(C_m)_{N_p}\right]_{T_c=0} = \left[\left(\frac{dC_N}{d\alpha_T}\right)_p\right]_{T_c=0}\left(1 + \frac{d\epsilon}{d\alpha_w}\right)\frac{l_p S_p n}{S_w \bar{c}_w a_w} C_{L_w} \qquad (4)$$

for the windmilling condition. In most cases, $\left[\left(\frac{dC_N}{d\alpha_T}\right)_p\right]_{T_c=0}$ may be taken

as 0.00165 for two-bladed propellers and 0.00235 for three-bladed propellers; however, for more precise values, charts for particular propellers are given in reference 8. More precise values may also be obtained by use of figures 22 to 24 of the present report. The factor $1 + \frac{d\epsilon}{d\alpha_w}$ refers

to the upwash at the propeller and may be obtained from figure 25 (modified from ref. 9).

Since even the windmilling propeller produces some additional downwash at the tail, the corresponding additional moment is then (ref. 6, p. 241),

$$\left[(C_m)_{\epsilon_p}\right]_{T_c=0} = \frac{a_t S_t l_t \eta_t}{a_w S_w \bar{c}_w (0.97)}\left[\left(\frac{dC_N}{d\alpha_T}\right)_p\right]_{T_c=0}\left(1 + \frac{d\epsilon}{d\alpha_w}\right)C_{L_w} \qquad (5)$$

There is probably some change in the dynamic pressure at the tail due to the windmilling propeller; however, the change is usually so slight as to be negligible. All other effects of the windmilling propeller may be considered to be negligible, and, in particular, it is assumed that the thrust is exactly zero.

In order to predict the elevator deflection required to land, it is necessary to account for the effect of the ground on the flow field in the vicinity of the airplane. The major effects of ground proximity are (1) to reduce the downwash at the tail, thereby increasing the angle of attack of the tail and altering the slope of the tail lift curve and (2) to alter the wing lift-curve slope by reducing the induced drag, which in turn arises from the changed downwash.

The change in wing lift-curve slope effectively changes the wing angle of attack by an amount

$$\Delta\alpha_w = \frac{C_{L_w}}{a_w}\left(\frac{1}{K} - 1\right) \qquad (6)$$

The factor K (ref. 3), which is the ratio of lift-curve slope near the ground to lift-curve slope far from the ground, is shown in figure 26.

The same factor may be used to obtain the slope of the tail lift curve in the presence of the ground.

Proximity to the ground causes a very large reduction in the downwash at the tail, thereby requiring much greater elevator deflections to achieve satisfactory landing attitudes when the landing gear is of the tail-wheel type; for an airplane with a tricycle landing gear this condition is not important except under certain special circumstances. The downwash and wake charts presented earlier may be used here, with some slight modifications (ref. 3), to determine downwash angles near the ground. The procedure to be outlined is for the case of flapped wings (however, the simplification to plain wings is obvious):

(1) Determine all geometric quantities as before (notation is shown in fig. 27); the distance h_o may be found from figure 28.

(2) From figures 29 and 30 determine h_w due to the plain wing and h_f due to the flap.

(3) Determine the net value of h by the equation

$$h = C_{L_w} h_w + C_{L_f} h_f \tag{7}$$

(4) From the downwash charts (figs. 4 to 13) determine ϵ by

$$\epsilon = C_{L_w}\left[\epsilon_w(x,\ m+h) - \epsilon_w(x,\ 2z+m-h)\right] +$$

$$C_{L_f}\left[\epsilon_f(x,\ m+h) - \epsilon_f(x,\ 2z+m-h)\right] \tag{8}$$

where the subscripts of ϵ_w and ϵ_f signify that these values are to be read from the downwash charts for the plain wing and flap, respectively.

(5) Add the wake corrections of figure 31 (this correction is usually negligible for unflapped wings).

Introductory discussion of effects of center-of-gravity location.- Of all of the variables which influence the equilibrium equation, one of the most important is the center-of-gravity location. Flight tests have shown (refs. 1 and 2) that for typical personal-type aircraft a rearward shift of longitudinal center-of-gravity location of 1 percent mean aerodynamic chord results in a decrease of elevator deflection required to trim, at large angles of attack, of approximately 1.25°; thus a shift of 5 percent mean aerodynamic chord will change the elevator deflection by almost 7°. As will be shown later, however, this effect can be altered by employing an elevator having a small area compared with the stabilizer

area so that rather large deflections are employed to give a certain
tail-depressing moment or by employing an elevator of rather large area
so that only small deflections are necessary to produce the same moment
(see also the flight-test results reported in ref. 2).

Generally speaking, limits on the longitudinal movement of the center
of gravity are provided by the stability and control requirements. The
rearward location of the center of gravity is limited by the requirement
that the airplane possess at least some degree of static longitudinal sta-
bility. The forward location of the center of gravity is limited by the
requirement that the airplane be trimmed at or near $C_{L_{max}}$ with full up
elevator. Within this center-of-gravity range the designer must provide
for satisfactory control under varying power conditions.

A large center-of-gravity travel with a given limited elevator deflec-
tion will entail a low-speed performance loss in the nose-heavy condition
because the critical angle of attack (see "Introduction") can be attained
only in the tail-heavy condition. Thus the designer would attempt to
minimize this loss by providing a small center-of-gravity travel. The
minimum speed would not be greatly affected.

The desired trim condition could be achieved with a large center-of-
gravity travel by having two or more limitations of elevator deflection
corresponding to various conditions of loading. Such a method could con-
ceivably be developed through suitable mechanical devices, and these might
well be practical even considering such diverse factors as economy, relia-
bility, compactness, and simplicity.

Numerical examples.- Some of the design variables which may be adjusted
in an effort to provide adequate control within the center-of-gravity range
described above are tail length, tail aspect ratio, tail incidence angle,
vertical location of the horizontal tail, and, to some extent, the vertical
center-of-gravity location. The effects of power are considered in a later
section, and it is found that the spanwise location of the elevators on the
horizontal tail is an extremely important parameter because of the very
large effect of the slipstream. The numerical examples which follow are
intended to demonstrate the effects of some of the more important of these
design variables, as well as to demonstrate the use of the data and pro-
cedures described in the preceding sections. The first numerical example
is for a typical high-wing light airplane (ref. 1), and the other is for
a low-wing light airplane (ref. 2). The geometric and aerodynamic data
for these two aircraft are shown in tables I and II and figures 32 and 33.

High-wing airplane: As a numerical example to demonstrate the use
of the analytical methods presented in the foregoing sections, the elevator
deflections required for longitudinal trim for the high-wing airplane shown
in figure 32, having the dimensional and aerodynamic qualities shown in
table I, will now be calculated.

The analysis will be made for $\alpha_w = 15.8^\circ$. Since $\alpha_{ZL} = -1.2^\circ$, $\alpha_a = 15.8^\circ + 1.2^\circ = 17.0^\circ$. From figure 3, $a_w = 0.081$ and $a_t = 0.055$. Hence

$$C_{L_w} = (0.081)(17) = 1.38$$

This simplified procedure was used to demonstrate what might be done in the absence of more detailed and accurate information. The essential simplification here is the assumption of a perfectly linear lift curve; in reality, the lift curve is nonlinear in the region under consideration and therefore the value 1.38 for the lift coefficient is somewhat too high; a value of 1.25 is more realistic.

The position of the one-quarter root chord on the body in percent of body length is 27.3; therefore, from figure 2, $K_{fu} = 0.008$ and from equation (2)

$$C_{m_{fu}} = \frac{(0.008)(3.5)^2(21.77)(1.25)}{(180)(4.98)(0.081)} = 0.036$$

In order to determine the downwash angle it will be necessary to interpolate for $A_w = 7.2$. From figure 4 it is found that, for

$$x = \left(\frac{14.33}{18}\right)(100) = 80, \quad h_w = (7)(1.25) = 8.7. \text{ Then } h_w + m = 8.7 - $$

$\left(\dfrac{0.83}{18}\right)(100) = 4.1$ so that the contour chart yields $\epsilon_6 = (5.7)(1.25)$

$(1.03) = 7.3^\circ$, where the correction factor 1.03 has been obtained from figure 14. Now, from figure 5, $h_w = (5.0)(1.25) = 6.2$ so that

$h_w + m = 6.2 - \left(\dfrac{0.83}{18}\right)(100) = 1.6$ and $\epsilon_9 = (3.5)(1.25)(1.03) = 4.5^\circ$.

Interpolating between the two values of ϵ just calculated gives $\epsilon_{7.2} = 6.2^\circ$.

The effect of the wake on the downwash angle will be neglected.

From figure 20, the elevator effectiveness factor is found to be 0.6.

It will be assumed that the dynamic pressure in the vicinity of the tail is about 5 percent less than the free-stream dynamic pressure so that $\eta_t = 0.95$.

A value has now been obtained for every quantity appearing in equation (1), except the one unknown δ_e. Thus

$$\left[1.25 \cos(15.8° - 3.8°) + 0.175 \sin(15.8° - 3.8°)\right]\left(\frac{0.33}{4.98}\right) +$$

$$\left[0.175 \cos(15.8° - 3.8°) - 1.25 \sin(15.8° - 3.8°)\right]\left(\frac{2.85}{4.98}\right) - 0.008 +$$

$$0.036 - 0.055(15.8° - 6.2° - 3.8° + 0° + 0.6\delta_e)\left(\frac{25.8}{180}\right)\left(\frac{13.16}{4.98}\right)(0.95) = 0$$

from which there is obtained

$$\delta_e = -\frac{0.053}{(0.6)(0.0198)} = -4.5°$$

This value compares favorably with the flight-test value of $-4.4°$ (ref. 1); however, the flight test was conducted with the propeller wind-milling, so that factor will now be introduced into the analysis.

From figure 25, the upwash factor at the propeller is $1 + \dfrac{d\epsilon}{d\alpha_w} = 0.8$.

From equation (4),

$$\left[(C_m)_{N_p}\right]_{T_c=0} = (0.00165)(0.8)\left(\frac{6.21}{180}\right)\left(\frac{28.3}{4.98}\right)\left(\frac{1}{0.081}\right)(1.25) = 0.004$$

and, from equation (5),

$$\left[(C_m)_{\epsilon_p}\right]_{T_c=0} = \left(\frac{0.055}{0.081}\right)\left(\frac{25.8}{180}\right)\left(\frac{13.16}{4.98}\right)\left(\frac{0.95}{0.07}\right)(0.00165)(0.8)(1.25) = 0.006$$

Therefore,

$$(\delta_e)_{T_c=0} = \frac{1}{(0.6)(0.0198)}(-0.053 + 0.004 + 0.006) = -3.6°$$

This value is in close agreement with the flight-test value and is there-fore quite acceptable. Again when comparing computed and measured eleva-tor deflections, one should bear in mind the ideas discussed in the "Introduction" concerning the correlation of such results.

The effect of ground proximity on the elevator deflection required to trim (no windmilling propeller) will now be determined.[2]

The important vertical distances z and d_g are taken to be $z = 4.5$ feet and $d_g = 2.5$ feet. From figure 26, then, $K = 1.13$. The change in wing angle of attack is, from equation (6),

$$\Delta\alpha_W = \left(\frac{1.25}{0.081}\right)\left(\frac{1}{1.13} - 1\right) = -1.8^\circ$$

so that $\alpha_{W_g} = 15.8^\circ - 1.8^\circ = 14.0^\circ$.

To determine the downwash angle, again interpolate between figures 4 and 5. For $A_W = 6$ (using figs. 29 and 30 to evaluate h),

$$\frac{m - h + 2z}{b/2}(100) = \left(-\frac{0.83}{18} - 0.028 + \frac{9}{18}\right)(100) = 42.6$$

so that, from the contour chart, $\epsilon_6 = (4.1)(1.25)(1.03) = 5.3^\circ$. For $A_W = 9$,

$$\frac{m - h + 2z}{b/2}(100) = \left(-\frac{0.83}{18} - 0.027 + \frac{9}{18}\right)(100) = 42.7$$

so that $\epsilon_9 = (2.5)(1.25)(1.03) = 3.2^\circ$. By linear interpolation, then, $\epsilon_{7.2} = 4.5^\circ$. Now, from equation (8),

$$\epsilon_g = 6.2^\circ - 4.5^\circ = 1.7^\circ$$

since multiplication by C_{L_W} has already been performed. The wake correction is neglected.

---

[2]If calculated results are to be compared here with values measured during actual landings, the actual angle of attack at landing should perhaps be employed in the calculations. However, since the major purpose of this report is to show the effects of changes in various quantities rather than to compare calculated and measured values, the previous value of $\alpha_W = 15.8^\circ$ will again be employed. It may be mentioned that the effect of using $\alpha_{W_{land}}$ would be to increase the elevator deflection, and, as will be seen at the end of the present computation, this would tend to reduce the difference between calculated and measured values (also see discussion in the following section "Low-wing airplane").

With the above values for α_{w_g} and ϵ_g and also

$$a_{t_g} = (0.055)(1.13) = 0.062$$

δ_{e_g} may be evaluated from equation (1):

$$\left[1.25 \cos (14.0° - 3.8°) + 0.175 \sin (14.0° - 3.8°)\right]\frac{0.33}{4.98} +$$

$$\left[0.175 \cos (14.0° - 3.8°) - 1.25 \sin (14.0° - 3.8°)\right]\frac{2.85}{4.98} - 0.008 +$$

$$\frac{0.036}{1.13} - (0.062)(14.0° - 1.7° - 3.8° + 0.6\delta_e)\left(\frac{25.8}{180}\right)\left(\frac{13.16}{4.98}\right)(0.95) = 0$$

From this there is obtained

$$\delta_{e_g} = \frac{-0.112}{(0.6)(0.0222)} = -8.4°$$

In order to make a comparison with the flight-test value of $-10.1°$, the effect of the windmilling propeller as corrected for the effect of the ground on the wing lift-curve slope should be added. Thus

$$\left(\delta_{e_g}\right)_{T_c=0} = \frac{1}{(0.6)(0.0222)}\left(-0.112 + \frac{0.004}{1.13} + \frac{0.006}{1.13}\right) = -7.6°$$

Low-wing airplane: As a second numerical example to demonstrate the use of the analytical methods presented in the foregoing sections, the elevator deflection required for longitudinal trim for the low-wing airplane shown in figure 33, having the dimensional and aerodynamic qualities shown in table II, will now be calculated.

The analysis will be made for $\alpha_w = 17.5°$ (ref. 2). Since $\alpha_{ZL} = -4.2°$, $\alpha_a = 17.5° + 4.2° = 21.7°$. From figure 3, $a_w = 0.072$ and $a_t = 0.071$. Hence[3]

$$C_{L_w} = (0.072)(21.7) = 1.56$$

---

[3]The only available information seems to indicate that the lift curve is linear up to this angle of attack.

The position of the one-quarter root chord on the body in percent of body length is 28.8; therefore, from figure 2, $K_{fu} \approx 0.01$ and, from equation (2),

$$C_{m_{fu}} = \frac{(0.01)(3.33)^2(27.2)(1.56)}{(290)(7.5)(0.072)} = 0.030$$

In order to determine the downwash angle it will be necessary to extrapolate for $A_W = 5.5$. From figure 4 one finds, for $x = \left(\frac{18.3}{19.9}\right)(100) = 92$, $h_W = (7.5)(1.56) = 11.7$. Thus $h_W + m = 11.7 + \left(\frac{2.50}{19.9}\right)(100) = 24.3$ so that the contour chart yields $\epsilon_6 = (4.8)(1.56)$ $(1.08) = 8.1°$, where the correction factor 1.08 has been obtained from figure 14. Now, from figure 5, $h_W = (5.5)(1.56) = 8.6$ so that $h_W + m = 8.6 + \left(\frac{2.50}{19.9}\right)(100) = 21.2$ and $\epsilon_9 = (3.0)(1.56)(1.08) = 5.0°$. Extrapolating from these two values of ϵ just calculated gives $\epsilon_{5.5} = 8.6°$.

The effect of the wake on the downwash angle will be neglected.

From figure 20, the elevator effectiveness is found to be 0.56.

It will be assumed that the dynamic pressure in the vicinity of the tail is about 5 percent less than the free-stream dynamic pressure so that $\eta_t = 0.95$.

A value has now been obtained for every quantity appearing in equation (1), except the one unknown δ_e. Thus

$$1.56 \cos (17.5° - 2.0°) + 0.197 \sin (17.5° - 2.0°)\left(\frac{0.167}{7.5}\right) +$$

$$\left[0.197 \cos (17.5° - 2.0°) - 1.56 \sin (17.5° - 2.0°)\right]\left(\frac{-0.031}{7.5}\right) - 0.031 +$$

$$0.030 - 0.071(17.5° - 8.6° - 2.0° - 0.5° + 0.56\delta_e)\left(\frac{53.5}{290}\right)\left(\frac{16.8}{7.5}\right)(0.95) = 0$$

from which there is obtained

$$\delta_e = \frac{-0.143}{(0.56)(0.0278)} = -9.2°$$

The effect of the windmilling propeller will now be considered. From figure 25, $1 + \frac{d\epsilon}{d\alpha_w} = 0.85$. From equation (4),

$$\left[(C_m)_{N_p}\right]_{T_c=0} = (0.00165)(0.85)\left(\frac{8.33}{290}\right)\left(\frac{44.3}{7.5}\right)\left(\frac{1}{0.072}\right)(1.56) = 0.005$$

and, from equation (5),

$$\left[(C_m)_{\epsilon_p}\right]_{T_c=0} = \left(\frac{0.071}{0.072}\right)\left(\frac{53.5}{290}\right)\left(\frac{16.8}{7.5}\right)\left(\frac{0.95}{0.07}\right)(0.00165)(0.85)(1.56) = 0.012$$

Therefore

$$(\delta_e)_{T_c=0} = \frac{1}{(0.56)(0.0278)}(-0.143 + 0.005 + 0.012) = -8.1^\circ$$

This result is in reasonably close agreement with the flight-test value of -10.5° (ref. 2).

The effect of ground proximity on the elevator deflection required to trim (no windmilling propeller) will now be determined. Before performing the computation, however, a comment concerning the landing characteristics of this airplane is in order. The airplane is so designed that the attitude of the wing with respect to the ground, when the airplane is at rest, is 11° (including the 2° incidence angle). This is in contrast with many light aircraft, with conventional-type landing gear, for which the wing attitude at rest is very nearly the angle for maximum lift (see footnote 2). Therefore, it will be assumed, for purposes of the following computations, that the flight path of the airplane is parallel to the ground and that the airplane is in landing attitude so that $\alpha_w = 11^\circ$. The wing lift coefficient at this angle of attack is taken as 1.08 and the wing drag coefficient, as 0.095.

The important vertical distances z and d_g are taken to be 3.8 feet and 4.5 feet, respectively. From figure 26, then, $K = 1.13$. The change in wing angle of attack due to the presence of the ground is, from equation (6),

$$\Delta\alpha_w = \left(\frac{1.08}{0.072}\right)\left(\frac{1}{1.13} - 1\right) = -1.7^\circ$$

so that $\alpha_{w_g} = 11.0^\circ - 1.7^\circ = 9.3^\circ$

To determine the downwash angle, again extrapolate from figures 4 and 5. The downwash angle without ground effect and then with ground effect must first be computed in order to take the difference as required by equation (8). Thus, for $A_W = 6$, it is found first that $h_W = (7)$ $(1.08) = 7.6$. Then $h_W + m = 7.6 + \left(\dfrac{2.50}{19.9}\right)(100) = 20.2$ so that the contour chart yields $\epsilon_6 = (4.9)(1.08)(1.08) = 5.7°$. To include the ground effect one has (evaluating h from fig. 29)

$$\frac{m - h_W + 2z}{b/2}(100) = \left(\frac{2.5}{19.9} - 0.022 + \frac{7.6}{19.9}\right)(100) = 48.6$$

so that the contour chart yields $\epsilon_6 = (3.7)(1.08)(1.08) = 4.3°$. Therefore, by equation (8), $\epsilon_{6g} = 5.7 - 4.3 = 1.4°$.

For $A_W = 9$, $h_W = (5.5)(1.08) = 5.9$. Then $h_W + m = 5.9 + \left(\dfrac{2.50}{19.9}\right)(100) = 18.5$ so that the contour chart yields $\epsilon_9 = (3.1)(1.08)$ $(1.08) = 3.6°$. To include the ground effect (evaluating h from fig. 30),

$$\frac{m - h_W + 2z}{b/2}(100) = \left(\frac{2.5}{19.9} - 0.020 + \frac{7.6}{19.9}\right)(100) = 48.8$$

so that the contour chart yields $\epsilon_9 = (2.3)(1.08)(1.08) = 2.7°$. Therefore, by equation (8), $\epsilon_{9g} = 3.6 - 3.1 = 0.5°$

By extrapolation, $\epsilon_{5.5g} = 1.5°$. Corrections due to the wake have again been omitted.

With the above values for α_{W_g} and ϵ_g and also

$$a_{t_g} = (0.071)(1.13) = 0.080$$

equation (1) may be evaluated:

$$\left[1.08 \cos (9.3° - 2.0°) + 0.095 \sin (9.3° - 2.0°)\right]\left(\frac{0.167}{7.5}\right) +$$

$$\left[0.095 \cos (9.3° - 2.0°) - 1.08 \sin (9.3° - 2.0°)\right]\left(\frac{-0.031}{7.5}\right) - 0.031 +$$

$$\frac{0.030}{1.13} - 0.080(9.3° - 1.5° - 2.0° - 0.5° + 0.56\delta_e)\left(\frac{53.5}{290}\right)\left(\frac{16.8}{7.5}\right)(0.95) = 0$$

From this there is obtained

$$\delta_{e_g} = \frac{-0.146}{(0.56)(0.0314)} = -8.3°$$

In order to make a comparison with the flight-test value, the contribution of the windmilling propeller should be added (corrected for the effect of the ground on the wing lift-curve slope). Thus

$$\left(\delta_{e_g}\right)_{T_c=0} = \frac{1}{(0.56)(0.0314)}\left[-0.146 + \frac{(0.005)(1.08)}{(1.13)(1.56)} + \frac{(0.012)(1.08)}{(1.13)(1.56)}\right] = -7.7°$$

This result is in excellent agreement with the measured value of -6.5°.

Power On

Introductory remarks.- It may be well to emphasize at this time that the effects of running propellers on the longitudinal stability characteristics are exceedingly complex. The flow along and around the fuselage and in the vicinity of the tail is difficult to evaluate from theoretical considerations and therefore wind-tunnel tests of powered models are usually resorted to in order to determine the stability characteristics. The light-plane designer is not often in a position to have such tests performed and therefore must employ what analytical methods are available, however meager they may be. Consequently, the analytical methods that are available are either very simple approximations or have been developed by means of semiempirical analyses. Unfortunately, the information of this type that is available does not appear to be directly applicable to light-aircraft design, and the analyst must therefore be content with methods which may offer to him a result valid only in the first approximation.

An attempt has been made, in the sections which follow, to present only those simple formulas and other data which appear to be valid for light aircraft. Elevator deflections required for longitudinal trim for several different cases, involving two different light aircraft, have been calculated by the methods presented and all agree well with deflections measured in flight; therefore, this may constitute a justification for the inclusion of such simplified and approximate methods. The designer is cautioned, nevertheless, that indiscriminate use of these methods may not be satisfactory.

Direct effects of power.- The application of power contributes directly to the equilibrium condition through the forces created by the propeller and indirectly through the effects of the slipstream on the wing and tail surfaces. The present discussion will be concerned only with the direct effects of power application.

Defining the forces and dimensions as shown in figure 34 and defining the thrust and normal-force coefficients as

$$T_c = T/2qD^2$$

$$C_{N_p} = N_p/qS_p$$

(9)

the contribution of the direct power effects to the equilibrium equation is (for small angles of thrust-line tilt)

$$C_{m_p} = T_c \frac{2D^2}{S_w \bar{c}_w}\left(h_p - \phi l_p\right)n + C_{N_p} \frac{S_p}{S_w \bar{c}_w}\left(l_p + \phi h_p\right)n$$

(10)

The thrust coefficient T_c is given by

$$T_c = \frac{P(550)\rho^{1/2}\eta_p}{\left(\dfrac{2W}{S_w C_{L_w}}\right)^{3/2} D^2}$$

(11)

where the propeller efficiency η_p may be obtained from figure 35 (ref. 6). The activity factor, used in figure 35, is defined as (for a propeller having $\bar{n}$ blades)

$$A.F. = \bar{n}(6,250) \int_{0.2}^{1.0} \left(\frac{r}{R}\right)^3 \left(\frac{b}{D}\right) d\left(\frac{r}{R}\right)$$

(12)

and usually has a value of from 150 to 300. The parameter C_{PX}, also appearing in figure 35, is

$$C_{PX} = C_P/X$$

(13)

where the power coefficient C_P is given by

$$C_P = \frac{\dfrac{P}{1,000}}{2\sigma\left(\dfrac{N}{1,000}\right)^3\left(\dfrac{D}{10}\right)^5} \tag{14}$$

The advance ratio J is given by

$$J = 60V/ND \tag{15}$$

If propeller charts are available for the proposed design, they should be used to determine η_p in preference to figure 35.

The normal-force coefficient may be written in the form

$$C_{N_p} = \left(\frac{dC_N}{d\alpha_T}\right)_p \left(1 + \frac{d\epsilon}{d\alpha_w}\right)\frac{CL_w}{a_w} \tag{16}$$

which includes the effect of the upwash field ahead of the wing. This equation is identical with equation (4) for the windmilling propeller (aside from a moment arm and certain nondimensionalizing quantities) except that the derivative $\left(\dfrac{dC_N}{d\alpha_T}\right)_p$ is to be evaluated for the particular value of thrust coefficient T_c involved, instead of for $T_c = 0$. This is accomplished by means of charts developed in reference 9 and presented here as figures 22 to 24. These figures may also be used for a better estimate of the normal-force coefficient in the case of a windmilling propeller. The factor $1 + \dfrac{d\epsilon}{d\alpha_w}$ is evaluated from figure 25, as before.

The use of figures 22 to 24 involves a new quantity dependent upon the propeller geometry, the "side-force factor." The propeller side-force factor, which is very similar in form to the activity factor mentioned earlier, is expressed as

$$\text{Propeller side-force factor} = (3,125)\int_{0.2}^{1.0} \frac{b}{D}\sin\left(\beta - \beta_{0.75R} + 25°\right) d\!\left(\frac{r}{R}\right)$$

$$\tag{17}$$

An approximate evaluation of this factor may be made according to the formula (ref. 10)

$$\text{S.F.F.} = 525\left(\frac{b}{D}\right)_{0.3R} + 525\left(\frac{b}{D}\right)_{0.6R} + 270\left(\frac{b}{D}\right)_{0.9R} \tag{18}$$

Indirect effects of power.- In addition to the direct forces just discussed, the running propeller produces many indirect effects as a result of the interaction of the slipstream with the horizontal tail and the wing. The indirect effects are no less important than are the direct effects, and in many cases they are more important; they are, however, exceedingly complex in nature and are therefore difficult to account for accurately. Some of the more important of these indirect effects are:

(a) Increase in wing lift due to the slipstream over a portion of the wing
(b) Change in wing moment coefficient due to the slipstream
(c) Change in the downwash at the tail due to the slipstream
(d) Increase in dynamic pressure at the tail due to the slipstream

The increment in wing lift coefficient due to the slipstream over a portion of the wing may be estimated from the equation (ref. 9)

$$\Delta C_{L_W} = 0.57 T_{c_A} C_{L_0} \frac{c_w}{\bar{c}_w} \frac{D^2}{S_w}$$ (19)

The increment in wing moment coefficient due to the slipstream over a portion of the wing may be estimated from the equation (ref. 9)

$$\Delta C_{m_W} = (c_{m_{ac}})_i \frac{c_{w_i}^2}{c_w} \frac{b_{w_i}}{S_w} \frac{8}{\pi} T_c + \left[\left(\frac{dC_m}{dC_L} \right)_{wf} \right]_0 \Delta C_{L_W}$$ (20)

In equation (19), c_w is the wing chord at spanwise station $0.75R$ from the airplane center line. The subscript 0 in equations (19) and (20) refers to power-off conditions. The derivative $\left[\left(\frac{dC_m}{dC_L} \right)_{wf} \right]_0$ in equation (20) may be obtained from the power-off analysis given earlier by omitting the contribution of the tail or it may be obtained from wind-tunnel data, if available; the subscript wf designates wing-fuselage combination (i.e., no tail).

The effects of the slipstream on the downwash and dynamic pressure at the tail probably constitute the most important of the power effects; but they are also the most difficult to evaluate. There seem to be available several analyses for determining the downwash and dynamic pressure with running propellers.

One of these is based on a theoretical analysis of an isolated running propeller. The increment of downwash at the tail due to the running propeller may be expressed in the simple form (ref. 10)

$$\epsilon_p = \left\{ A + B\left[\left(\frac{dC_N}{d\alpha_T}\right)_p\right]_{T_c=0} \right\} \frac{C_{L_W}}{a_W} \qquad (21)$$

where A and B are functions of the thrust coefficient, as given in figure 36.

The dynamic pressure at the tail is obtained from this elementary theory by considering the tail to be far behind the propeller; thus

$$\eta_t = 1 + \frac{8}{\pi} T_c \qquad (22)$$

The other methods (see, e.g., refs. 9 and 11) generally involve the use of semiempirical data obtained from wind-tunnel tests of powered models. The test results used in the analyses were for high-performance fighter-type aircraft; however, it was thought that the results of such analyses might be applicable to light aircraft as well (ref. 9, p. 14) in view of certain correlations of thrust coefficients for personal- and fighter-type aircraft. Computations for elevator deflection required to trim by the method of reference 9 do not agree with available flight-test values for the airplanes considered in this report and, therefore, the applicability of this method to light aircraft is subject to consid-erable doubt. Although no computations were made using the method of reference 11, it, too, is semiempirical in nature and is based on tests of powered models of rather high performance aircraft and therefore may not lead to reliable results for light aircraft.

Additionally, since the effects of power on longitudinal trim char-acteristics cannot be accounted for in a completely rational manner, it is doubtful that these methods, with their increased complexity, can offer any advantage over the simplified method of reference 10.

One must consider, however, only those portions of the horizontal stabilizer and elevators that are immersed in the slipstream, and these will depend upon the spanwise location of the elevators on the horizontal tail and upon the vertical location of the horizontal tail. There is little information available as to the shape and location of the slip-stream in the vicinity of the tail plane; the computations of this report are based on the assumption that the slipstream remains cylindrical.[4]

---

[4]This assumption, although neglecting the "swirl" of the slipstream, effect of wing downwash on the slipstream, and so forth, seems to give results, at least for the present analysis, which are in fairly good agreement with experiment (see ref. 11, p. 19, for some additional comments).

Further considerations of power-on lift and moment coefficients.-
Tilt of the propeller thrust axis produces no appreciable change in
downwash (for small angles of tilt); however, there is a noticeable
change in lift coefficient given by

$$\Delta C_{L_p} = T_c \frac{2D^2}{S_w} \sin \alpha_T \tag{23}$$

The total lift coefficient is thus given by the power-off lift
coefficient plus the contributions of equations (19) and (23). Since
the thrust coefficient varies with lift coefficient, the following iter-
ation procedure is recommended:

(1) Evaluate ΔC_{L_w} by equation (19).

(2) Evaluate ΔC_{L_p} by equation (23) with T_c corresponding to
$\left(C_{L_{wf}}\right)_0 + \Delta C_{L_w}$.

(3) Evaluate ΔC_{L_p} by equation (23) with T_c corresponding to
$\left(C_{L_{wf}}\right)_0 + \Delta C_{L_w} + \left(\Delta C_{L_p}\right)_2$, where $\left(\Delta C_{L_p}\right)_2$ is the value obtained from
step (2) above.

(4) The final lift coefficient is given by $\left(C_{L_{wf}}\right)_0$ plus ΔC_{L_w}
from step (1) plus ΔC_{L_p} from step (3).

The final power-on wing-fuselage pitching-moment coefficient is
given by

$$C_{m_{wf}} = \left(C_{m_{wf}}\right)_0 + C_{m_p} + \Delta C_{m_w} \tag{24}$$

The terms C_{m_p} and ΔC_{m_w} are found from equations (10) and (20), with
values of T_c based on $\left(C_{L_{wf}}\right)_p$ from step (4) of the procedure given
above.

The computation of the power-on tail pitching-moment coefficient
consists merely of adding the increments produced by the altered down-
wash at the tail and increased tail effectiveness to $\left(C_{m_t}\right)_0$.

The final power-on complete pitching-moment coefficient is given by

$$C_{m_p} = \left(C_{m_{wf}}\right)_p + \left(C_{m_t}\right)_p \tag{25}$$

Inasmuch as

$$\left(C_{L_t}\right)_p = -\frac{\left(C_{m_t}\right)_p}{l_t/\bar{c}_w} \tag{26}$$

the complete power-on lift coefficient may be formed by adding this result to that from step (4) of the procedure given above.

Introductory discussion of effect of thrust-line location.- A detailed analysis of the effect of tilting the thrust axis (ref. 11) has shown that downward tilt will reduce the destabilizing effects of power by a significant amount. Tilt affects the direct propeller forces but is less important in causing changes in the indirect effects (ref. 9, p. 7). Thus, the effects of tilt are easy to estimate and may prove to be a significant design variable for use in obtaining desirable trim characteristics.

The effect of vertical location of the thrust axis with respect to the airplane center-of-gravity location is a most important parameter. The destabilizing effect of power application may be altered very effectively by shifting the vertical location of the thrust axis; this may be accomplished, obviously, by tilt as well as by actual vertical shifts since tilting will change the moment arm between the center of gravity and the line of action of the thrust.

Numerical examples.- The numerical examples which follow are intended to illustrate the methods of analysis outlined in the preceding section for power effects and to demonstrate the effects of changes in the various design variables on longitudinal trim characteristics.

The two aircraft studied previously for power-off flight will now be analyzed for power-on flight. The geometric and aerodynamic data for the two aircraft are shown in figures 32 and 33 and tables I and II.

High-wing airplane: For purposes of comparison with the power-off analysis, the computations for the high-wing airplane which follow are based on $\alpha_w = 15.8^\circ$. The flight conditions are taken to be

$$P = 49.5 \text{ bhp at } 3,000\text{-ft altitude and } 2,000 \text{ rpm}$$

$$V = 63 \text{ fps}$$

From equation (12) the activity factor for the particular propeller is

$$A.F. = 2(6,250) \int_{0.2}^{1.0} \left(\frac{r}{R}\right)^3 \left(\frac{b}{D}\right) d\left(\frac{r}{R}\right) \approx 217$$

From figure 35, $X = 0.25$, and, from equation (14),

$$C_P = \frac{\dfrac{49.5}{1,000}}{(2)(0.951)\left(\dfrac{2,000}{1,000}\right)^3 \left(\dfrac{6}{10}\right)^5} = 0.0418$$

so that

$$C_{PX} = \frac{0.0418}{0.25} = 0.167$$

and also

$$\left(C_P\right)^{1/3} = 0.347$$

From equation (15),

$$J = \frac{(60)(63)}{(2,000)(6)} = 0.315$$

so that

$$\frac{J}{\left(C_P\right)^{1/3}} = \frac{0.315}{0.347} = 0.908$$

Using these values, one finds, from figure 35, $\eta_p = 0.61$. Now T_{c_A} may be computed from equation (11) as

$$T_{c_A} = \frac{(49.5)(550)(0.002176)^{1/2}(0.61)}{\left[\dfrac{(2)(1,050)}{(180)(1.25)}\right]^{3/2}(6)^2} = 0.744$$

The increment in wing lift coefficient due to the slipstream is estimated from equation (19):

$$\Delta C_{L_W} = (0.57)(0.744)(1.25)\left(\frac{5.25}{4.98}\right)\left(\frac{36}{180}\right) = 0.112$$

so that

$$C_{L_1} = 1.25 + 0.11 = 1.36$$

Now, from equation (11),

$$T_{c_1} = \frac{(49.5)(550)(0.002176)^{1/2}(0.61)}{\left[\dfrac{(2)(1,050)}{(180)(1.36)}\right]^{3/2}(6)^2} = 0.855$$

so that, from equation (23),

$$\left(\Delta C_{L_p}\right)_2 = (0.855)\frac{(2)(6)^2}{(180)}\sin(15.8° - 3.8°) = 0.071$$

Now

$$C_{L_2} = 1.25 + 0.11 + 0.07 = 1.43$$

so that

$$T_{c_2} = \frac{(49.5)(550)(0.002176)^{1/2}(0.61)}{\left[\dfrac{(2)(1,050)}{(180)(1.43)}\right]^{3/2}(6)^2} = 0.925$$

and therefore

$$\left(\Delta C_{L_p}\right)_3 = (0.925)\frac{(2)(6)^2}{(180)}\sin 12° = 0.077$$

Now

$$\left(C_{L_w}\right)_p = 1.25 + 0.11 + 0.08 = 1.44$$

Because this value is so near to C_{L_2}, no further iterations for T_c are necessary.

In order to evaluate the quantity $\left[\left(\dfrac{dC_m}{dC_L}\right)_{wf}\right]_0$, in the absence of wind-tunnel data, the results of the power-off analysis presented earlier may be utilized in the following approximate manner:

At $C_{L_w} = 1.25$ there was obtained for $C_{m_{wf}}$

$$C_{m_{wf}} = \left[1.25 \cos (15.8^\circ - 3.8^\circ) + 0.175 \sin (15.8^\circ - 3.8^\circ)\right]\left(\frac{0.33}{4.98}\right) +$$

$$\left[0.175 \cos (15.8^\circ - 3.8^\circ) - 1.25 \sin (15.8^\circ - 3.8^\circ)\right]\left(\frac{2.85}{4.98}\right) -$$

$$0.008 + 0.036$$
$$= 0.061$$

At $C_{L_w} = 0$, where $C_{D_w} = 0.010$ and $\alpha_w = -1.2^\circ$,

$$C_{m_{wf}} = \left[0.010 \sin (-1.2^\circ - 3.8^\circ)\right]\left(\frac{0.33}{4.98}\right) + \left[0.010 \cos (-1.2^\circ - \right.$$

$$\left. 3.8^\circ)\right]\left(\frac{2.85}{4.98}\right) - 0.008 = -0.002$$

Therefore, approximately,

$$\left[\left(\frac{dC_m}{dC_L}\right)_{wf}\right]_0 = \frac{0.061 - (-0.002)}{1.25} = 0.050$$

Now the increment in wing moment coefficient may be evaluated from equation (20):

$$\Delta C_{m_w} = (-0.008)\frac{(5.25)^2}{(4.98)}\frac{(6.5)}{(180)}\frac{(8)}{\pi}(0.925) + (0.050)(0.112) = 0.002$$

In order to evaluate C_{m_p} and thus obtain the complete wing-fuselage power-on pitching-moment coefficient, the propeller normal-force coefficient C_{N_p} must first be found.

From figure 22, using $\beta = 28^\circ$ at 0.75R, it is found that

$$\left[\left(\frac{dC_N}{d\alpha_T}\right)_0\right]_{\text{Ham Std}} = 0.00201/\text{deg}$$

From figure 23, with the propeller side-force factor from equation (18) as

$$\text{S.F.F.} = 525(0.0555 + 0.0694) + 270(0.039) = 75.5$$

it is found that

$$\frac{\left(\dfrac{dC_N}{d\alpha_T}\right)_0}{\left[\left(\dfrac{dC_N}{d\alpha_T}\right)_0\right]_{\text{Ham std}}} = 0.935$$

or

$$\left(\frac{dC_N}{d\alpha_T}\right)_0 = (0.935)(0.00201) = 0.00187 \,^5$$

From figure 24, with $T_c = 0.925$,

$$\frac{\left(\dfrac{dC_N}{d\alpha_T}\right)_p}{\left(\dfrac{dC_N}{d\alpha_T}\right)_0} = 1.55$$

or

$$\left(\frac{dC_N}{d\alpha_T}\right)_p = (1.55)(0.00187) = 0.0029$$

Also, from figure 25, $1 + \dfrac{d\epsilon}{d\alpha_w} = 0.80$. Using equation (16), there is obtained

$$C_{N_p} = (0.0029)(0.80)(15.8) = 0.0367$$

---

[5]Compare this value with the value of 0.00165 used for the power-off (windmilling-propeller) analysis.

The moment contributed by the direct power effects may be evaluated from equation (10), using the values obtained above and certain of those listed in table I:

$$C_{m_p} = (0.925)\frac{(2)(6)^2}{(180)(4.98)}(-0.85)(1) + (0.0367)\frac{(28.3)}{(180)(4.98)}(6.21)(1) = -0.056$$

Thus, from equation (24),

$$\left(C_{m_{wf}}\right)_p = 0.061 - 0.056 + 0.002 = 0.007$$

The contribution of the tail to the equilibrium equation must now be evaluated by determining the power-on downwash angle and tail dynamic pressure. From figure 36, $A = 0.35$ and $B = 0.225$. Introducing these values into equation (21) gives

$$\epsilon_p = \left[0.35 + (0.225)(0.00187)\right](15.8) = 5.53°$$

From equation (22),

$$\eta_t = 1 + \frac{(8)(0.925)}{\pi} = 3.35$$

From equation (1), then,[6]

$$\left(C_{m_t}\right)_p = (-0.055)(15.8 - 6.2 - 5.5 - 3.8 + 0 + 0.60\delta_e)\left(\frac{20.0}{180}\right)\left(\frac{13.16}{4.98}\right)(3.35) +$$

$$(-0.055)(15.8 - 6.2 - 3.8 + 0.59\delta_e)\left(\frac{5.8}{180}\right)\left(\frac{13.16}{4.98}\right)(1.0)$$

$$= -0.043 - 0.035\delta_e$$

The elevator deflection required for trim may now be calculated using equation (25):

$$0 = 0.007 - 0.043 - 0.035\delta_e$$

or

$$\delta_e = -1.0°$$

which agrees very well with the flight-test value (ref. 1).

_____

[6]Considering only a portion of the horizontal tail equal in span to the propeller diameter to be immersed in the slipstream.

Low-wing airplane: For comparison with flight-test results (ref. 2) the analysis for the low-wing airplane will be made for $\alpha_W = 14.5^\circ$. The other flight conditions are taken to be

$$P = 178 \text{ bhp at } 3{,}000\text{-ft altitude and } 2{,}250 \text{ rpm}$$

$$V = 65.7 \text{ fps}$$

$$\left(C_{L_W}\right)_0 = 1.35$$

$$\left(C_{D_W}\right)_0 = 0.138$$

From equation (12) the activity factor for the particular propeller is

$$\text{A.F.} = 2(6{,}250) \int_{0.2}^{1.0} \left(\frac{r}{R}\right)^3 \left(\frac{b}{D}\right) d\left(\frac{r}{R}\right) \approx 205$$

From figure 35, $X = 0.25$, and, from equation (14),

$$C_P = \frac{\dfrac{178}{1{,}000}}{(2)(0.951)\left(\dfrac{2{,}250}{1{,}000}\right)^3 \left(\dfrac{7.5}{10}\right)^5} = 0.0346$$

so that

$$C_{PX} = \frac{0.0346}{0.25} = 0.1384$$

and also

$$\left(C_P\right)^{1/3} \doteq 0.326$$

From equation (15),

$$J = \frac{(60)(65.7)}{(2{,}250)(7.5)} = 0.234$$

so that

$$\frac{J}{\left(C_P\right)^{1/3}} = \frac{0.234}{0.326} = 0.718$$

Using these values, one finds, from figure 35, $\eta_p = 0.520$. Now T_{c_A} may be computed from equation (11) as

$$T_{c_A} = \frac{(178)(550)(0.002176)^{1/2}(0.52)}{\left[\dfrac{(2)(2,700)}{(290)(1.35)}\right]^{3/2}(7.5)^2} = 0.823$$

The increment in wing lift coefficient due to the slipstream is estimated from equation (19):

$$\Delta C_{L_w} = (0.57)(0.823)(1.35)\left(\frac{7.5}{7.5}\right)\frac{(7.5)^2}{(290)} = 0.123 \quad .$$

so that

$$C_{L_1} = 1.35 + 0.12 = 1.47$$

Now, from equation (11),

$$T_c = \frac{(178)(550)(0.002176)^{1/2}(0.52)}{\left[\dfrac{(2)(2,700)}{(290)(1.47)}\right]^{3/2}(7.5)^2} = 0.945$$

so that, from equation (23),

$$\left(\Delta C_{L_p}\right)_2 = (0.945)\frac{(2)(7.5)^2}{(290)}\sin(14.5° - 2.0° - 5.0°) = 0.0478$$

Now

$$C_{L_2} = 1.35 + 0.12 + 0.05 = 1.52$$

so that

$$T_{c_2} = \frac{(178)(550)(0.002176)^{1/2}(0.52)}{\left[\dfrac{(2)(2,700)}{(290)(1.52)}\right]^{3/2}(7.5)^2} = 0.997$$

and therefore

$$\left(\Delta C_{L_p}\right)_3 \ (0.997)\frac{(2)(7.5)^2}{(290)} \sin 7.5° = 0.0505$$

Now

$$\left(C_{L_w}\right)_p = 1.35 + 0.12 + 0.05 = 1.52$$

In order to evaluate the quantity $\left[\left(\dfrac{dC_m}{dC_L}\right)_{wf}\right]_0$, an approximate procedure based on the power-off analysis will again be used.

At $C_{L_w} = 1.35$

$$C_{m_{wf}} = \left[1.35 \cos (14.5° - 2.0°) + 0.138 \sin (14.5° - 2.0°)\right]\left(\frac{0.167}{7.5}\right) +$$

$$\left[0.138 \cos (14.5° - 2.0°) - 1.35 \sin (14.5° - 2.0°)\right]\left(\frac{-0.031}{7.5}\right) -$$

$$0.031 + 0.030$$

$$= 0.029$$

At $C_{L_w} = 0$, where $C_{D_w} = 0.015$ and $\alpha_w = -4.2°$,

$$C_{m_{wf}} = (0.015)\left(\frac{0.167}{7.5}\right) \sin (-4.2° - 2.0°) +$$

$$(0.015)\left(\frac{-0.031}{7.5}\right) \cos (-4.2° - 2.0°) - 0.031$$

$$= -0.031$$

Therefore, approximately,

$$\left[\left(\frac{dC_m}{dC_L}\right)_{wf}\right]_0 = \frac{0.029 - (-0.031)}{1.35} = 0.044$$

Now the increment in wing moment coefficient may be evaluated from equation (20):

$$\Delta C_{m_W} = (-0.031)\frac{(7.5)^2}{(7.5)}\frac{(8.5)}{(290)}\left(\frac{8}{\pi}\right)(0.997) + (0.044)(0.123) = -0.012$$

In order to evaluate C_{m_p} and thus obtain the complete wing-fuselage power-on pitching-moment coefficient, the propeller normal-force coefficient C_{N_p} must first be found.

From figure 22, using $\beta = 30°$ at 0.75R, it is found that

$$\left[\left(\frac{dC_N}{d\alpha_T}\right)_0\right]_{Ham\ Std} = 0.00218/deg$$

From figure 23, with the propeller side-force factor from equation (18) as

$$S.F.F. = 525(0.1112) + 270(0.0445) = 70.5$$

$$\frac{\left(\dfrac{dC_N}{d\alpha_T}\right)_0}{\left[\left(\dfrac{dC_N}{d\alpha_T}\right)_0\right]_{Ham\ Std}} = 0.875$$

or

$$\left(\frac{dC_N}{d\alpha_T}\right)_0 = (0.875)(0.00218) = 0.00191\ [7]$$

From figure 24, with $T_c = 0.997$,

$$\frac{\left(\dfrac{dC_N}{d\alpha_T}\right)_p}{\left(\dfrac{dC_N}{d\alpha_T}\right)_0} = 1.58$$

---

[7]Again compare value with the value of 0.00165 used for the power-off analysis.

or

$$\left(\frac{dC_N}{d\alpha_T}\right)_p = (1.58)(0.00191) = 0.00302$$

Also, from figure 25, $1 + \frac{d\epsilon}{d\alpha_w} = 0.85$. Using equation (16), there is obtained

$$C_{N_p} = (0.00302)(0.85)(14.5) = 0.0372$$

The moment contribution of the direct power effects may be evaluated from equation (10), using the values obtained above and certain of those listed in table II:

$$C_{m_p} = (0.997)\frac{(2)(7.5)^2}{(290)(7.5)}\left[-0.25 - \left(\frac{5}{57.3}\right)(8.33)\right] +$$

$$(0.0372)\frac{(44.3)}{(290)(7.5)}\left[8.33 + \left(\frac{5}{57.3}\right)(-0.25)\right]$$

$$= -0.044$$

Thus, from equation (24),

$$\left(C_{m_{wf}}\right)_p = 0.029 - 0.044 - 0.012 = -0.027$$

The contribution of the tail to the equilibrium equation must now be evaluated by determining the power-on downwash angle and tail dynamic pressure as outlined previously.[8] From figure 36, $A = 0.36$ and $B = 0.22$. Introducing these values into equation (21) gives

$$\epsilon_p = \left[0.36 + (0.22)(0.00191)\right](14.5) = 5.2°$$

From equation (22),

$$\eta_t = 1 + \frac{(8)(0.997)}{\pi} = 3.54$$

In order to calculate the contribution of the tail to the moment-coefficient equation, the power-off downwash angle for the conditions

---

[8]Again, these values apply only to that portion of the horizontal tail immersed in the slipstream, which has been taken as equal to the propeller diameter in these computations. Note that, for this airplane, much of the elevator area lies outside of the slipstream.

of this example is needed. By methods used earlier, it is found that $\epsilon = 7.4^\circ$. Thus

$$\left(C_{m_t}\right)_p = (-0.071)(14.5 - 7.4 - 5.2 - 2.0 - 0.5 + 0.43\delta_e)\left(\frac{18.0}{290}\right)\left(\frac{16.8}{7.5}\right)(3.54) +$$

$$(-0.071)(14.5 - 7.4 - 2.0 - 0.5 + 0.62\delta_e)\left(\frac{35.5}{290}\right)\left(\frac{16.8}{7.5}\right)(1.0)$$

$$= -0.0688 - 0.0271\delta_e$$

The elevator deflection required for trim may now be calculated from equation (25):

$$0 = -0.027 - 0.0688 - 0.0271\delta_e$$

or

$$\delta_e = -3.5^\circ$$

which compares well with the flight-test value (ref. 2) of -1.0°.

RESULTS AND DISCUSSION

It has long been known that the elevator deflections required to trim in power-off flight at low speeds are usually greater than those required for power-on flight and that those required for landing are even greater. The flight tests of references 1 and 2 provided some quantitative information on the elevator deflections required, under varying conditions, for several light aircraft.

If the objective is to design an aircraft which has adequate lateral control in low-speed flight, and the method of achieving this objective is to maintain the elevator deflection within the greatest value that will still result in satisfactory lateral control characteristics, then the requirement for at least a nearly constant elevator setting for longitudinal trim, under all conditions of power setting and center-of-gravity location, becomes a most stringent one. The designer may, however, be able to meet this requirement by altering certain design parameters. The actual realization of this objective has been achieved in flight tests with a particular airplane (ref. 2).

To provide some quantitative information concerning the effects of changes in some of the more important design variables, the results of

a number of computations for elevator trim angle for various conditions
are shown in tables III to VI. The airplanes used for these studies are
the same two that were used earlier as examples of the analytical proce-
dures. All computations have been performed in a fashion similar to
that of the detailed examples presented earlier.

Variation of design parameters independently for power-on conditions.-
Each airplane is first ·subjected to a basic analysis. The effects of
windmilling propeller and ground proximity are accounted for, and then
some of the more important design parameters, such as center-of-gravity
location, horizontal tail location, elevator area, and tail length, are
varied. The effect of altering the wing from high-wing to midwing and
low-wing positions is also shown. It should be pointed out that the
changes in the design parameters used to obtain the results shown are
often exaggerated so as to bring out clearly the resulting change in the
elevator deflection required to trim. For the power-on studies the
important parameters are center-of-gravity location and orientation of
the thrust axis. Some results are given for the low-wing airplane with
flaps deflected.

In cases where flight-test results were available, they have been
compared with the calculated elevator deflections; these comparisons are
shown in table III and figure 37. It has been stated previously that a
correlation between measured and calculated values of $\pm 4^\circ$ would be con-
sidered acceptable, and it may be seen from figure 37 that the results
are in very good agreement.

In table IV there are presented the results of many computations
which are intended to show the quantitative effects of changes in various
design parameters as discussed above. Results are given for both power-
on and power-off conditions for the two airplanes under consideration.
This type of quantitative information may be of some use to designers
when considering the effects of design changes in their particular con-
figuration in attempting to provide for a minimum difference in trim
between power-off and power-on condition.

Looking first at the power-off results, one sees at once that the
most effective factors which may be employed to reduce the elevator
deflection required to trim are those which relate the location of the
tail to the wing wake. Additionally, the tail incidence angle is an
important factor as is the longitudinal location of the center of gravity.
From these results alone it would appear that the midwing configuration
is more favorable in this regard than is either the low- or high-wing
configuration (this point will be discussed in more detail in a later
paragraph).

For the power-on results the most important parameters are tail
incidence angle, longitudinal center-of-gravity position, and thrust-
line orientation.

Effects on trim of applying power with changes in various design
parameters.- In table V there is presented a comparison of calculated
and measured effects of power on the elevator deflection required to
trim. Unfortunately, only a few comparisons are possible because of the
scarcity of data; nevertheless, one sees immediately that the methods
of this report are adequate for predicting such results.

When such comparisons are made, several points should be kept in
mind. First, the measured values should be considered to be accurate
only to within about $\pm 1^{\circ}$. Since the values in the table refer to differ-
ences of measured values, it is very possible that the errors may be
cumulative so that here an accuracy of $\pm 2^{\circ}$ in the flight-test values is
about all that may be expected.

The results for the high-wing airplane are especially good if one
considers the fact that the one poor comparison for this airplane (rear-
ward center-of-gravity location) was also the case that exceeded, by a
small amount only, the limit of acceptable correlation for the power-off
analysis (table III and fig. 37). Also, some of the experimental data
for this particular case appear to be out of line with the data for the
other cases. Therefore, one need not be unduly concerned with the magni-
tude of the discrepancy observed in this instance.

The wing angle of attack for each case used in the comparison should
be carefully noted. The elevator deflection angles obtained from flight
tests (given in table III) correspond, in each case, to those obtained
at the "critical" angle of attack, that is, the maximum angle of attack
for satisfactory lateral control (refs. 1 and 2). For the high-wing air-
plane the flight-test values[9] obtained were $\alpha_W = 15.2^{\circ}$ with power on
and 15.8° with power off. For all corresponding calculations the value
$\alpha_W = 15.8^{\circ}$ was used. The discrepancy is slight, in this instance, and
should not have an excessive effect on the comparison between calculated
and test results. However, for the low-wing airplane $\alpha_W = 14.5^{\circ}$ with
power on and 17.5° with power off with flaps up, and $\alpha_W = 17.0^{\circ}$ with
power on and 13.0° with power off with flaps down for the flight-test
values. Therefore, a direct evaluation of the effect on trim of power
is not available from flight tests with which the calculated values may
be compared; however, an attempt has been made to determine from the
available data the appropriate values, holding angle of attack constant.
The comparison shown for the low-wing airplane in table V is made on that
basis.

It would appear then that the effects of power may be accounted for
adequately for use in preliminary design.

---

[9]Average values over the span.

In order to assist the designer further in estimating the effects
of changes in various design parameters on the trim conditions, with
power off and power on, additional numerical studies are presented in
table VI. In this table calculated values of elevator deflection required
to trim are shown for propeller-off, propeller-windmilling, and power-on
conditions. The calculations have been carried out using a constant
angle of attack so as to obtain results which show only the effects on
trim of applying power. For the high-wing airplane $\alpha_w = 15.8°$; for the
low-wing airplane $\alpha_w = 17.5°$. Thus, this table constitutes a rather
complete survey of the effects on trim of applying power.

The designer would normally wish to have the trim characteristics
of the airplane such that the difference in elevator deflection required
to trim with power off and power on is zero, or very nearly so. The
results of table VI provide much information concerning the possibility
of achieving the objective. It may be noted immediately that many of
the design parameters that seemed promising when considered for the
power-off or power-on condition alone are no longer so promising. The
elevator area does, however, seem to be important; but perhaps even more
important in this regard is the spanwise location of the elevator, that
is, the degree of immersion in the slipstream.[10] In particular, all
factors which have to do with the location of the tail with respect to
the slipstream and wing wake are of primary importance in achieving the
stated goal. The orientation of the thrust line remains an important
parameter, as would be expected.

One may question why the midwing configuration appears to be better
than either the high- or low-wing configuration for the results shown.
The answer lies in the location of the horizontal tail with respect to
the wing wake. In the two extreme conditions the tail lies at the wake
edges, while in the midwing case it happens to fall squarely within the
wake and thus the maximum benefit of the downwash is achieved. Thus, it
appears that the relative locations of the horizontal tail and wing should
be carefully considered in preliminary design. The dynamic pressure at
the tail, which also influences the tail effectiveness, depends greatly
on the relative locations of the wing and tail (fig. 21).

In a further attempt to study these results, one might try to com-
pare the results for the high-wing and low-wing airplanes as shown in
table VI. Such a comparison is not useful in this case because the
parameter employed is a difference in elevator deflection; quite clearly,
this must depend on the particular configuration of the elevator, espe-
cially as regards area, spanwise location, elevator aspect ratio, and so
forth. The low-wing airplane used in these examples (fig. 33) has a

---

[10]Flight investigations dealing with this point are reported in
references 2 and 12.

rather narrow chord elevator placed, for the most part, outboard on the horizontal stabilizer so that large deflections are required, relative to the wide inboard elevators of the high-wing airplane (fig. 32).

General remarks and design recommendations.- The results of an interesting flight investigation of the effects of various design modifications on the qualitative flight characteristics of a light airplane are presented in reference 12. One of the most significant of the modifications employed was that of a limitation of the up-elevator deflection; the deflection could not be limited to such an extent that the airplane was made stallproof because of the elevator deflection required for landing with a tail-wheel-type landing gear; however, the airplane was made spinproof. The other modifications included changes in wing incidence angle, wing washout, area and aspect ratio of the tail, tilt of the thrust axis, and location of the elevators with respect to the slipstream. The general performance characteristics of the airplane were only very slightly impaired by the modifications employed.

If such modifications could be incorporated in the preliminary design stage, there is no reason to doubt that any adverse effects on performance could be eliminated almost entirely and, even more important, that longitudinal trim characteristics could be obtained such that a single limitation of up-elevator deflection would provide adequate low-speed lateral control under all conditions.

Although the effect of power on the elevator angle required for balance can be essentially eliminated by choosing certain combinations of design parameters, the conditions will apply strictly to only one center-of-gravity location. Since the rearmost center-of-gravity location is critical in that it requires the lowest maximum up-elevator deflection, the minimum speed will be somewhat higher for the most forward center-of-gravity location. In addition, a three-point landing requires a greater up-elevator deflection with the forward center-of-gravity location. In designs for certain purposes, such as personal transportation, it is often possible to minimize these conditions to the point where they are unimportant by (1) using a tricycle landing gear which eliminates the necessity for a three-point landing and (2) arranging for a small range of center-of-gravity positions by keeping all variable loads near the center of gravity. If it is necessary that the variable load have a large fore-and-aft distribution and a large center-of-gravity travel cannot be avoided, it is possible to use automatic means to give different maximum elevator deflections for different loads. The condition can be minimized also by use of a large horizontal tail surface.

It is very difficult to prescribe well-defined design procedures which will result in the longitudinal trim characteristics desired. However, it is apparent, in view of the preceding discussion and the numerical results shown in the tables, that the desired trim characteristic

of minimum power effect may be approached by a process of rational modi-
fication of the original design. In particular, a relatively small ele-
vator located essentially outside of the slipstream will help greatly in
achieving this goal, as will careful location of the horizontal tail
with respect to the wing wake in the power-off condition at the most
desirable incidence angle. Orientation of the thrust axis is also a
powerful aid in this regard.

It may be well to point out here that a tab provides a better way
of maintaining the critical angle of attack with a single elevator
setting than does an adjustable stabilizer. This is so because a tab
mainly influences the control force and not the tail lift coefficient.
For example, the Ag-1 airplane, which is treated as a numerical example
in this report and for which flight-test data were presented in refer-
ence 2, could be modified to have the stabilizer move with the flaps to
keep the relationship between the critical angle of attack and elevator
deflection the same; then speed trim could be made by use of the tab.

Some quantitative flight-test data regarding the effect of hori-
zontal tail configuration are given in reference 2. More specifically,
it is shown there that for a particular tricycle-gear airplane it was
possible to achieve a condition whereby the elevator deflection was
maintained within the greatest value that would still result in satis-
factory lateral control characteristics under varying flight conditions.
This was achieved most easily by providing elevators of relatively small
area located for the most part outside of the slipstream. Essentially
equivalent characteristics were achieved by using an elevator of some-
what larger area and much larger span but by restricting the maximum
deflection angle to a lower value than in the previous case.

It is believed that the methods of analysis presented and discussed
in this report will assist the designer in estimating quantitatively the
effects of changes in the various design parameters in his attempt to
provide for adequate control under all conditions.

CONCLUDING REMARKS

Many design parameters influence longitudinal trim characteristics.
By a process of rational design modification, using the simplified ana-
lytical methods presented in this report to predict the effects of
changes in the design parameters, the designer may approach the desired
condition of little or no change in elevator trim position upon appli-
cation of power. This procedure should result in a design in which for
one center-of-gravity position the maximum up-elevator deflection may

be maintained within the greatest value that will still result in satis-
factory lateral control characteristics under all flight conditions,
while, at the same time, adequate longitudinal control is available.

Texas Engineering Experiment Station,
     Texas Agricultural and Mechanical College System,
          College Station, Texas, May 20, 1955.

APPENDIX

SYMBOLS

A	aspect ratio
a	lift-curve slope
a_0	section lift-curve slope
b	span, ft; propeller width at r, ft
C_D	drag coefficient
C_L	lift coefficient
C_{L_f}	increase of lift coefficient, at particular angle of attack, upon deflecting flap
C_{L_w}	lift coefficient, at same angle of attack, flaps retracted
C_m	pitching-moment coefficient
$C_{m_{fu}}$	fuselage pitching-moment coefficient about fuselage aerodynamic center
C_{N_p}	propeller normal-force coefficient
$\dfrac{dC_N}{d\alpha_T}$	rate of change of propeller normal-force coefficient with angle of attack of thrust line
C_P	power coefficient
c	chord, ft
$\bar{c}$	mean aerodynamic chord, ft
c_{d_0}	section profile-drag coefficient
c_l	section lift coefficient
c_m	section pitching-moment coefficient

$\left(c_{m_{ac}}\right)_i$ average section pitching-moment coefficient about wing aerodynamic center for portion of wing immersed in slipstream

D propeller diameter, ft

d_g height of tail quarter-chord point above ground, ft

d_T vertical distance from elevator hinge line to thrust line, positive down, ft

h vertical displacement of wake center line, ft

h_o distance below wing trailing edge of wake origin, ft

h_p vertical distance from longitudinal component of thrust-line center of gravity, positive up, ft

i incidence angle with respect to airplane reference line, positive up, deg

J advance ratio

K ground-effect factor

K_{fu} fuselage moment factor

k factor for determining wake origin

L lift, lb; also length, ft

L_{fu} overall fuselage length, ft

l_p longitudinal distance from propeller disk to center of gravity, positive rearward, ft

l_t longitudinal distance from center of gravity to tail aerodynamic center, positive rearward, ft

M pitching moment, ft-lb

m vertical distance (with respect to airplane reference line) from wing trailing edge to elevator hinge axis, positive up, ft

N propeller rotational speed, rpm

N_p propeller normal force, lb

n number of propellers

$\bar{n}$ number of blades

P   power, bhp

q dynamic pressure, lb/sq ft, $\frac{1}{2}\rho V^2$

R   propeller radius, ft

r   radius to propeller blade element, ft

S   surface area, sq ft

S_p propeller disk area, sq ft

T   propeller thrust force, lb

T_c propeller thrust-force coefficient

T_{c_A} thrust coefficient corresponding to power-off lift coefficient

V   velocity, fps

W   airplane gross weight, lb

w_{fu} maximum width of fuselage, ft

X   power coefficient adjustment factor

x   longitudinal distance from wing quarter-chord point to elevator hinge axis, positive rearward, ft

x_{ac} longitudinal distance from center of gravity to wing aerodynamic center, positive forward, ft

z   vertical distance from wake origin to ground, ft

z_{ac} vertical distance from center of gravity to wing aerodynamic center, positive up, ft

α angle of attack, deg

α_a absolute angle of attack (measured from zero lift), deg

α_T angle of attack of thrust line, deg

α_{ZL} angle of attack for zero lift, deg

β propeller blade angle, deg

δ control-surface deflection, positive down, deg

ϵ average downwash angle, deg

η_p propeller efficiency

η_t tail efficiency factor, q_t/q

λ taper ratio

ρ density, slug/cu ft

σ density ratio

τ elevator effectiveness factor

ϕ tilt of thrust line, positive down, deg

Subscripts:

ac   aerodynamic center

e   elevator

f   flap

fu   fuselage

g   ground

i   immersed in slipstream

max   maximum

O   power off

p   propeller

T   thrust line

t   horizontal tail

w   wing

wf   wing-fuselage combination

REFERENCES

1. Weick, Fred E., Sevelson, Maurice S., McClure, James G., and Flanagan, Marion D.: Investigation of Lateral Control Near the Stall - Flight Investigation With a Light High-Wing Monoplane Tested With Various Amounts of Washout and Various Lengths of Leading-Edge Slot. NACA TN 2948, 1953.

2. Weick, Fred E., and Abramson, H. Norman: Investigation of Lateral Control Near the Stall - Flight Tests With High-Wing and Low-Wing Monoplanes of Various Configurations. NACA TN 3676, 1956.

3. Goranson, R. Fabian: A Method for Predicting the Elevator Deflection Required to Land. NACA WR L-95, 1944. (Supersedes NACA ARR L4I16.)

4. Gilruth, R. R., and White, M. D.: Analysis and Prediction of Longitudinal Stability of Airplanes. NACA Rep. 711, 1941.

5. Silverstein, Abe, and Katzoff, S.: Design Charts for Predicting Downwash Angles and Wake Characteristics Behind Plain and Flapped Wings. NACA Rep. 648, 1939.

6. Perkins, Courtland D., and Hage, Robert E.: Airplane Performance Stability and Control. John Wiley & Sons, Inc., c. 1949.

7. Wallace, Rudolf: Investigation of Full-Scale Split Trailing-Edge Wing Flaps With Various Chords and Hinge Locations. NACA Rep. 539, 1935.

8. Ribner, Herbert S.: Formulas for Propellers in Yaw and Charts of the Side-Force Derivative. NACA Rep. 819, 1945.

9. Weil, Joseph, and Sleeman, William C., Jr.: Prediction of the Effects of Propeller Operation on the Static Longitudinal Stability of Single-Engine Tractor Monoplanes With Flaps Retracted. NACA Rep. 941, 1949. (Supersedes NACA TN 1722.)

10. Ribner, Herbert S.: Notes on the Propeller and Slipstream in Relation to Stability. NACA WR L-25, 1944. (Supersedes NACA ARR L4I12a.)

11. Goett, Harry J., and Delaney, Noel K.: Effect of Tilt of the Propeller Axis on the Longitudinal-Stability Characteristics of Single-Engine Airplanes. NACA Rep. 774, 1944.

12. Hunter, P. A., and Vensel, J. R.: A Flight Investigation to Increase the Safety of a Light Airplane. NACA TN 1203, 1947.

TABLE I.- GEOMETRIC AND AERODYNAMIC DATA FOR HIGH-WING AIRPLANE[a]

Geometric Data

$i_W = 3.8°$ $b_W = 36$ ft

$i_t = 0°$ $b_t = 10$ ft

$\bar{c}_W = 4.98$ ft $w_{fu} = 3.5$ ft

$S_W = 180$ sq ft $L_{fu} = 21.77$ ft

$S_t = 25.8$ sq ft $D = 6$ ft

$S_e = 10.8$ sq ft $S_p = 28.3$ sq ft

$A_W = 7.2$ $R = 3$ ft

$A_t = 3.88$ $\lambda = 1$

                                      $\phi = 0°$

Center-of-Gravity

$W = 1,050$ lb $l_p = 6.21$ ft

Longitudinal c.g. = 30.4% M.A.C. $z_{ac} = 2.85$ ft

$x = 14.33$ ft $m = -0.83$ ft

$x_{ac} = 0.33$ ft $h_p = -0.85$ ft

$l_t = 13.16$ ft $d_T = 0.58$ ft

Aerodynamic Data

Wing section = NACA 23012

$\left(a_W\right)_{sec} = 0.100/$deg

$c_{m_{ac}} = -0.008$

$\alpha_{ZL} = -1.2°$

$C_{D_W} = 0.175$ at $\alpha_W = 15.8°$

---

[a]Values given here are from three sources: directly from design
data, estimated from design data, or actually measured.

TABLE II.- GEOMETRIC AND AERODYNAMIC DATA FOR LOW-WING AIRPLANE[a]

Geometric Data

$i_w = 2^\circ$ $b_w = 39.8$ ft

$i_t = -0.5^\circ$ flaps up (-6.9° flaps down) $b_t = 17.75$ ft

$\bar{c}_w = 7.5$ ft $w_{fu} = 3.33$ ft

$S_w = 290$ sq ft $L_{fu} = 27.2$ ft

$S_t = 53.5$ sq ft $D = 7.5$ ft

$S_e = 20.2$ sq ft $S_p = 44.3$ sq ft

$A_w = 5.5$ $R = 3.75$ ft

$A_t = 5.9$ $\lambda = 1$

                             $\phi = 5.0^\circ$

Center-of-Gravity Data

$W = 2,700$ lb $l_p = 8.33$ ft

Longitudinal c.g. = 25% M.A.C. $z_{ac} = 0.031$ ft

$x = 18.30$ ft $m = 2.50$ ft

$x_{ac} = 0.167$ ft $h_p = -0.250$ ft

$l_t = 16.8$ ft $d_T = -0.50$ ft

Aerodynamic Data

Wing section = NACA 64021 (modified)

$\left(a_w\right)_{sec} = 0.094$/deg

$c_{m_{ac}} = -0.031$

$\alpha_{ZL} = -4.2^\circ$ (-14.3° with flaps down 40°)

$C_{D_w} = 0.197$ at $\alpha_w = 17.5^\circ$

---

[a]Values given here are taken directly from design data or are estimated from design data.

TABLE III.- COMPARISON BETWEEN COMPUTED AND MEASURED ELEVATOR DEFLECTION REQUIRED TO TRIM

Airplane	Condition	α_W, deg	Elevator deflection required to trim, δ_e, deg		Power
			Calculated	Flight test (a)	
High-wing	Basic analysis	15.8	-4.5	------	Off
	Basic + Windmilling propeller	15.8	-3.6	-4.4	Off
	Basic + Ground effect + Windmilling propeller	15.8	-7.6	-10.1	Off
	Forward c.g. position (moved 3.1% M.A.C. forward)	15.8	-7.8	------	Off
	Forward c.g. + Windmilling propeller	15.8	-6.9	-9.5	Off
	Forward c.g. + Ground effect + Windmilling propeller	15.8	-10.4	-14.1	Off
	Rearward c.g. position (moved 1.9% M.A.C. rearward)	15.8	-1.2	------	Off
	Rearward c.g. + Windmilling propeller	15.8	-.3	-2.7	Off
	Rearward c.g. + Ground effect + Windmilling propeller	15.8	-4.7	-9.5	Off
Low-wing	Basic analysis	17.5	-9.2	------	Off
	Basic + Windmilling propeller	17.5	-8.1	-10.5	Off
	Basic + Ground effect + Windmilling propeller	11.0	-7.7	-6.5	Off
	Basic + Flaps down 40°	13.0	-6.8	------	Off
	Basic + Flaps down 40° + Windmilling propeller	13.0	-5.4	-1.0	Off
	Basic + Flaps down 40° + Ground effect + Windmilling propeller	11.0	-14.5	-13.0	Off
High-wing	Basic analysis	15.8	-1.0	-.3	On
	Forward c.g. position (moved 3.1% M.A.C. forward)	15.8	-2.1	-3.8	On
	Rearward c.g. position (moved 1.9% M.A.C. rearward)	15.8	-.2	+1.9	On
Low-wing	Basic analysis	14.5	-3.5	+1.0	On
	Basic + Flaps down 40°	17.0	4.0	+3.5	On

^aHigh-wing airplane, ref. 1; low-wing airplane, ref. 2.

TABLE IV.- EFFECT OF CHANGES IN DESIGN PARAMETERS ON ELEVATOR DEFLECTION REQUIRED TO TRIM

Airplane	Condition	α_w, deg	Power	δ_e, deg (a)
High-wing	Basic analysis	15.8	Off	-4.5
	Basic + Windmilling propeller	15.8	Off	-3.6
	Basic + Ground effect	15.8	Off	-8.4
	Basic + 50% tail-length increase	15.8	Off	-7.2
	Basic + 3° change (negative) in tail incidence angle	15.8	Off	-9.5
	Basic + 50% elevator-area increase[b]	15.8	Off	-3.7
	Basic + High horizontal tail position (raised 3 ft)	15.8	Off	-5.5
	Forward c.g. position (moved 5% M.A.C. forward)	15.8	Off	-9.8
	Rearward c.g. position (moved 5% M.A.C. rearward)	15.8	Off	+1.0
	High c.g. position (moved up 5% M.A.C.)	15.8	Off	-4.0
	Low c.g. position (moved down 5% M.A.C.)	15.8	Off	-4.8
	Midwing configuration	15.8	Off	-2.1
	Low-wing configuration	15.8	Off	-6.1
Low-wing	Basic analysis	17.5	Off	-9.2
	Basic + Windmilling propeller	17.5	Off	-8.1
	Basic + 50% tail-length increase	17.5	Off	-11.4
	Basic + 3° change (negative) in tail incidence angle	17.5	Off	-14.5
	Basic + 50% elevator-area increase[b]	17.5	Off	-7.4
	Basic + High horizontal tail position (raised 3 ft)	17.5	Off	-11.8
	Forward c.g. position (moved 5% M.A.C. forward)	17.5	Off	-14.2
	Rearward c.g. position (moved 5% M.A.C. rearward)	17.5	Off	-3.9
	High c.g. position (moved up 5% M.A.C.)	17.5	Off	-8.4
	Low c.g. position (moved down 5% M.A.C.)	17.5	Off	-10.0
	Basic + Flaps down 40°	13.0	Off	-3.1

[a]Power-on computations were made using method of ref. 10 for estimating downwash angle due to power and η_t due to power.

[b]Total horizontal tail area held constant.

TABLE IV.- EFFECT OF CHANGES IN DESIGN PARAMETERS ON ELEVATOR DEFLECTION REQUIRED TO TRIM - Concluded

Airplane	Condition	α_w, deg	Power	δ_e, deg (a)
High-wing	Basic analysis	15.8	On	-1.0
	Basic + 50% tail-length increase	15.8	On	-2.5
	Basic + 3° change (negative) in tail incidence angle	15.8	On	-5.8
	Basic + 50% elevator-area increase[b]	15.8	On	-.9
	Basic + High horizontal tail position (raised 3 ft)	15.8	On	-2.1
	Forward c.g. position (moved 5% M.A.C. forward)	15.8	On	-2.9
	Rearward c.g. position (moved 5% M.A.C. rearward)	15.8	On	+1.1
	High c.g. position (moved up 5% M.A.C.)	15.8	On	-.6
	Low c.g. position (moved down 5% M.A.C.)	15.8	On	-1.4
	Midwing configuration	15.8	On	-3.4
	Low-wing configuration	15.8	On	-2.7
Low-wing	Basic analysis	17.5	On	-4.5
		14.5	On	-3.5
	Basic + 50% tail-length increase	17.5	On	-6.4
	Basic + 3° change (negative) in tail incidence angle	17.5	On	-10.6
	Basic + 50% elevator-area increase[b]	17.5	On	-3.7
	Basic + High horizontal tail position (raised 3 ft)	17.5	On	-7.2
	High c.g. position (moved up 5% M.A.C.)	17.5	On	-4.1
	Low c.g. position (moved down 5% M.A.C.)	17.5	On	-4.9
	Forward c.g. position (moved 5% M.A.C. forward)	17.5	On	-7.3
		14.5	On	-6.1
	Rearward c.g. position (moved 5% M.A.C. rearward)	17.5	On	-1.6
		14.5	On	-.8
	Basic + High thrust line (moved up 10% M.A.C.)	14.5	On	-5.0
	Basic + Low thrust line (moved down 10% M.A.C.)	14.5	On	-2.1
	Basic + Additional 5° thrust-line tilt (down)	14.5	On	-4.9
	Basic + Flaps down 40°	17.0	On	+4.0

[a]Power-on computations were made using method of ref. 10 for estimating downwash angle due to power and η_t due to power.

[b]Total horizontal tail area held constant.

TABLE V.- COMPARISON BETWEEN CALCULATED AND MEASURED CHANGES IN ELEVATOR DEFLECTION

REQUIRED TO TRIM DUE TO APPLICATION OF POWER

Airplane	Condition	α_w, deg	Change in elevator deflection due to power, $\Delta\delta_e$,[a] deg	
			Calculated	Flight test
High-wing	Basic	15.8	-2.6	-4.1
	Forward c.g. position (moved 3.1% M.A.C.)	15.8	-4.8	-5.7
	Rearward c.g. position (moved 1.9% M.A.C.)	15.8	-.1	-4.6
Low-wing	Basic (flaps up)	17.5	-3.6	-4.5
	Basic (flaps down)	13.0	-5.4	-2.5

[a]$\Delta\delta_e = (\delta_e)_{\text{windmilling propeller}} - (\delta_e)_{\text{power on}}$.

TABLE VI.- EFFECT OF APPLICATION OF POWER ON ELEVATOR DEFLECTION REQUIRED TO TRIM

Airplane	Condition	α_w, deg	Elevator deflection required to trim, δ_e, deg			$\Delta\delta_e$,[a] deg
			Power off	Windmilling propeller	Power on	
High-wing	Basic	15.8	-4.5	-3.6	-1.0	-3.5
	Basic + 50% tail-length increase	15.8	-7.2	-6.1	-2.5	-4.7
	Basic + 3° change (negative) in tail incidence angle	15.8	-9.5	-8.7	-5.8	-3.7
	Basic + 50% elevator-area increase[b]	15.8	-3.7	-3.0	-.9	-2.8
	Basic + High horizontal tail position	15.8	-5.5	-3.6	-2.1	-3.4
	Forward c.g. position (moved 5% M.A.C. forward)	15.8	-9.8	-9.0	-2.9	-6.9
	Rearward c.g. position (moved 5% M.A.C. rearward)	15.8	+1.0	+1.9	+1.1	-.1
	High c.g. position (moved up 5% M.A.C.)	15.8	-4.0	-3.4	-.6	-3.6
	Low c.g. position (moved down 5% M.A.C.)	15.8	-4.8	-3.8	-1.4	-3.4
	Midwing configuration	15.8	-2.1	-1.3	-3.4	-1.3
	Low-wing configuration	15.8	-6.1	-5.2	-2.7	-3.4
Low-wing	Basic	17.5	-9.2	-8.1	-4.5	-4.7
	Basic + 50% tail-length increase	17.5	-11.4	-10.5	-6.4	-5.0
	Basic + 3° change (negative) in tail incidence angle	17.5	-14.5	-13.4	-10.6	-3.9
	Basic + 50% elevator-area increase[b]	17.5	-7.4	-6.6	-3.7	-3.7
	Basic + High horizontal tail position	17.5	-11.8	-10.7	-7.2	-4.6
	Forward c.g. position (moved 5% M.A.C. forward)	17.5	-14.2	-13.1	-7.3	-6.9
	Rearward c.g. position (moved 5% M.A.C. rearward)	17.5	-3.9	-2.8	-1.6	-2.3
	High c.g. position (moved up 5% M.A.C.)	17.5	-8.4	-7.3	-4.1	-4.3
	Low c.g. position (moved down 5% M.A.C.)	17.5	-10.0	-8.8	-4.9	-5.1
	Basic + Additional 5° thrust-line tilt (down)	17.5	-9.2	-9.2	-6.1	-3.1

[a]$\Delta\delta_e = (\delta_e)_{\text{power off}} - (\delta_e)_{\text{power on}}$.

[b]Total horizontal tail area held constant.
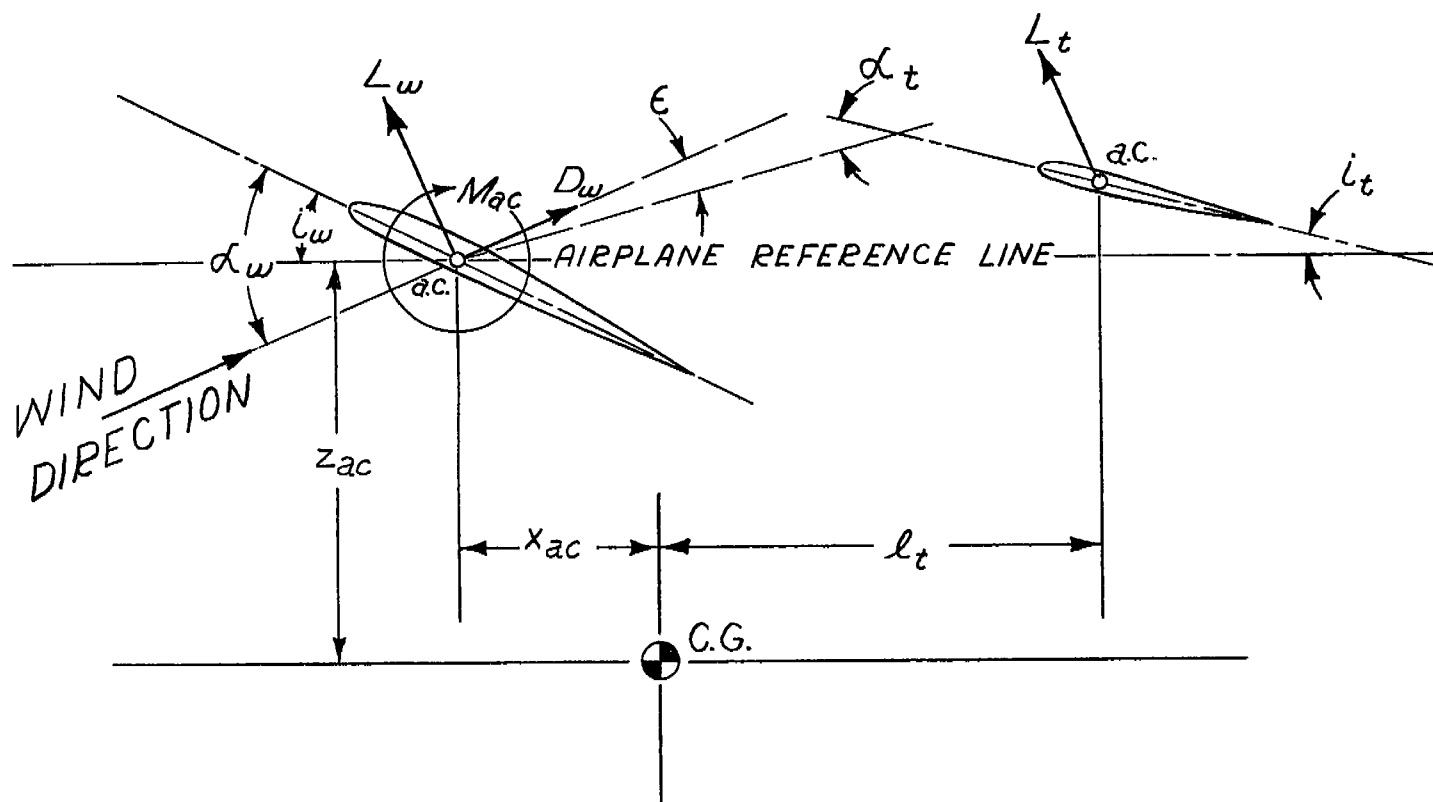
Figure 1.- Forces and moments in plane of symmetry.
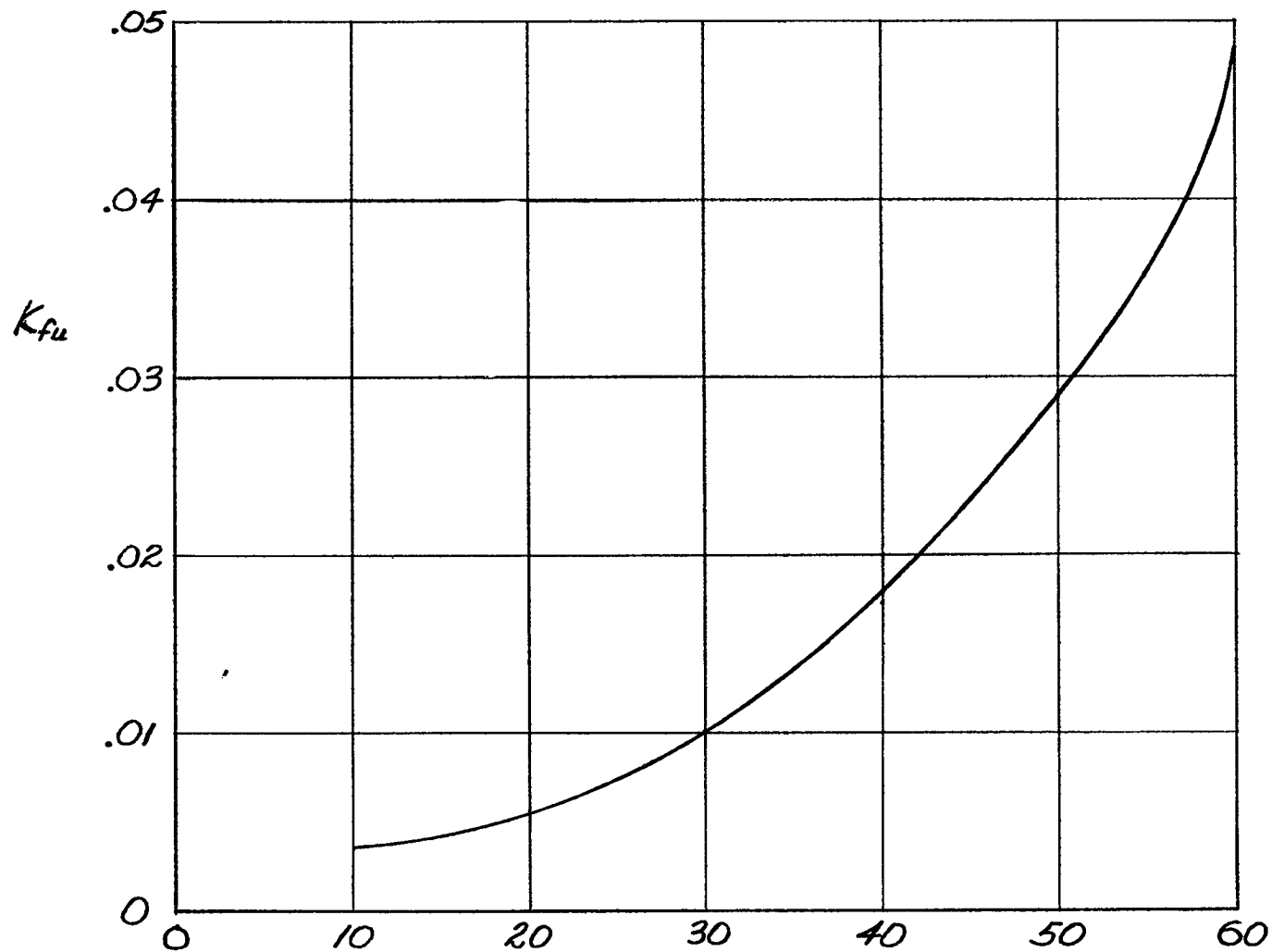
Position of 1/4 root chord in % body length.

Figure 2.- Fuselage moment factor (ref. 4).
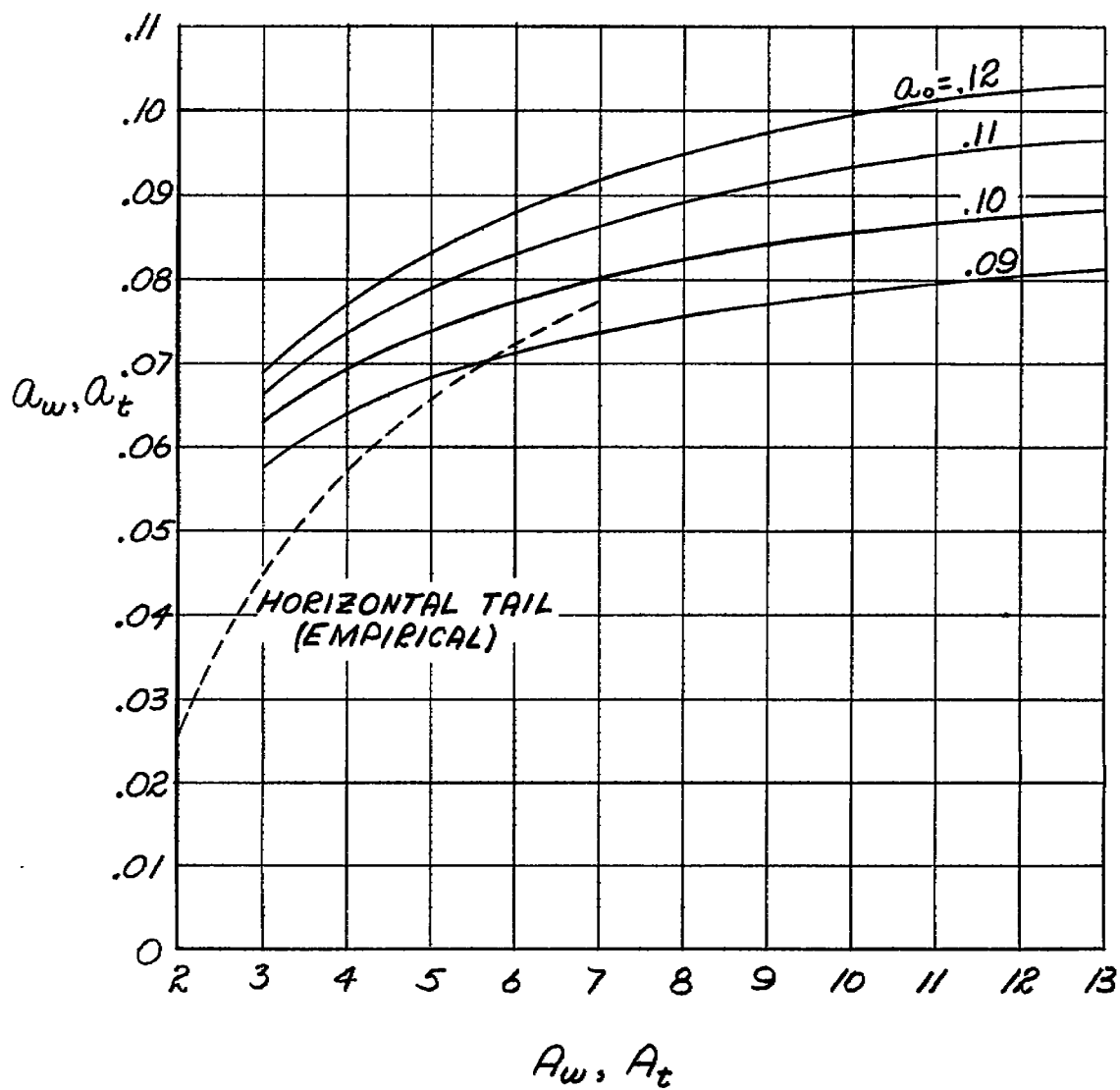
Figure 3.- Lift-curve slope versus aspect ratio (ref. 4).
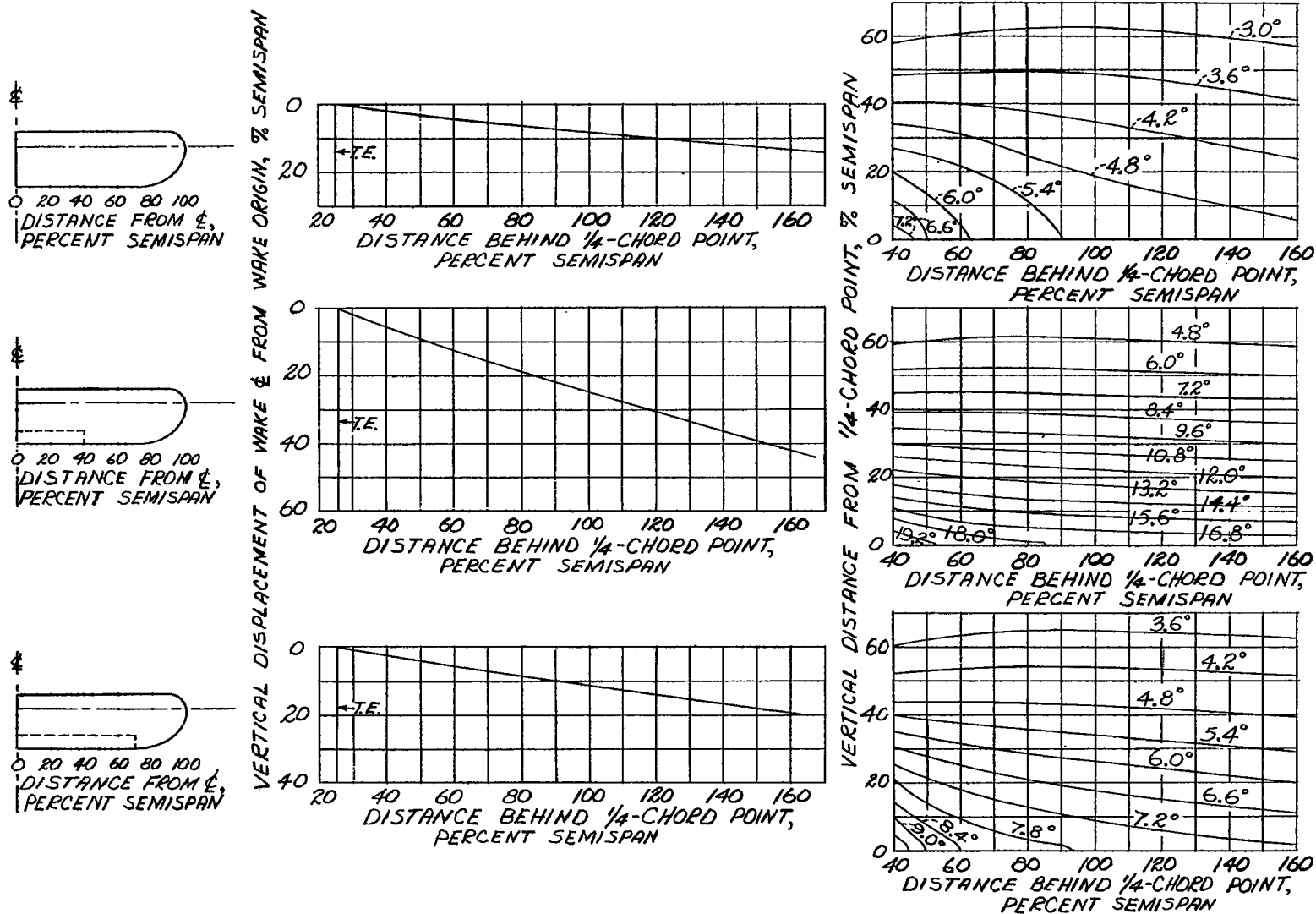
Figure 4.- Design chart for downwash displacement and angle (ref. 5).
$C_L = C_{L_f} = 1.0$; $\lambda = 1:1$; $A_W = 6$.
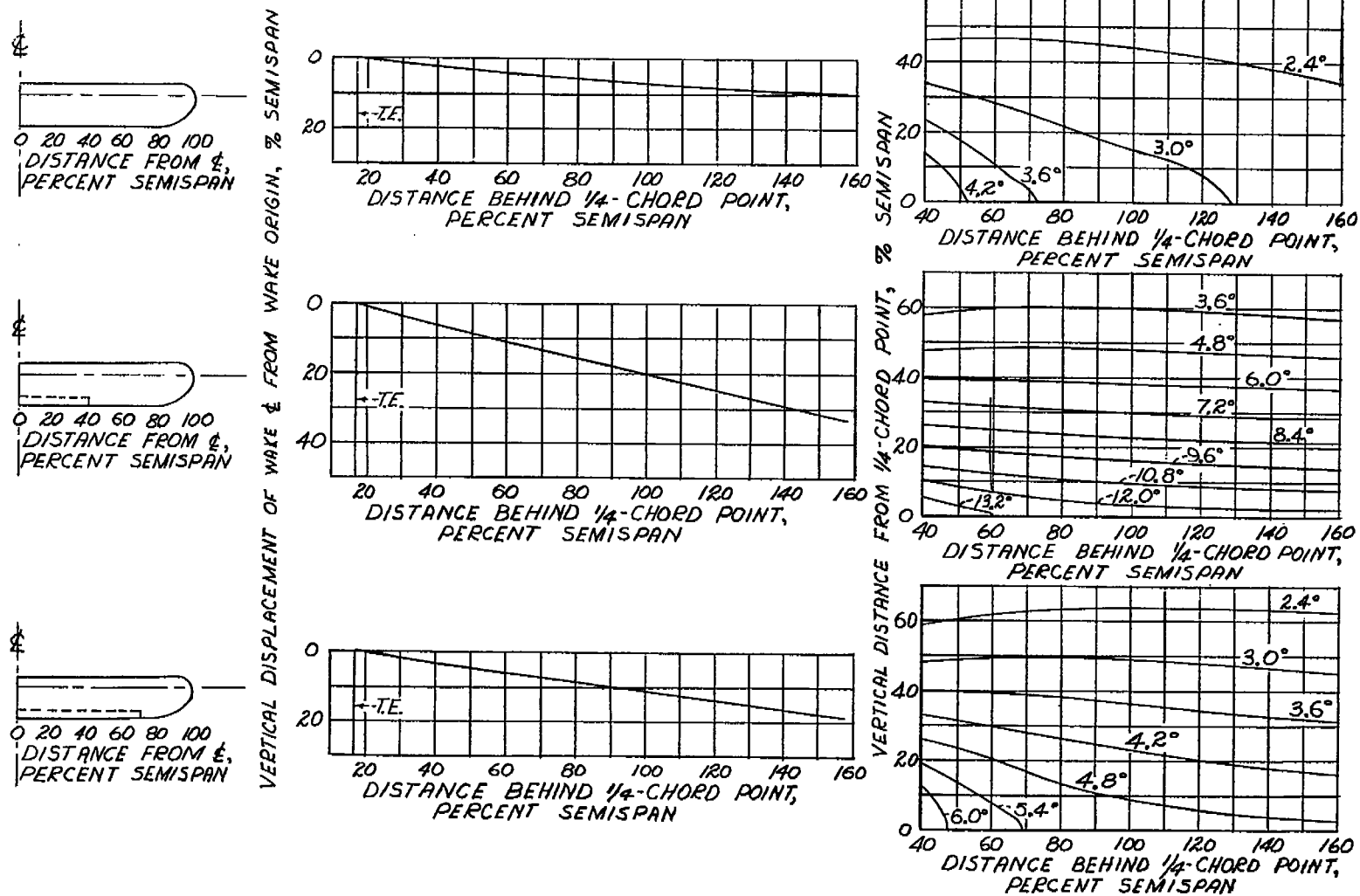
Figure 5.- Design chart for downwash displacement and angle (ref. 5).
$C_L = C_{L_f} = 1.0$; $\lambda = 1:1$; $A_w = 9$.
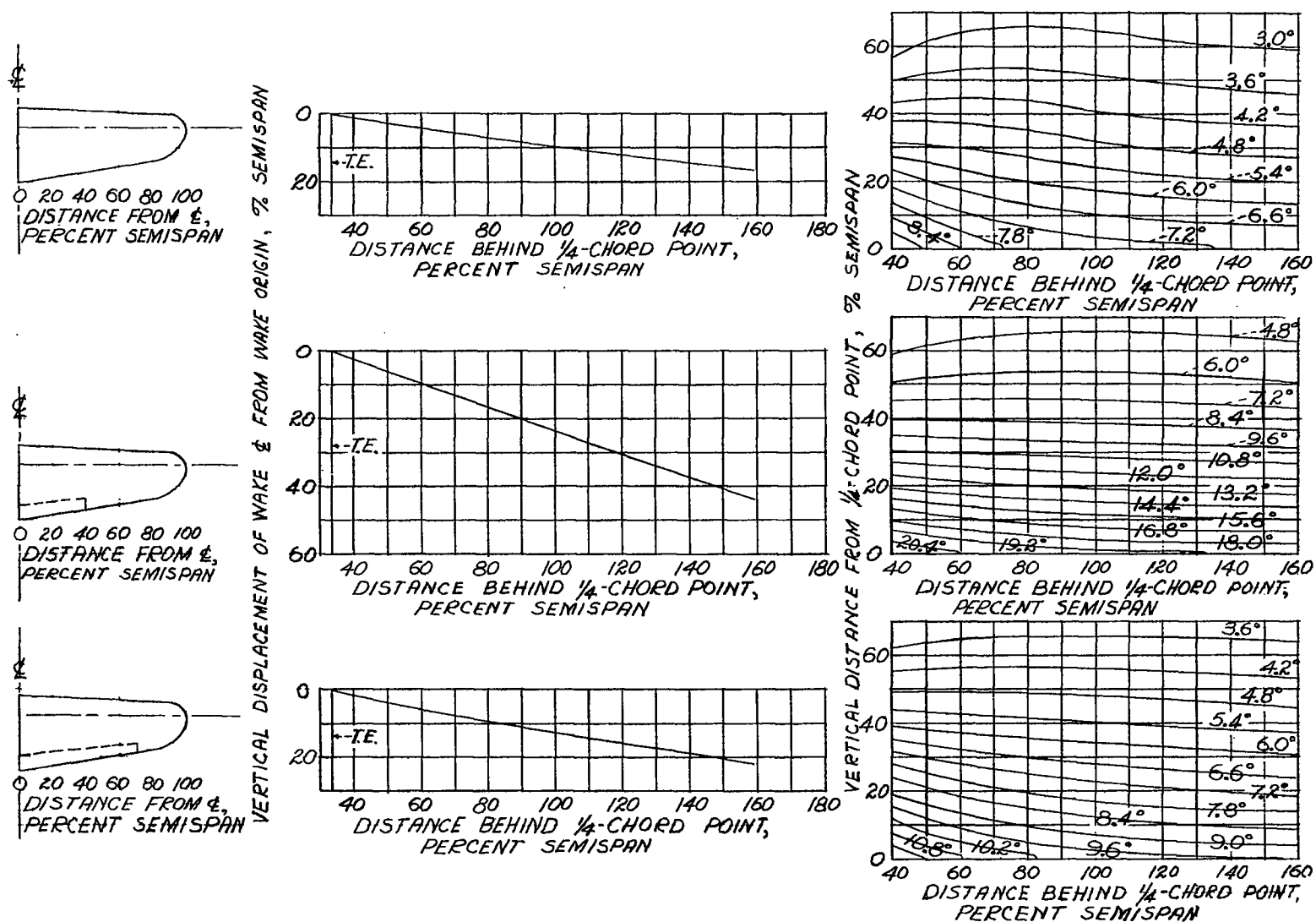
Figure 6.- Design chart for downwash displacement and angle (ref. 5).
$C_L = C_{L_f} = 1.0$; $\lambda = 2:1$; $A_W = 6$.
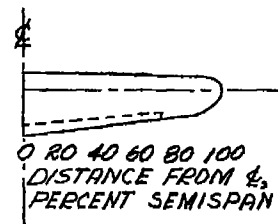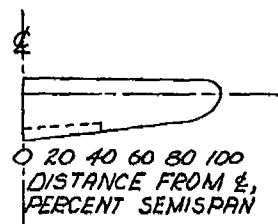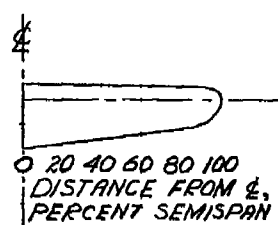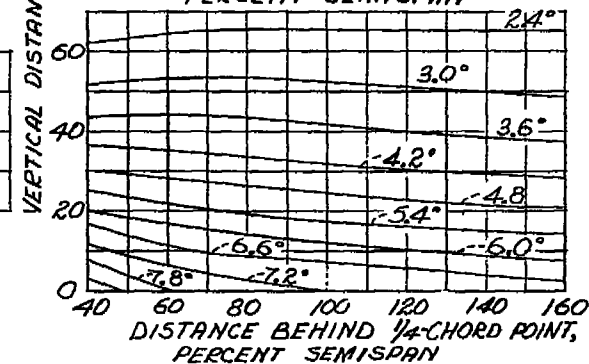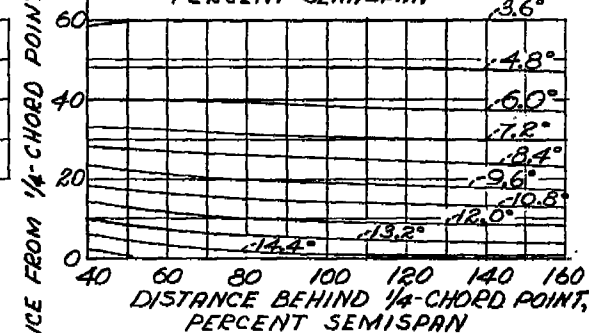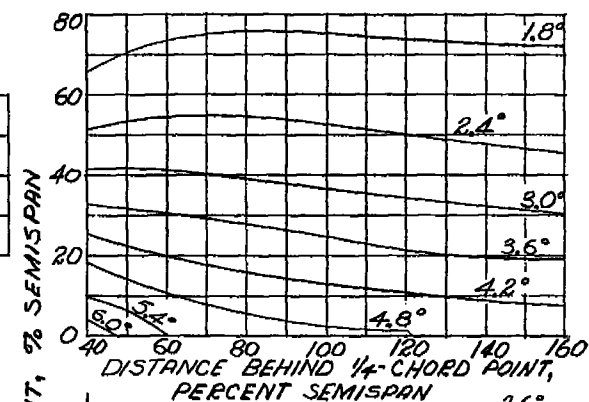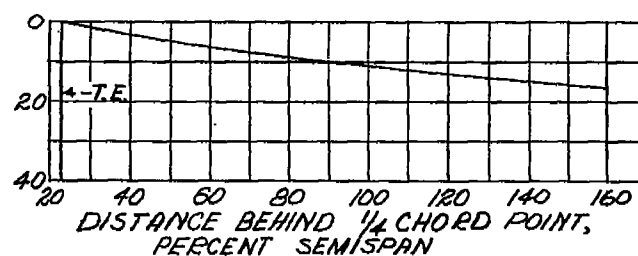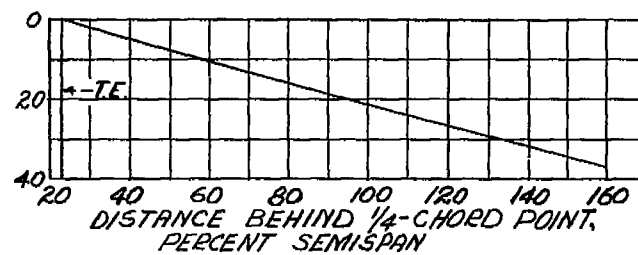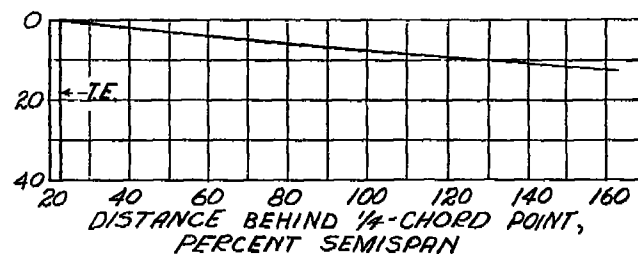
Figure 7.- Design chart for downwash displacement and angle (ref. 5).
$C_L = C_{L_f} = 1.0$; $\lambda = 2:1$; $A_w = 9$.
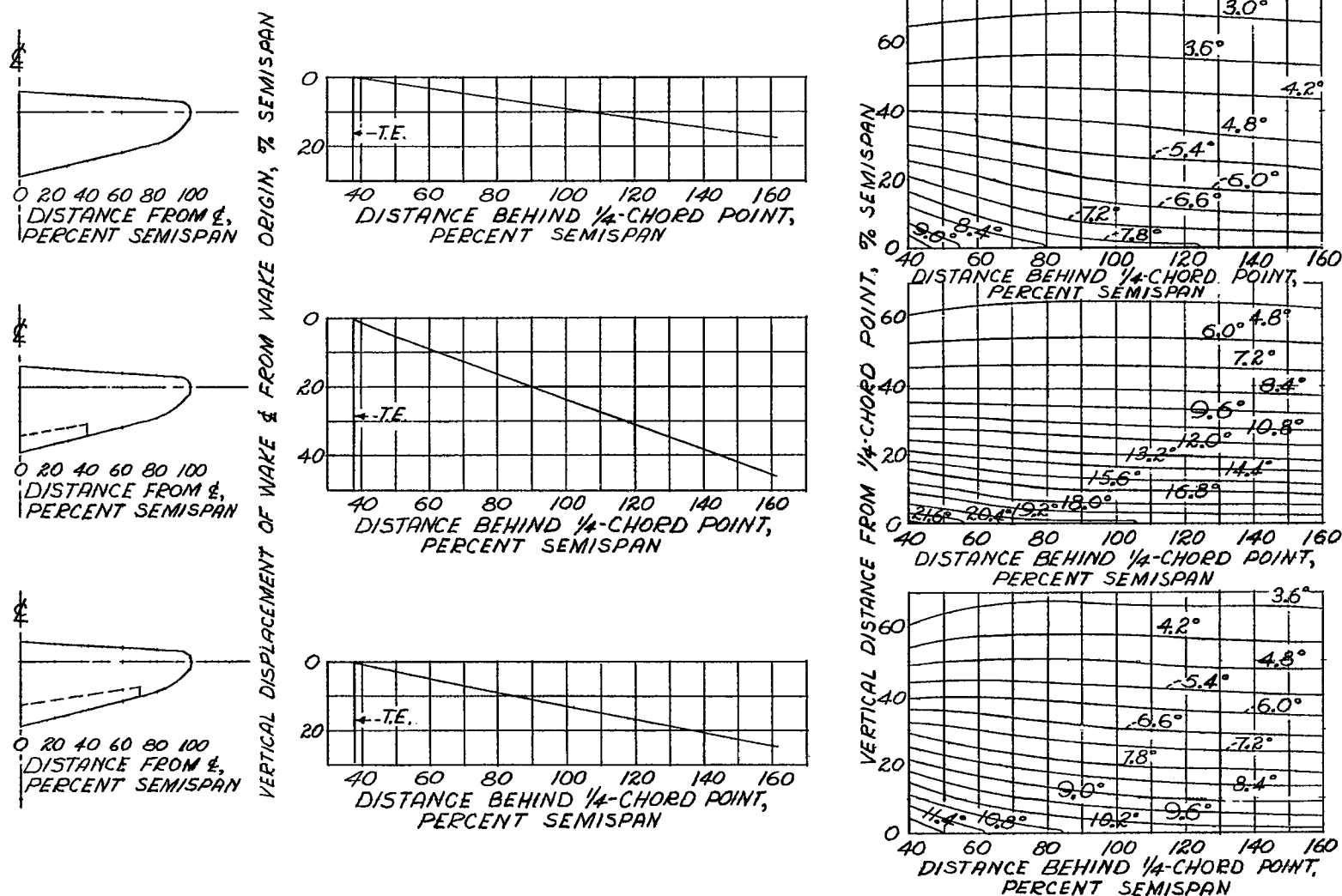
Figure 8.- Design chart for downwash displacement and angle (ref. 5).
$C_L = C_{L_f} = 1.0$; $\lambda = 3:1$; $A_W = 6$.
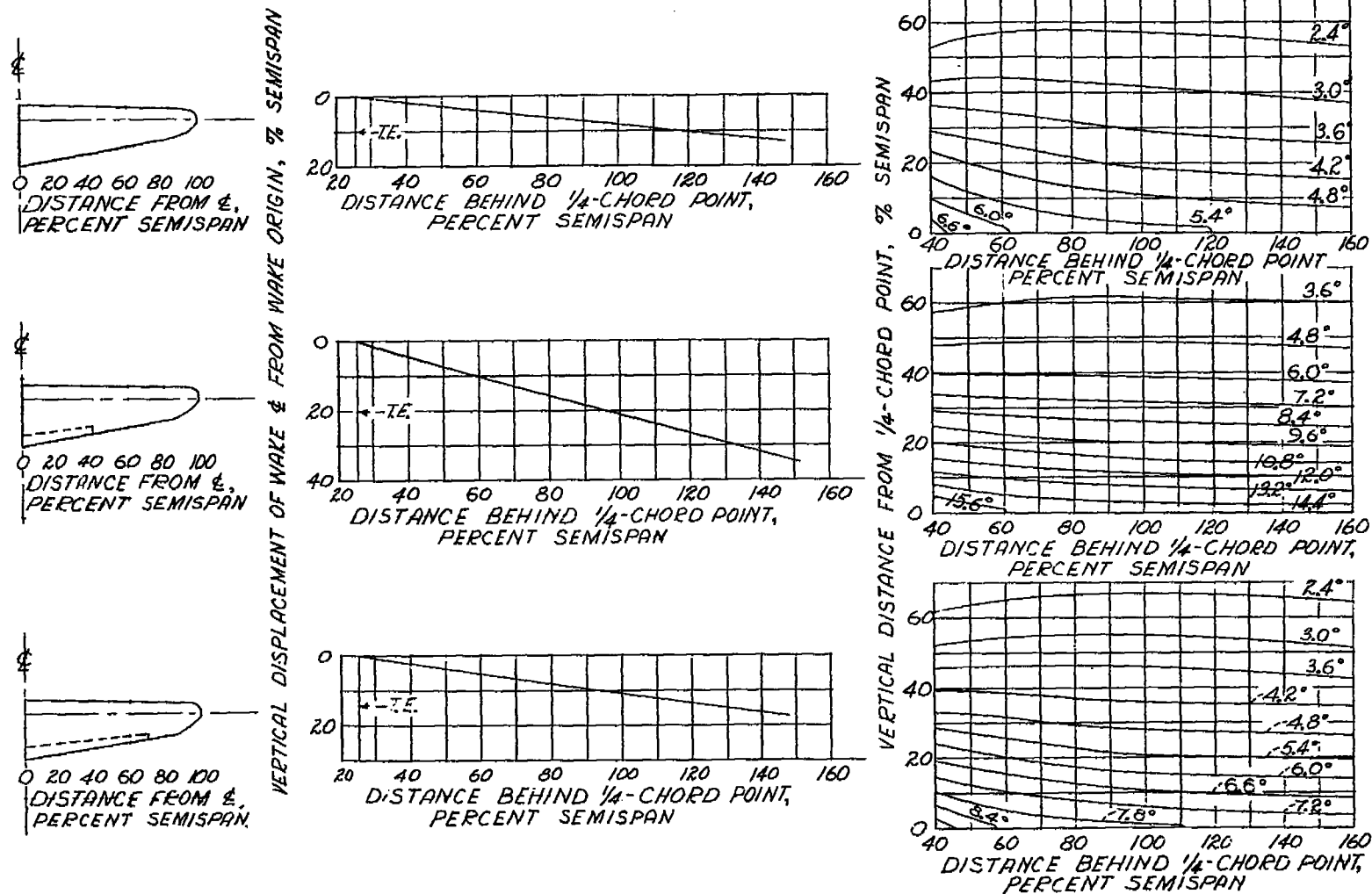
Figure 9.- Design chart for downwash displacement and angle (ref. 5).
$C_L = C_{L_f} = 1.0$; $\lambda = 3:1$; $A_W = 9$.
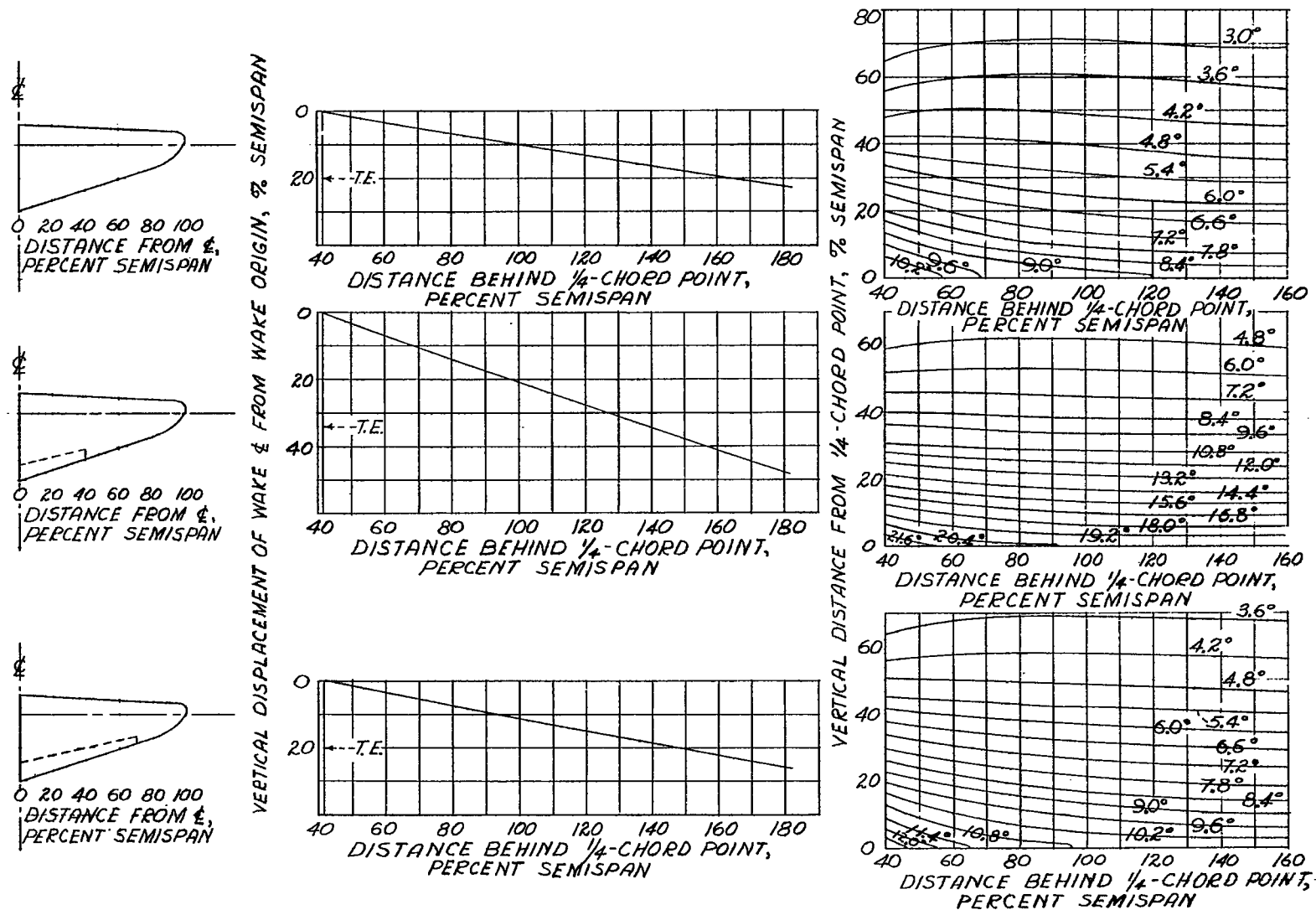
Figure 10.- Design chart for downwash displacement and angle (ref. 5).
$C_L = C_{L_f} = 1.0;$ $\lambda = 5:1;$ $A_W = 6.$
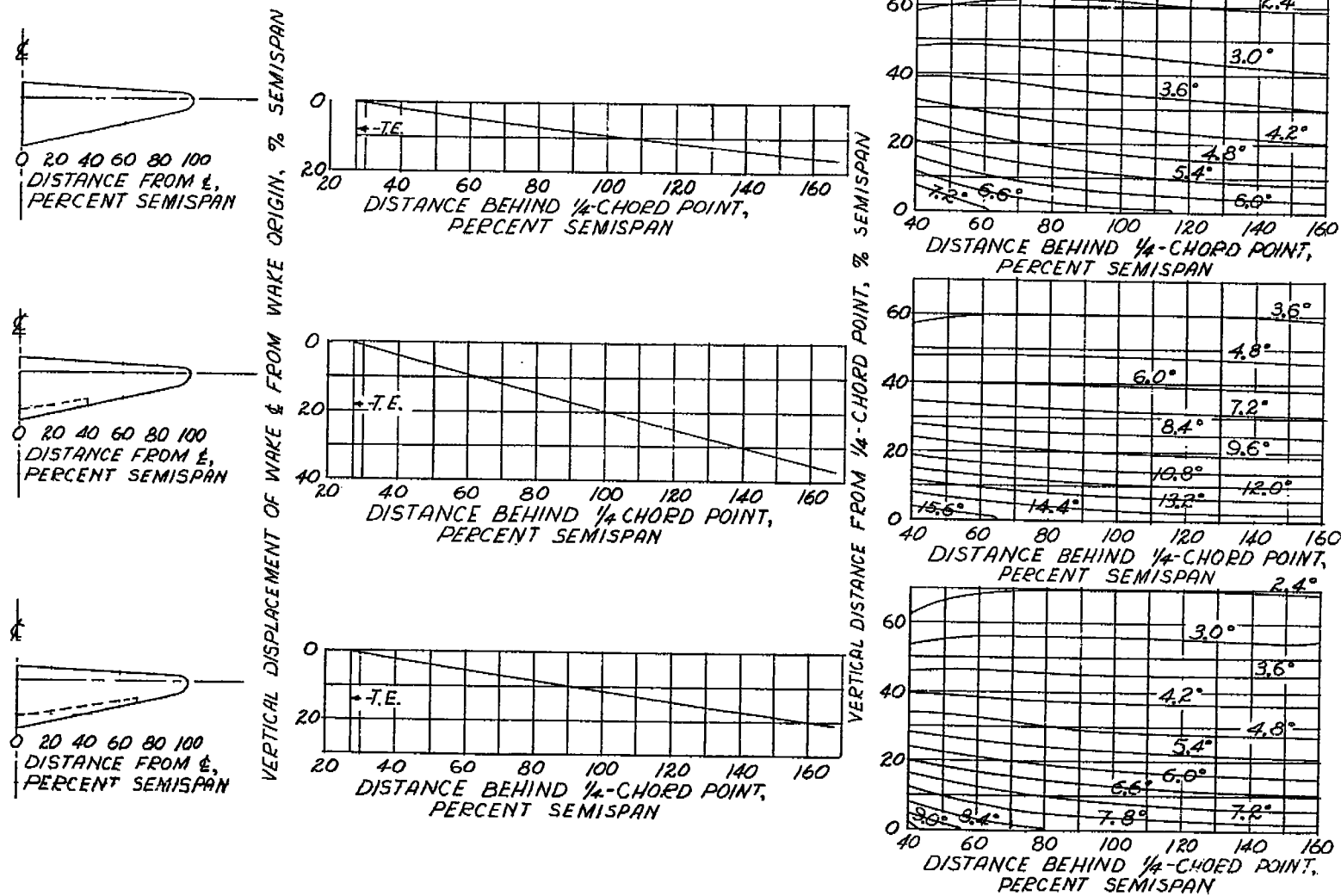
Figure 11.- Design chart for downwash displacement and angle (ref. 5).
$C_L = C_{Lf} = 1.0$; $\lambda = 5:1$; $A_W = 9$.
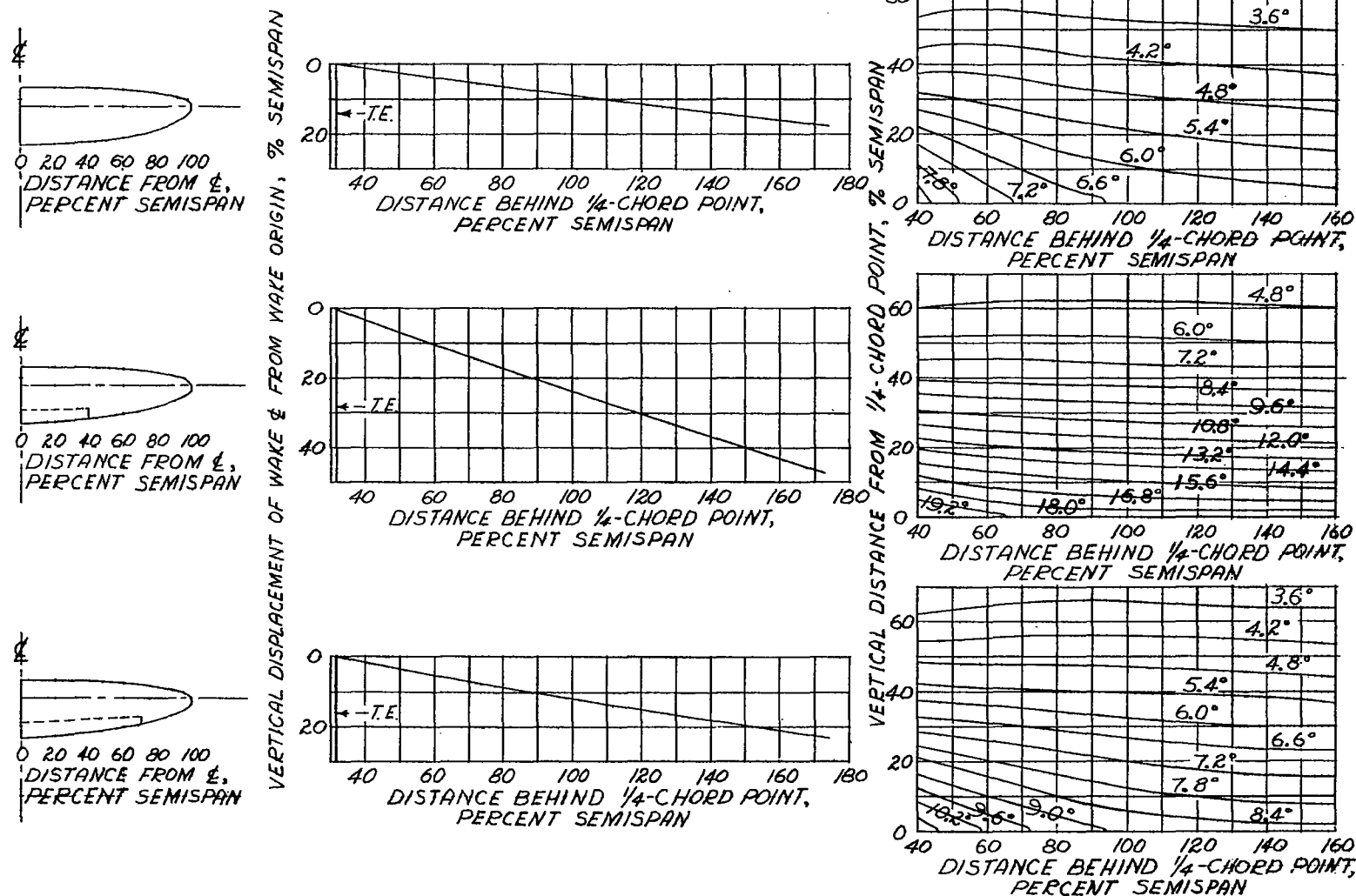
Figure 12.- Design chart for downwash displacement and angle (ref. 5). $C_L = C_{L_f} = 1.0$; elliptical; $A_W = 6$.
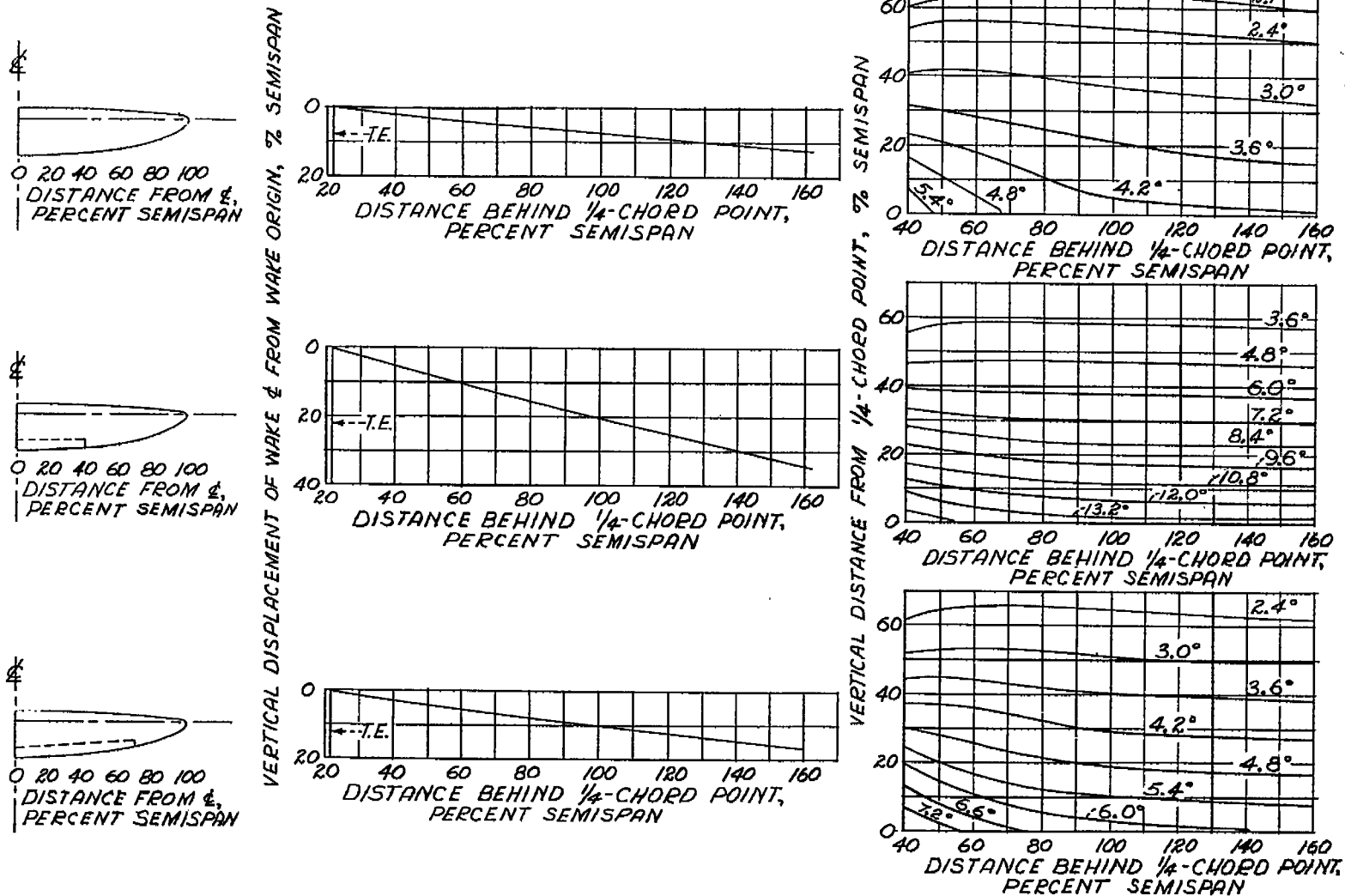
Figure 13.- Design chart for downwash displacement and angle (ref. 5).
$C_L = C_{L_f} = 1.0$; elliptical; $A_w = 9$.
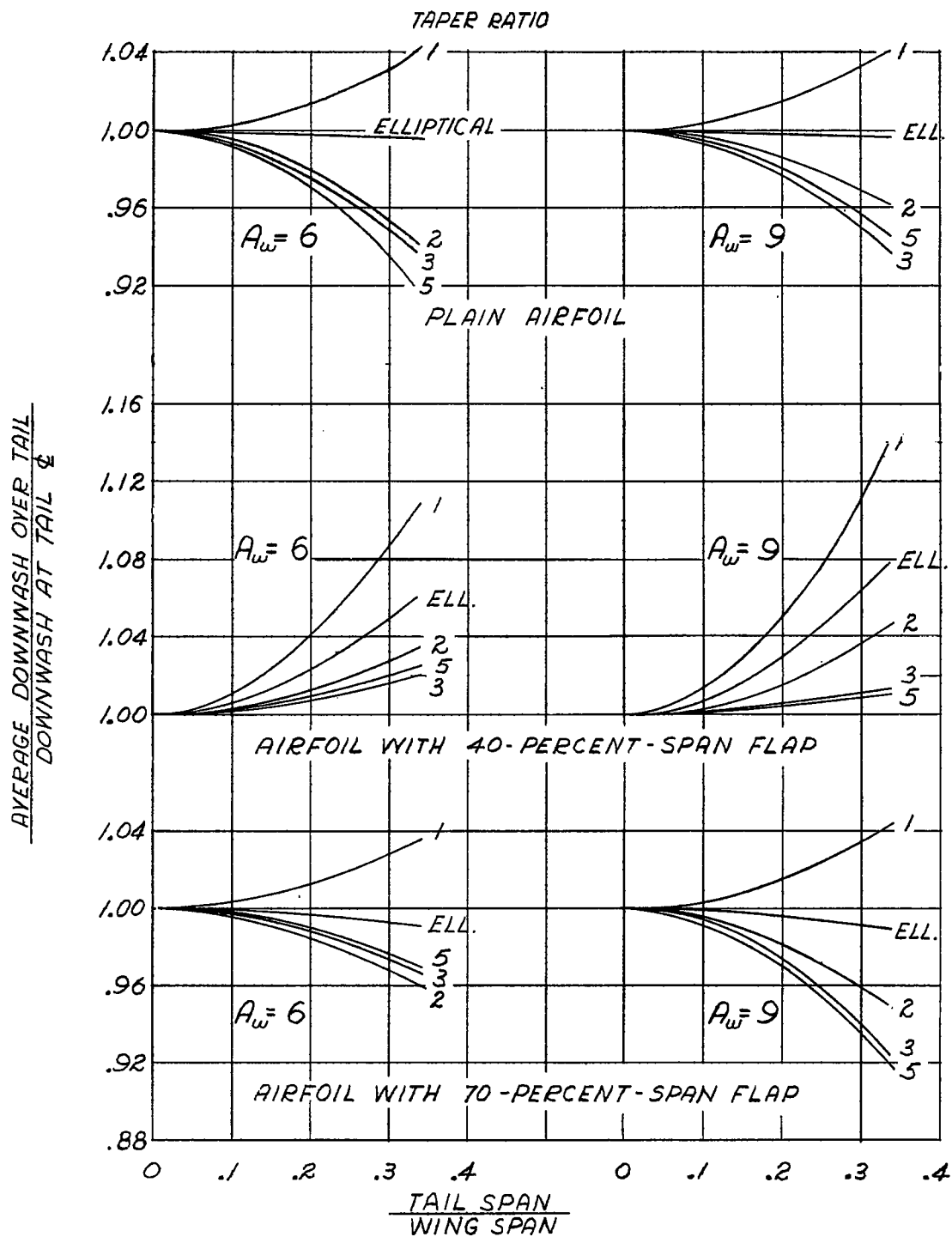
Figure 14.- Correction factor for variation of downwash across horizontal tail span (ref. 5).

FLAP DEFLECTION, δ_f, DEG
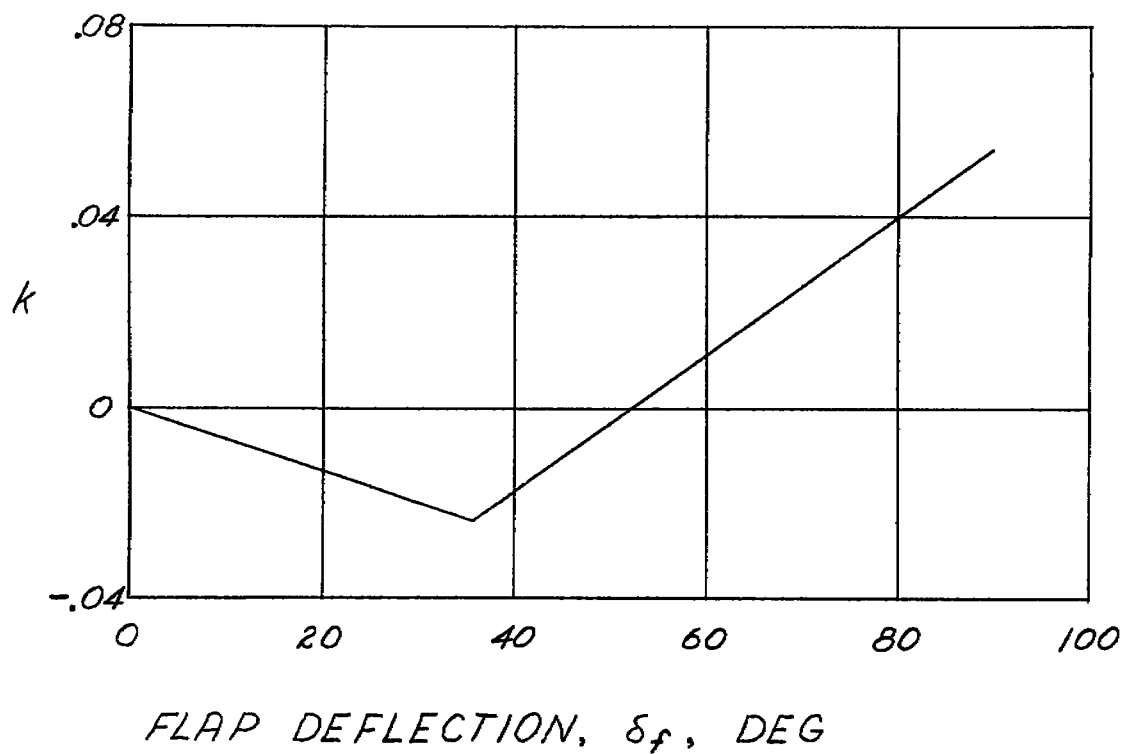
Figure 15.- Factor for locating wake origin for flapped wings (ref. 5).
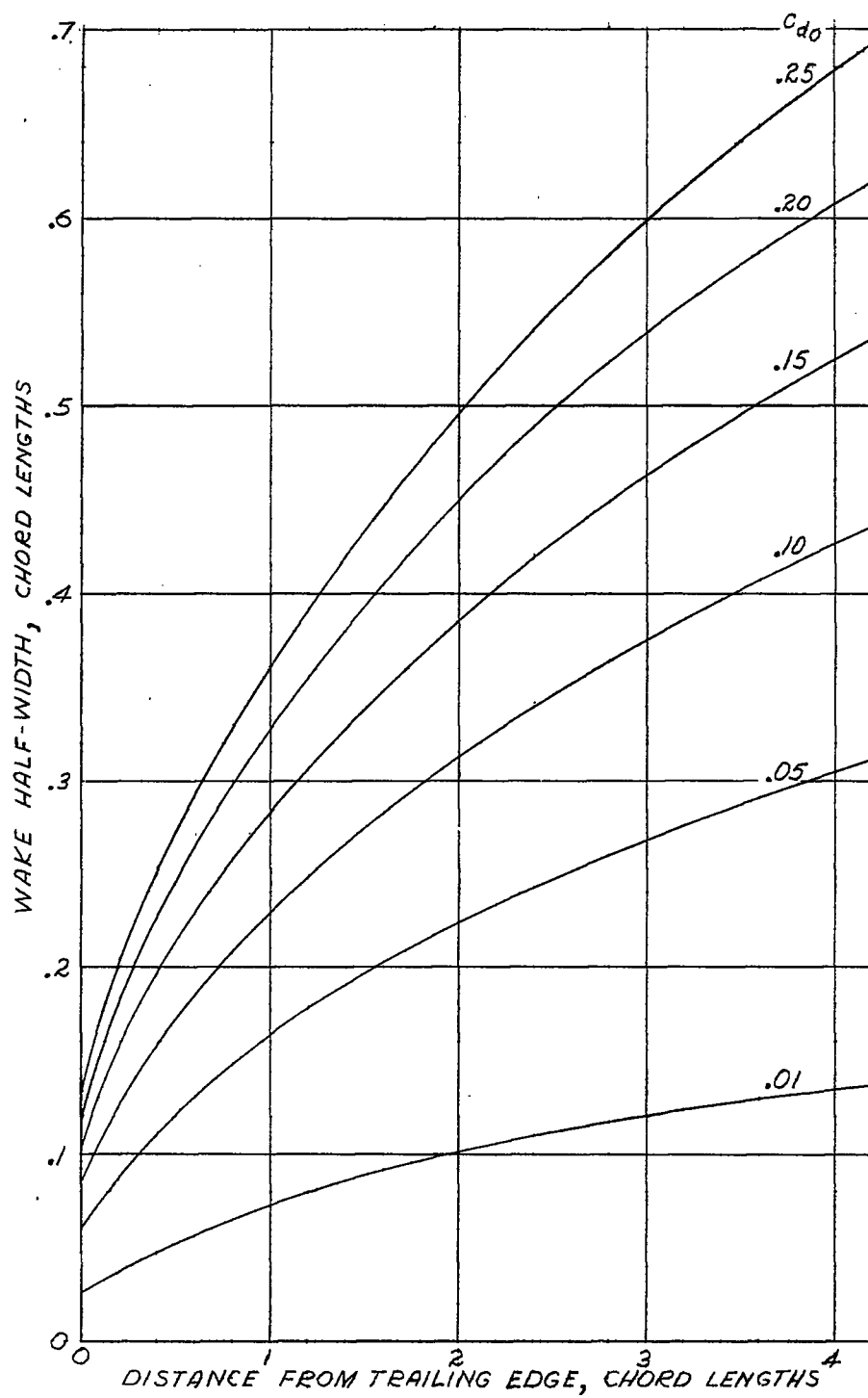
Figure 16.- Relation between wake width and distance from trailing
edge (ref. 5).
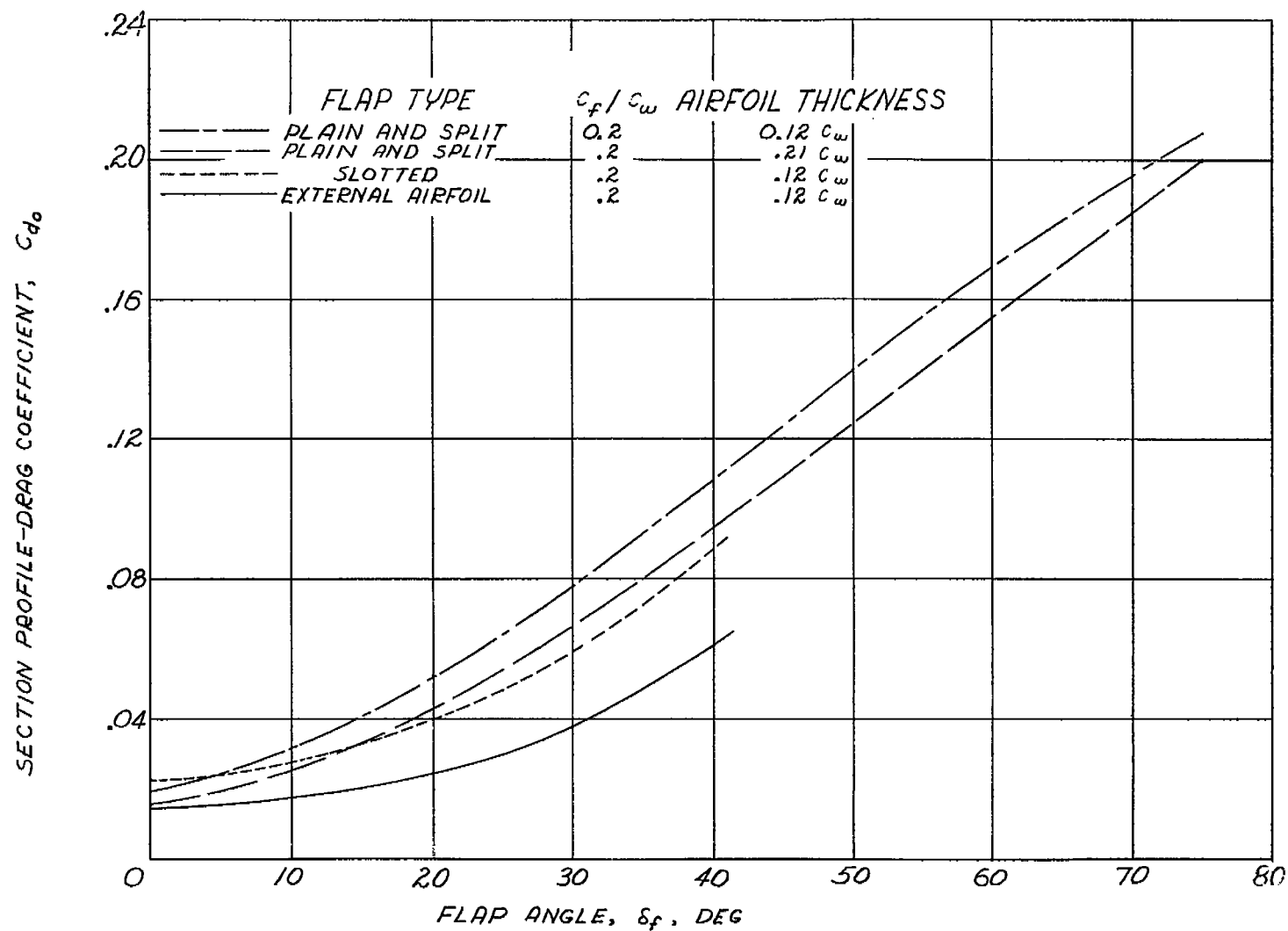
Figure 17.- Section profile-drag coefficients for different flaps (ref. 5).
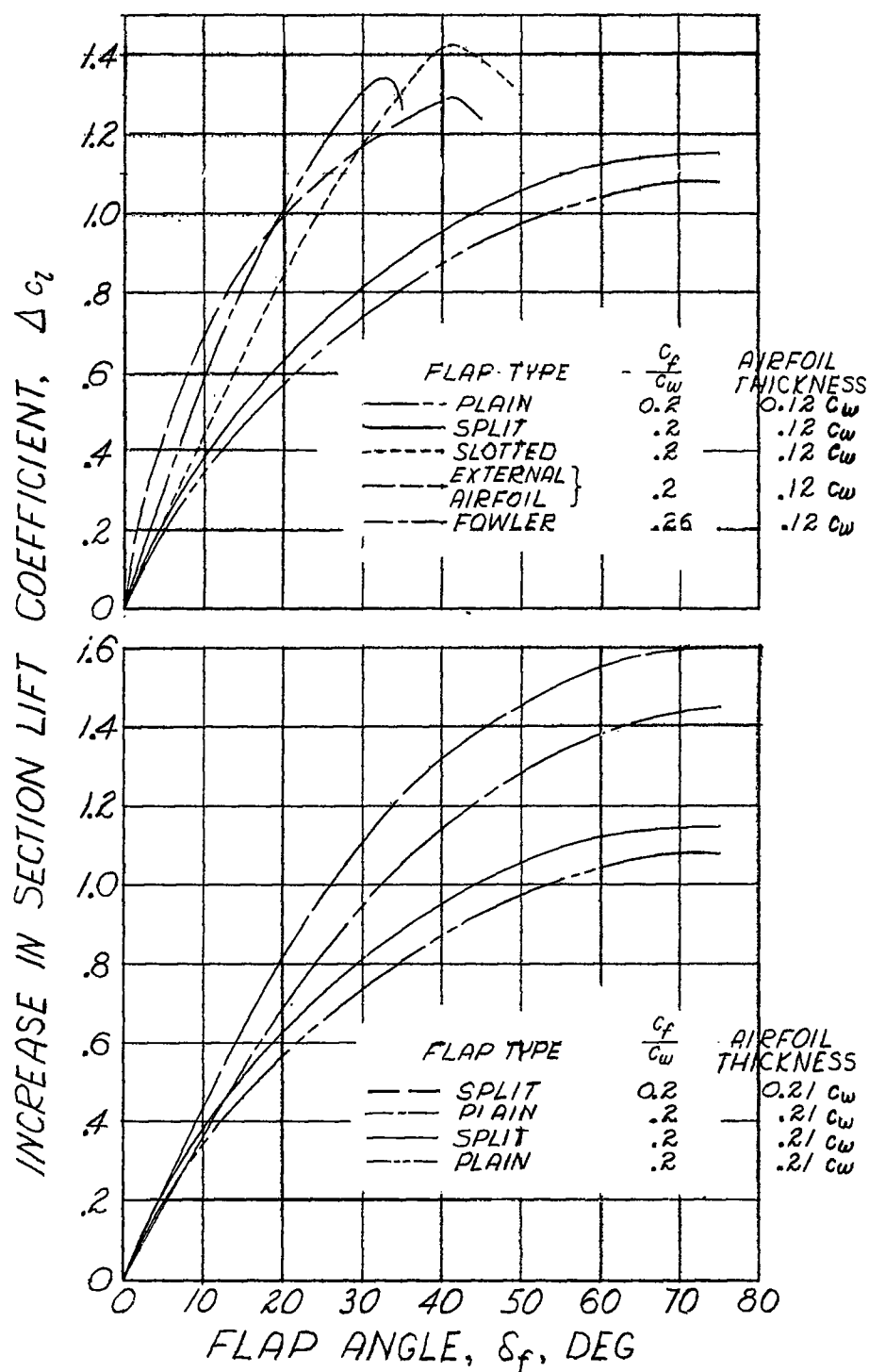
(a) Increment in section lift coefficient due to flaps.

Figure 18.- Effect of flap deflection on lift characteristics (ref. 5).

$$\frac{C_{L_f}}{\Delta c_l}$$
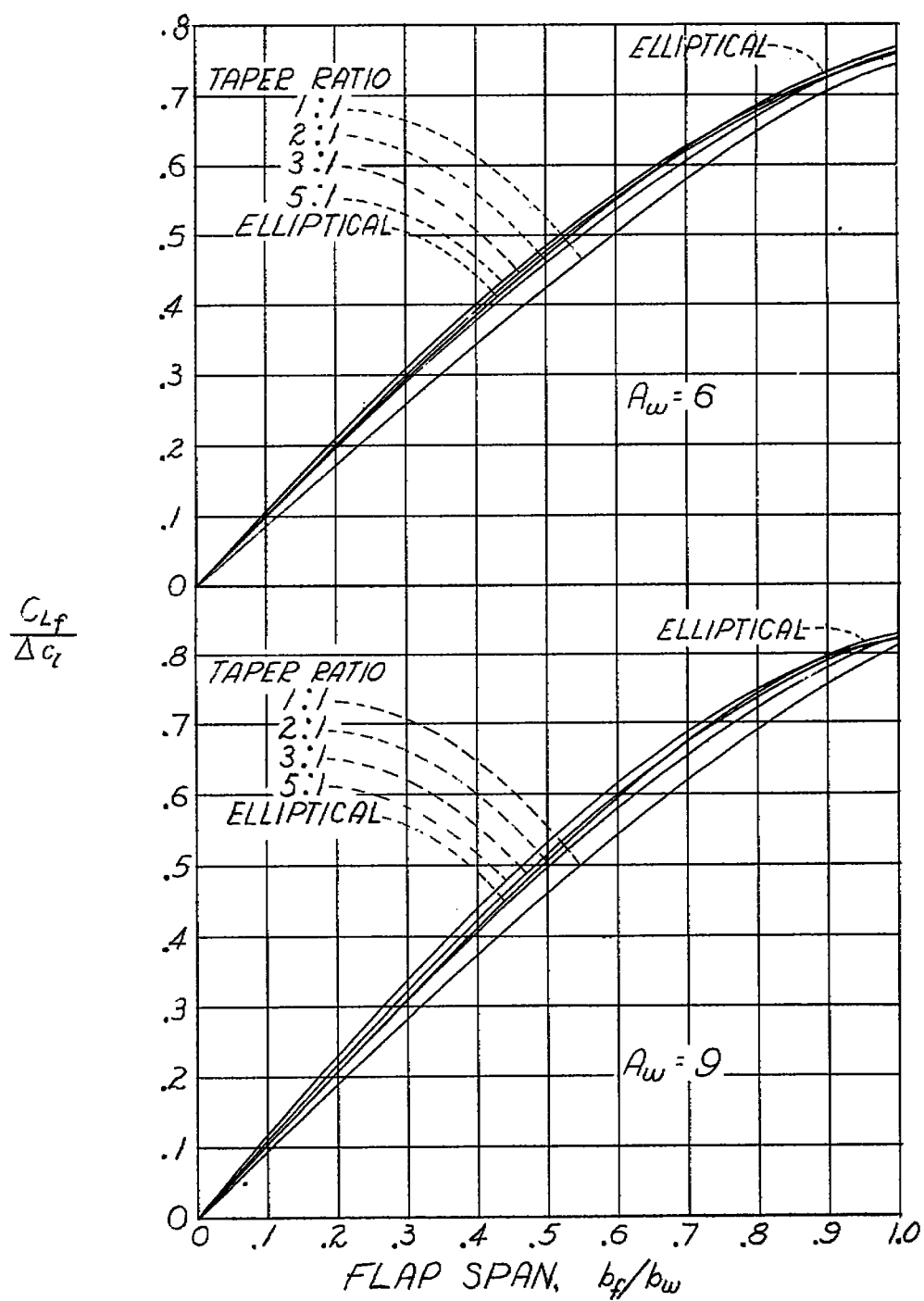
(b) Lift increments for flapped wings.

Figure 18.- Concluded.
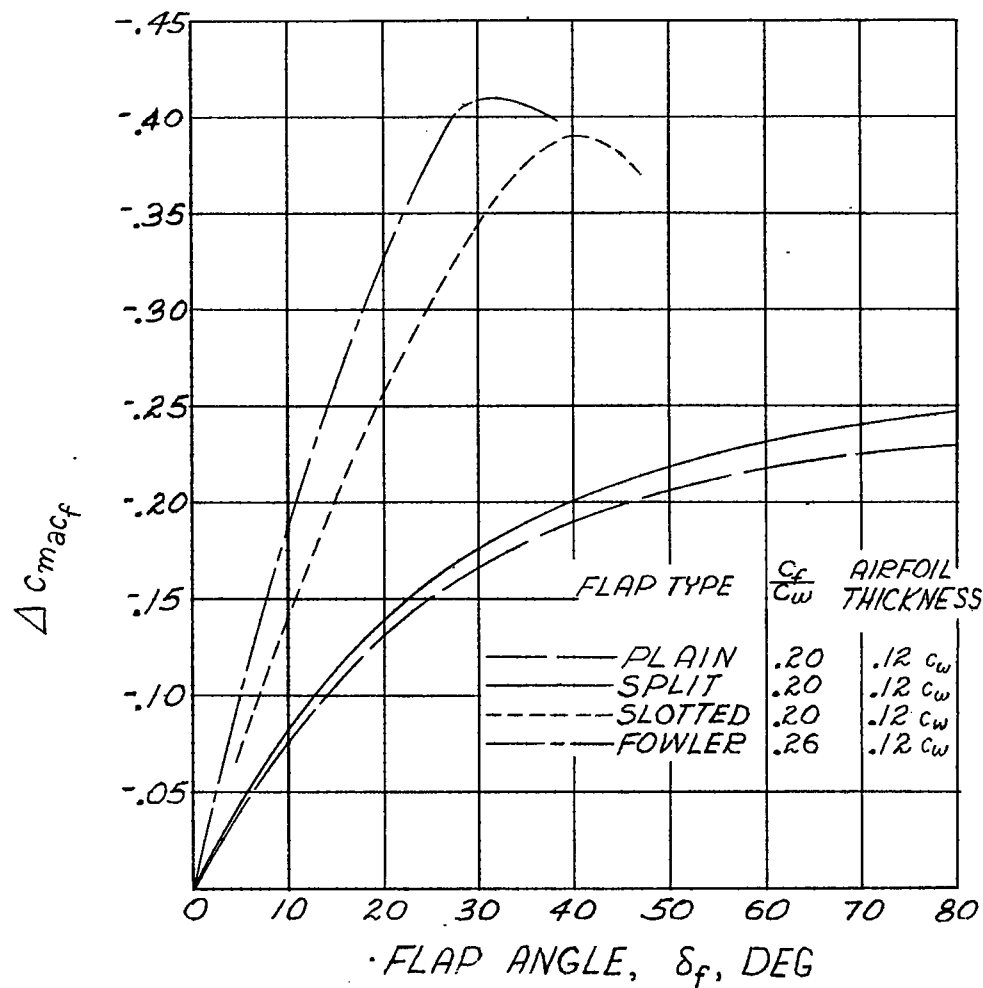
(a) Increment in section moment due to flaps.
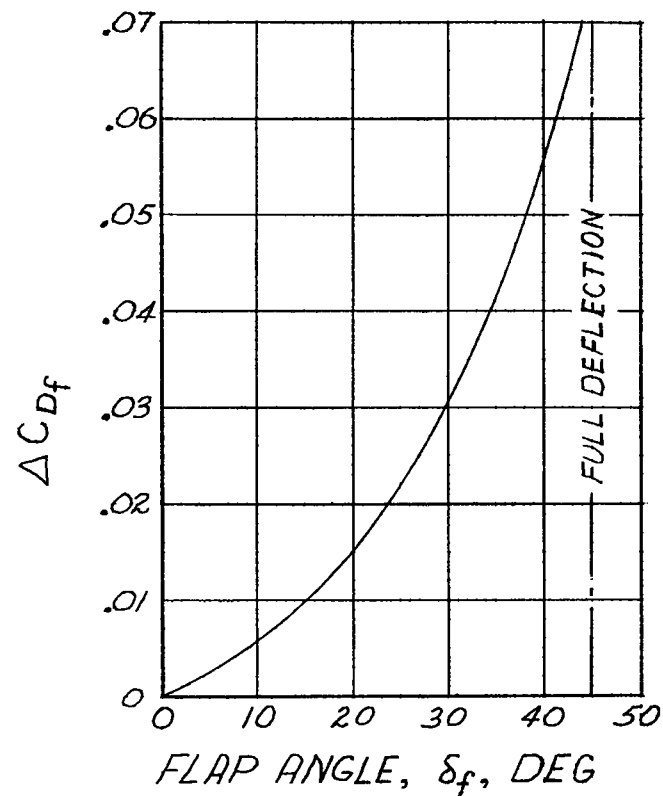
(b) Increment in total wing drag due to flaps.

Figure 19.- Effect of flap deflection on moment and drag characteristics. (Reprinted from ref. 6 with permission of John Wiley & Sons, Inc.)
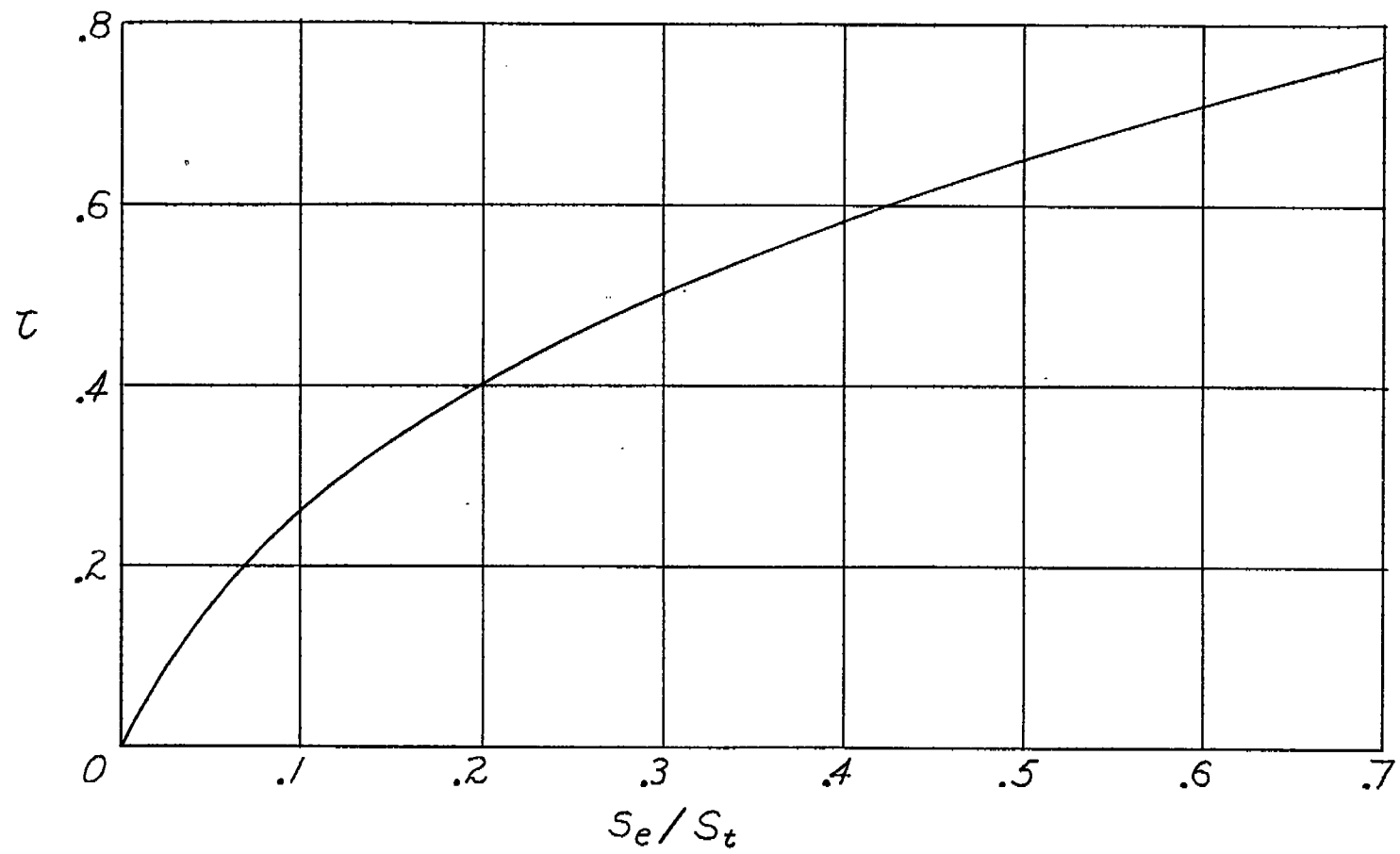
Figure 20.- Elevator effectiveness factor (ref. 4).
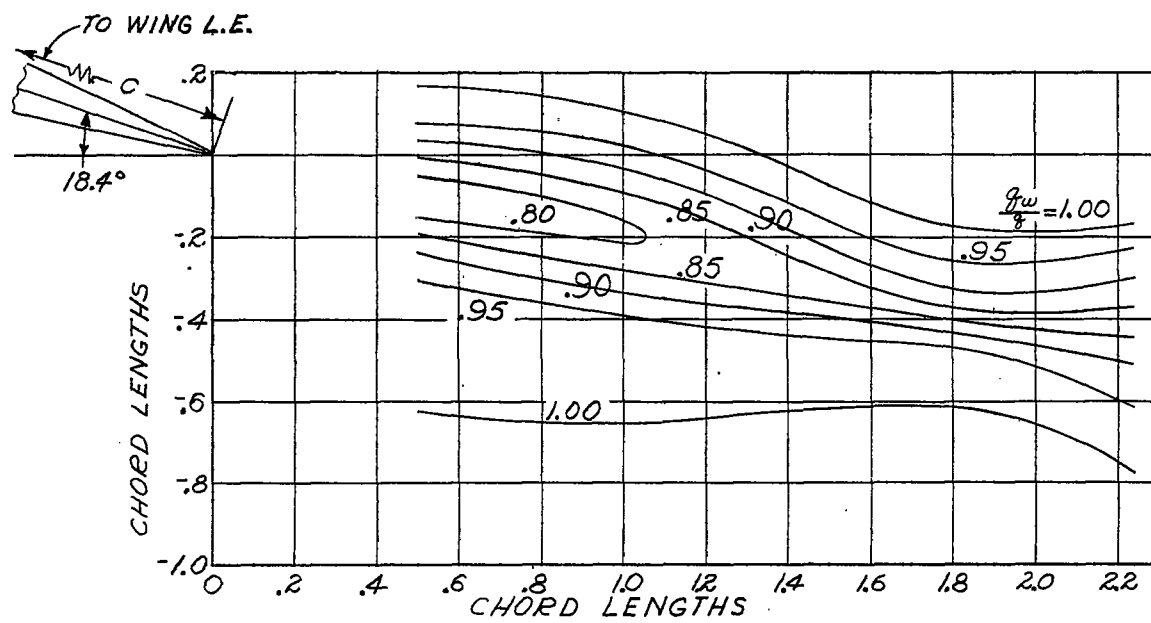
(a) Plain wing.
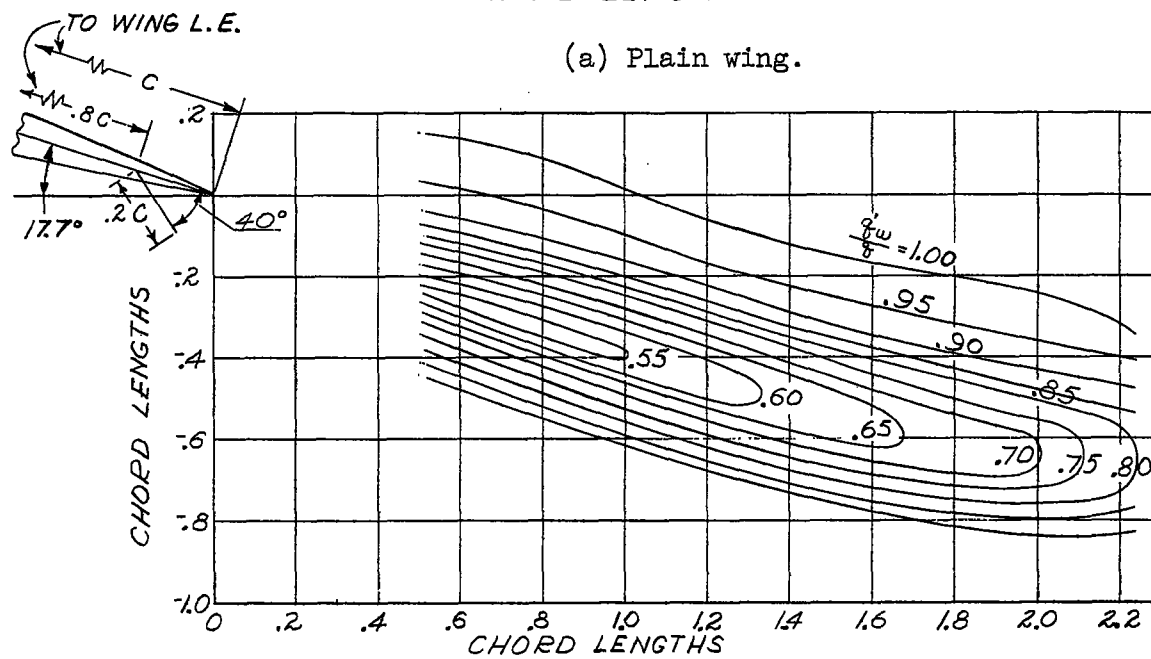
(b) Split flap.

Figure 21.- Velocity contours (ref. 7).
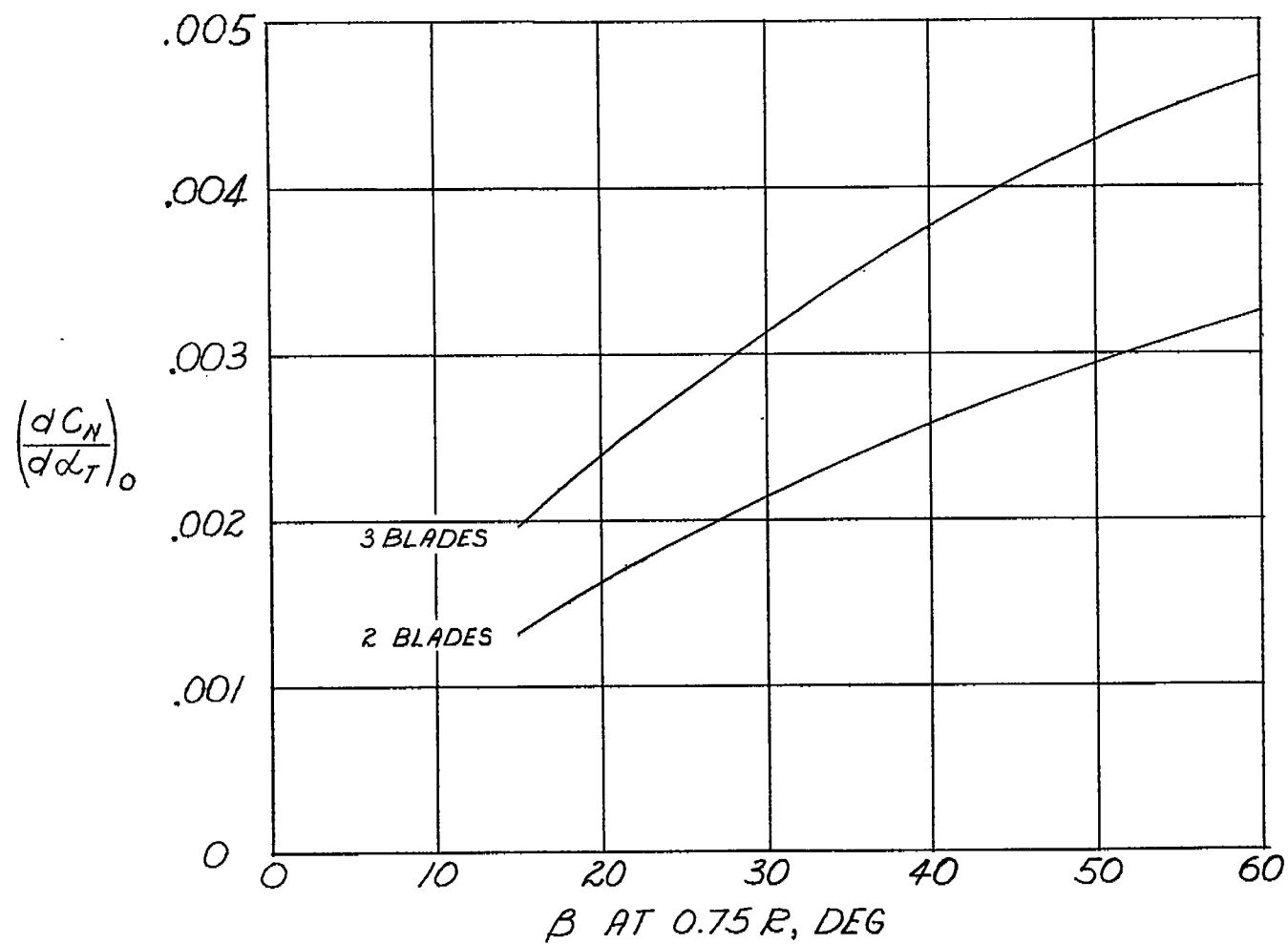
Figure 22.- Variation of $\dfrac{dC_N}{d\alpha_T}$ with β for Hamilton Standard 3155-6 propeller with 0.164-diameter spinner and side-force factor of 80.7 (ref. 9, modified).
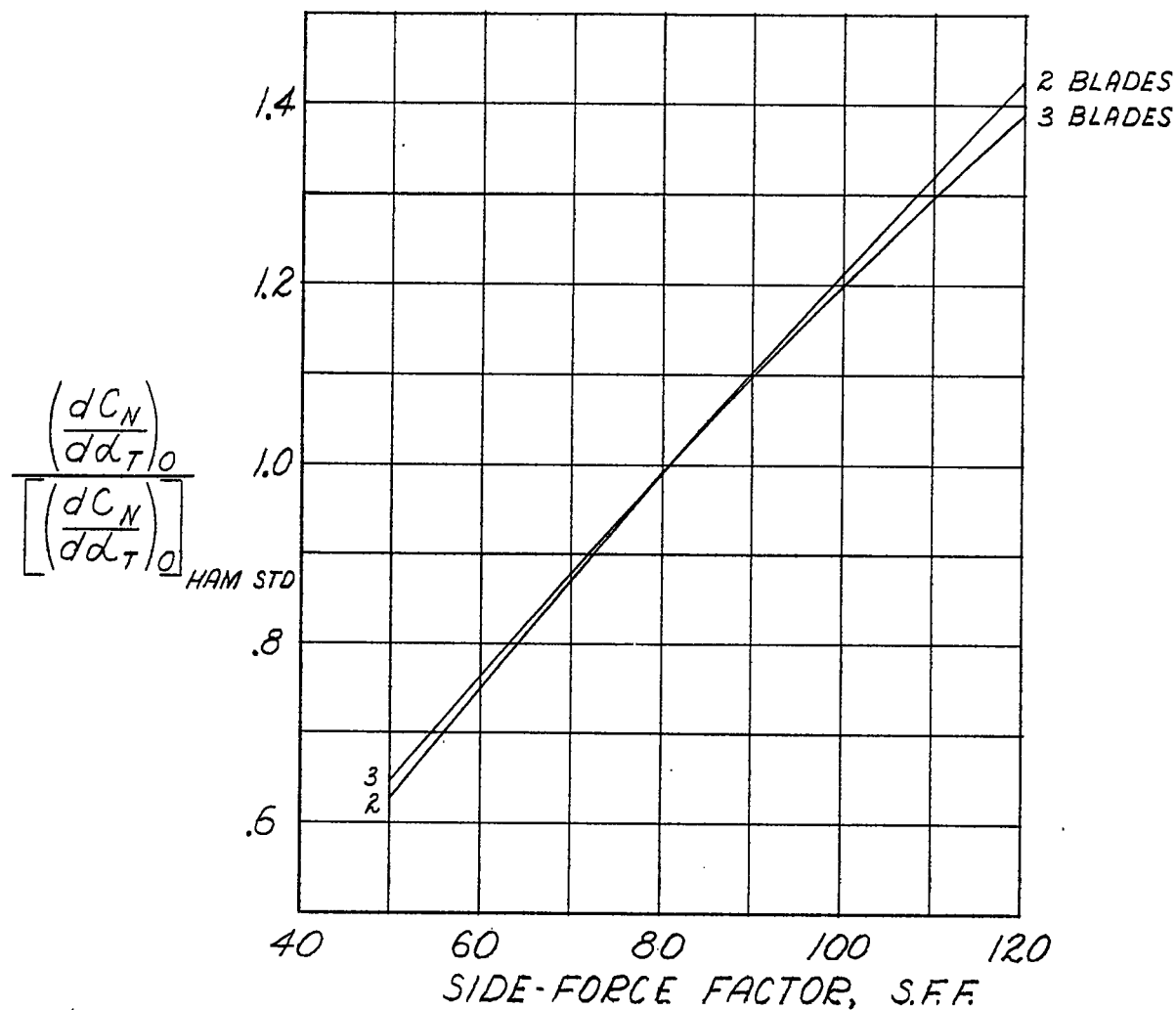
Figure 23.- Ratio of normal-force derivatives versus side-force
  factor (ref. 9). Hamilton Standard 3155-6 propeller; side-
  force factor, 80.7.

$$\frac{\left(\dfrac{dC_N}{d\alpha_T}\right)_P}{\left(\dfrac{dC_N}{d\alpha_T}\right)_O}$$

THRUST COEFFICIENT, T_C
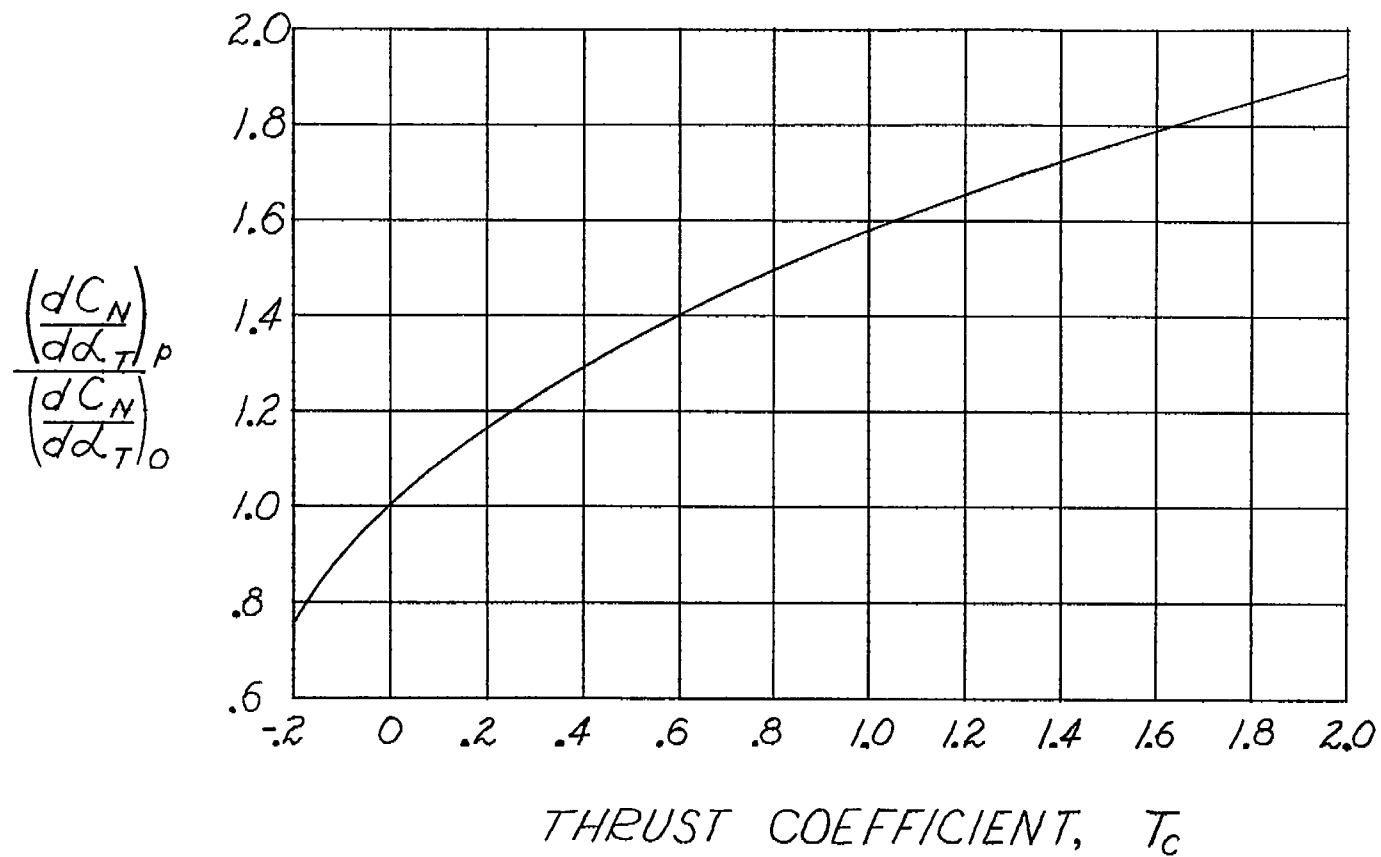
Figure 24.- Ratio of normal-force derivatives versus thrust coefficient T_c (ref. 9).
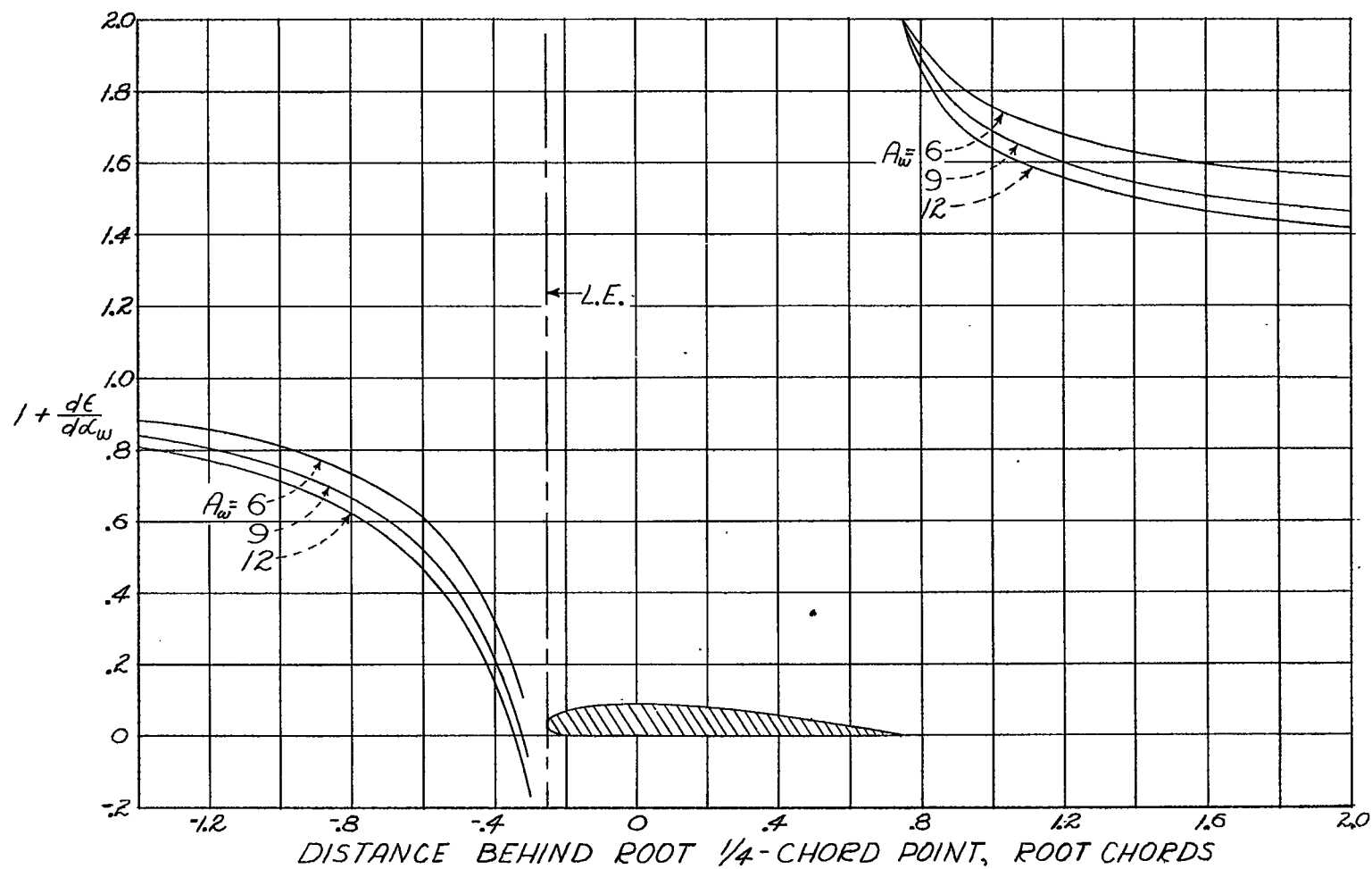
Figure 25.- Value of $1 + \dfrac{d\epsilon}{d\alpha_w}$ on longitudinal axis of elliptical

wing (ref. 9, modified).
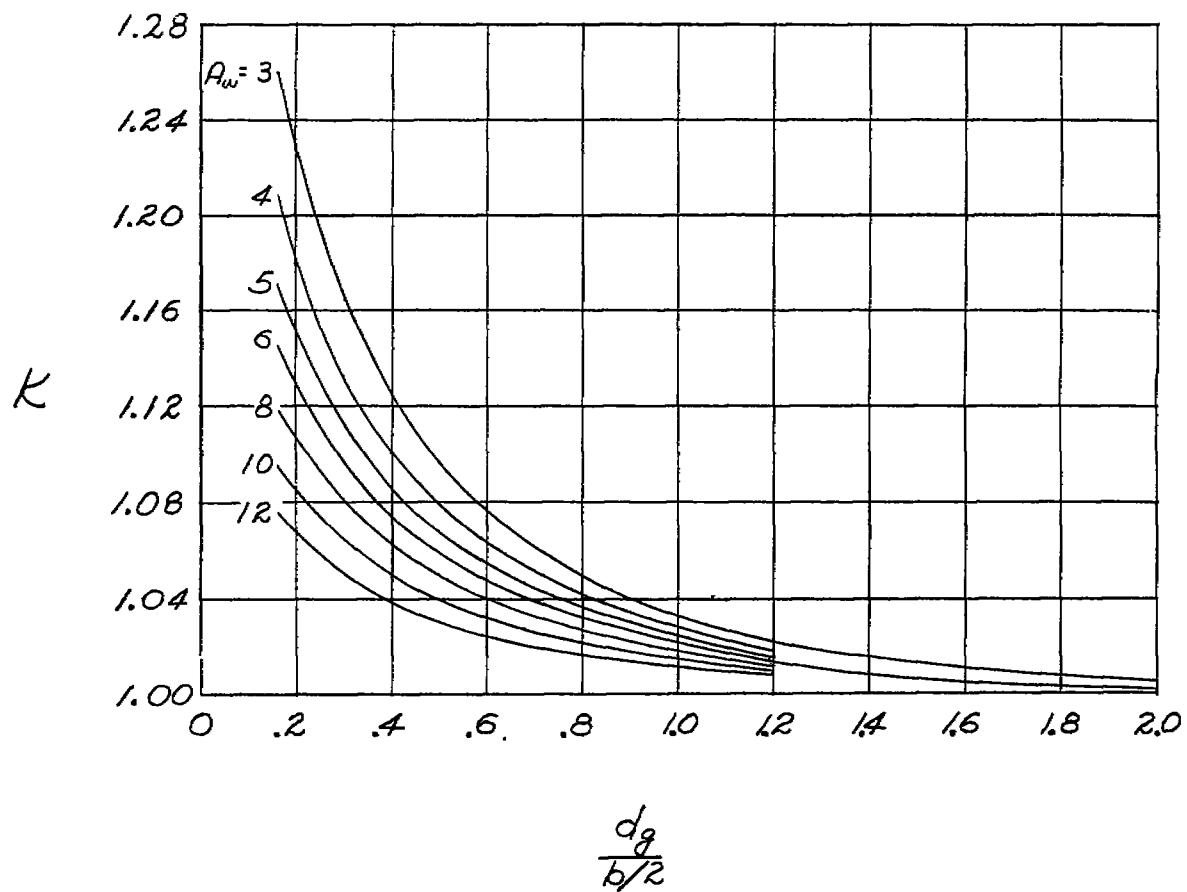
Figure 26.- Ground effect on lift-curve slope (ref. 3).
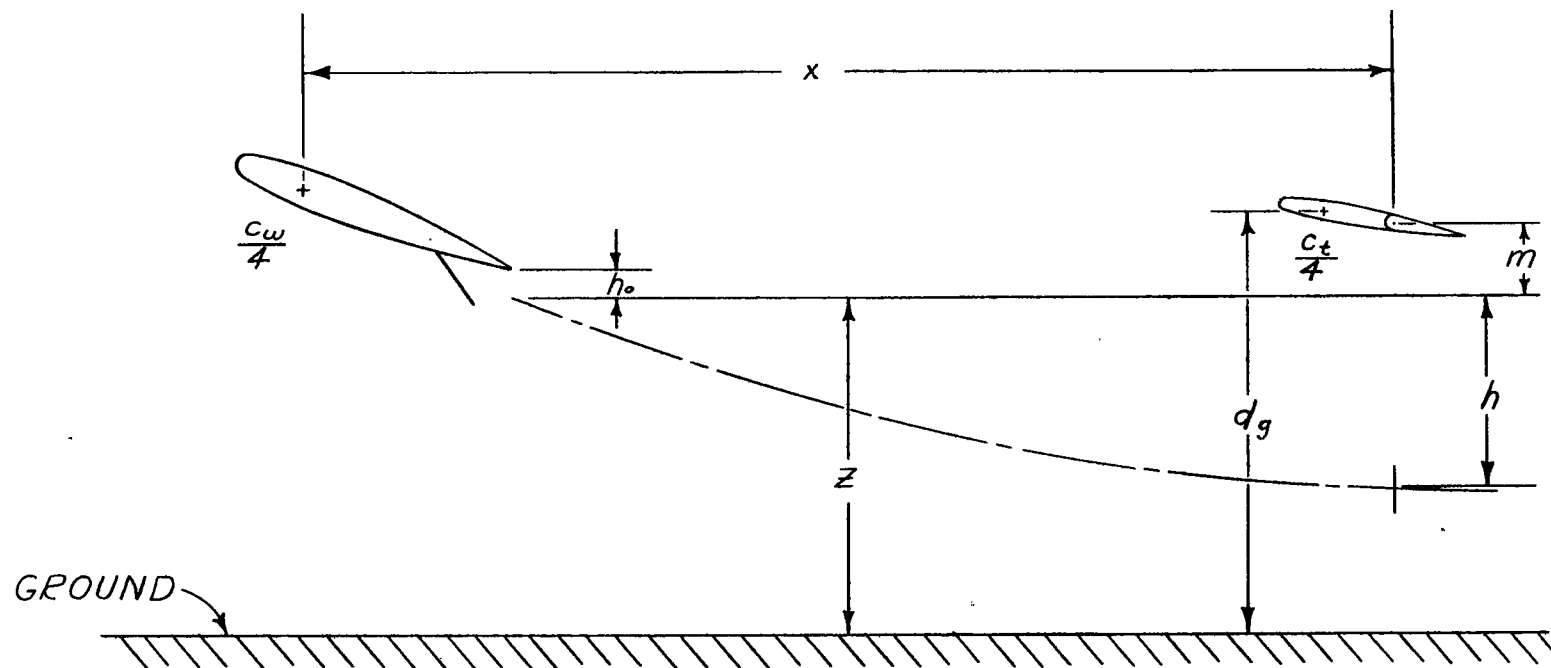
Figure 27.- Geometry for computing ground effect (ref. 3).
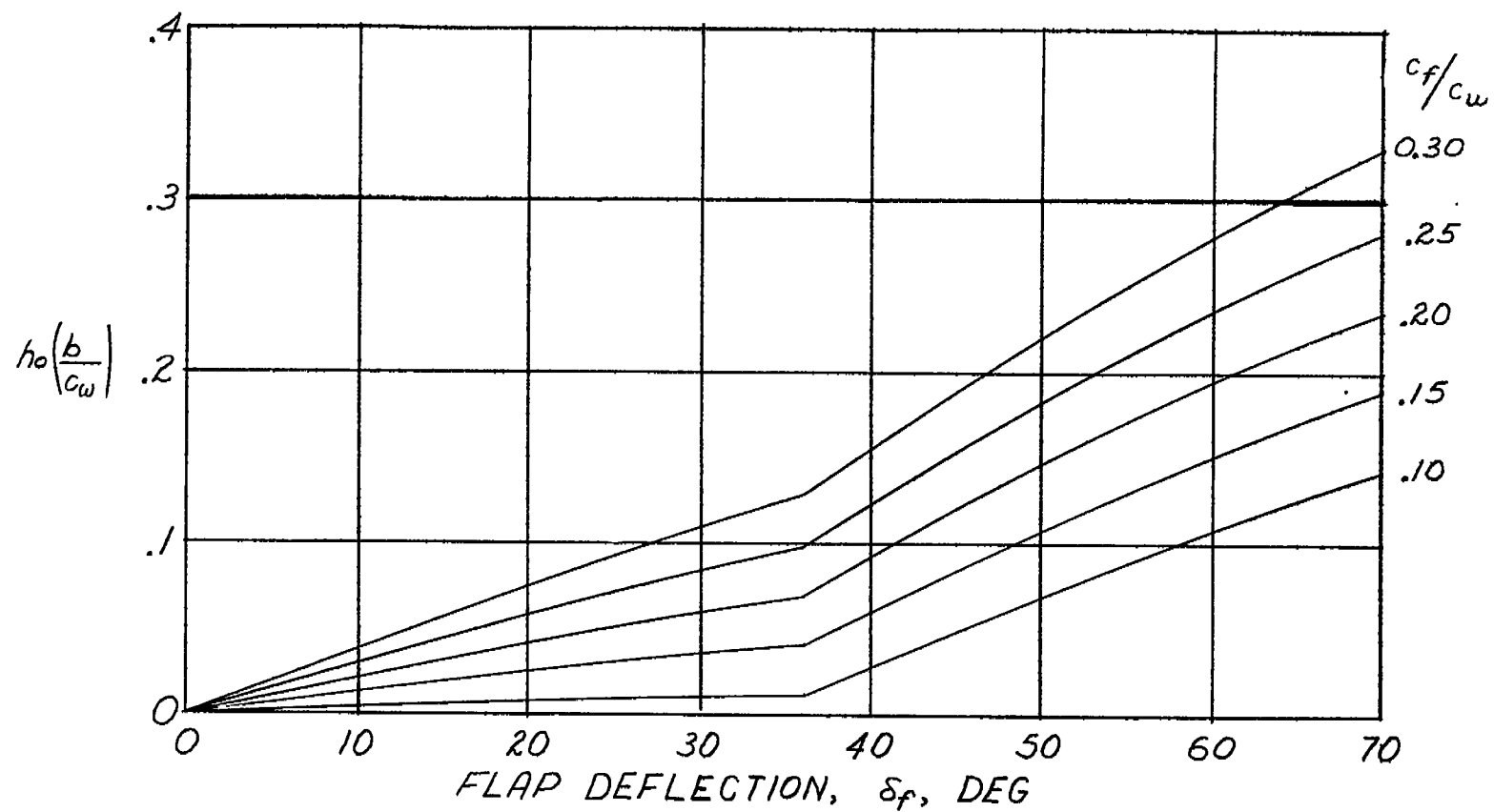
Figure 28.- Downward displacement of wake origin for flapped
wings (ref. 3).
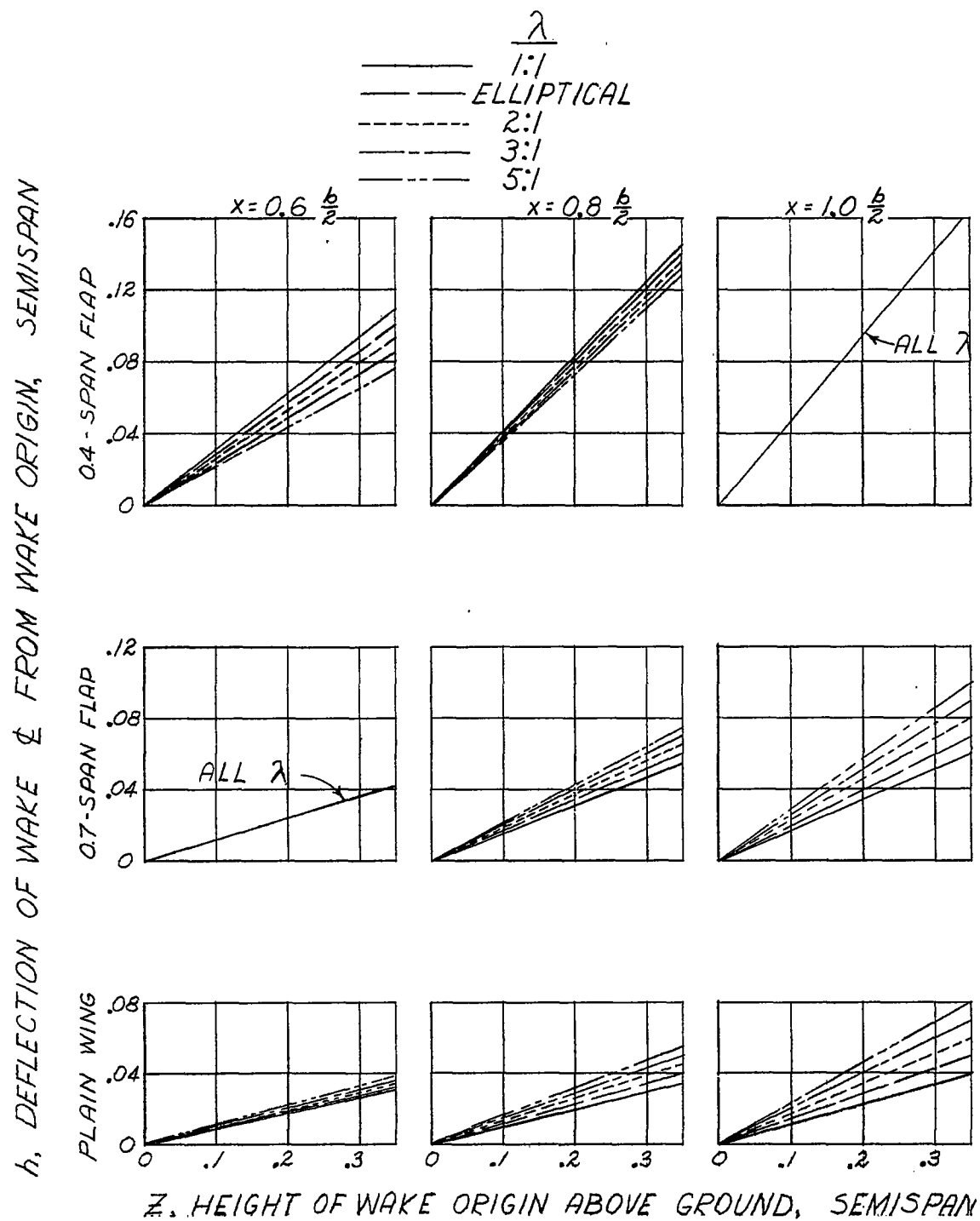
Figure 29.- Wake deflection near ground (ref. 3).
$C_L = C_{L_f} = 1.0$; $A_W = 6$.
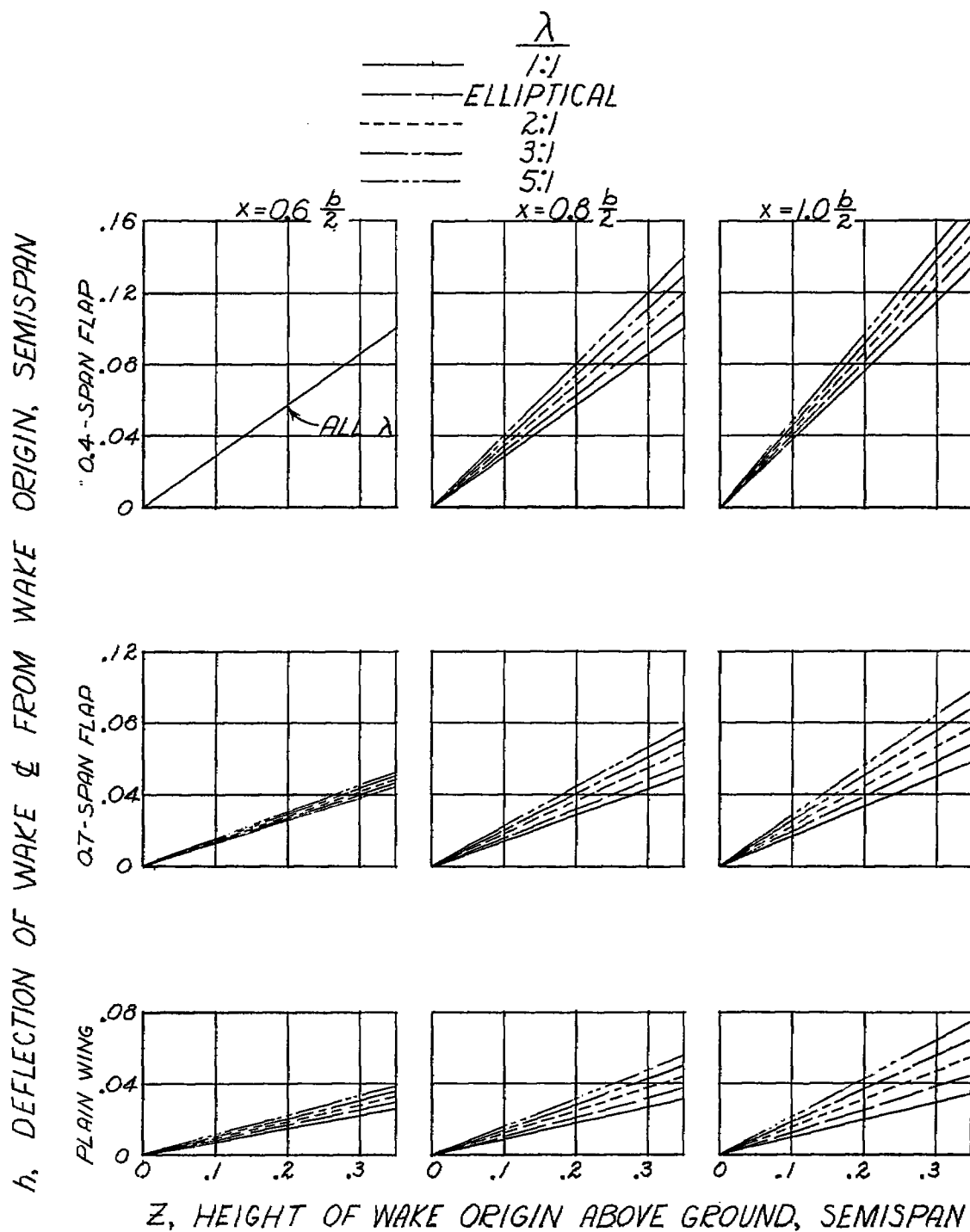
Figure 30.- Wake deflection near ground (ref. 3).
$C_L = C_{L_f} = 1.0$; $A_W = 9$.
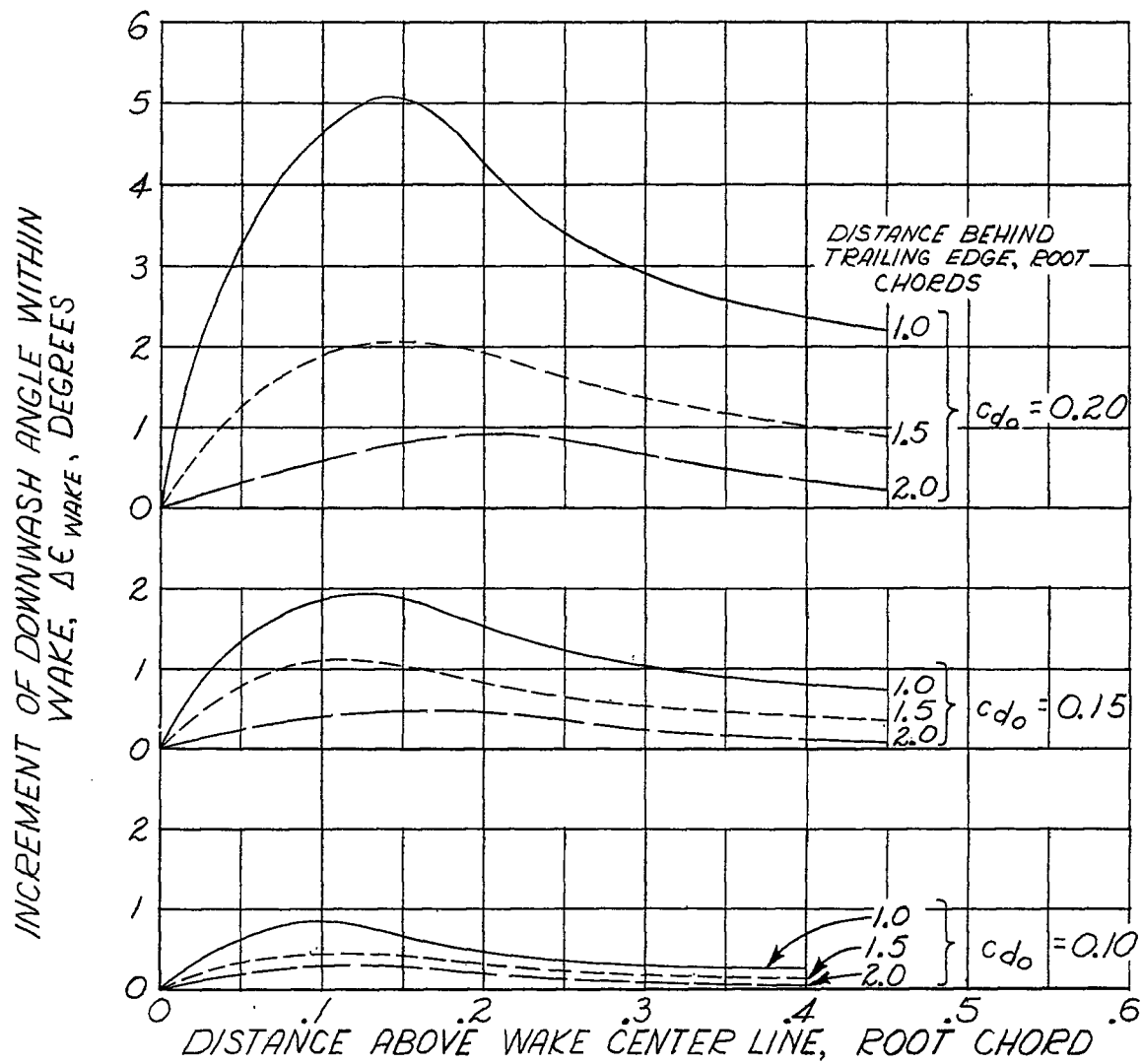
Figure 31.- Wake effect on downwash near ground (ref. 3).
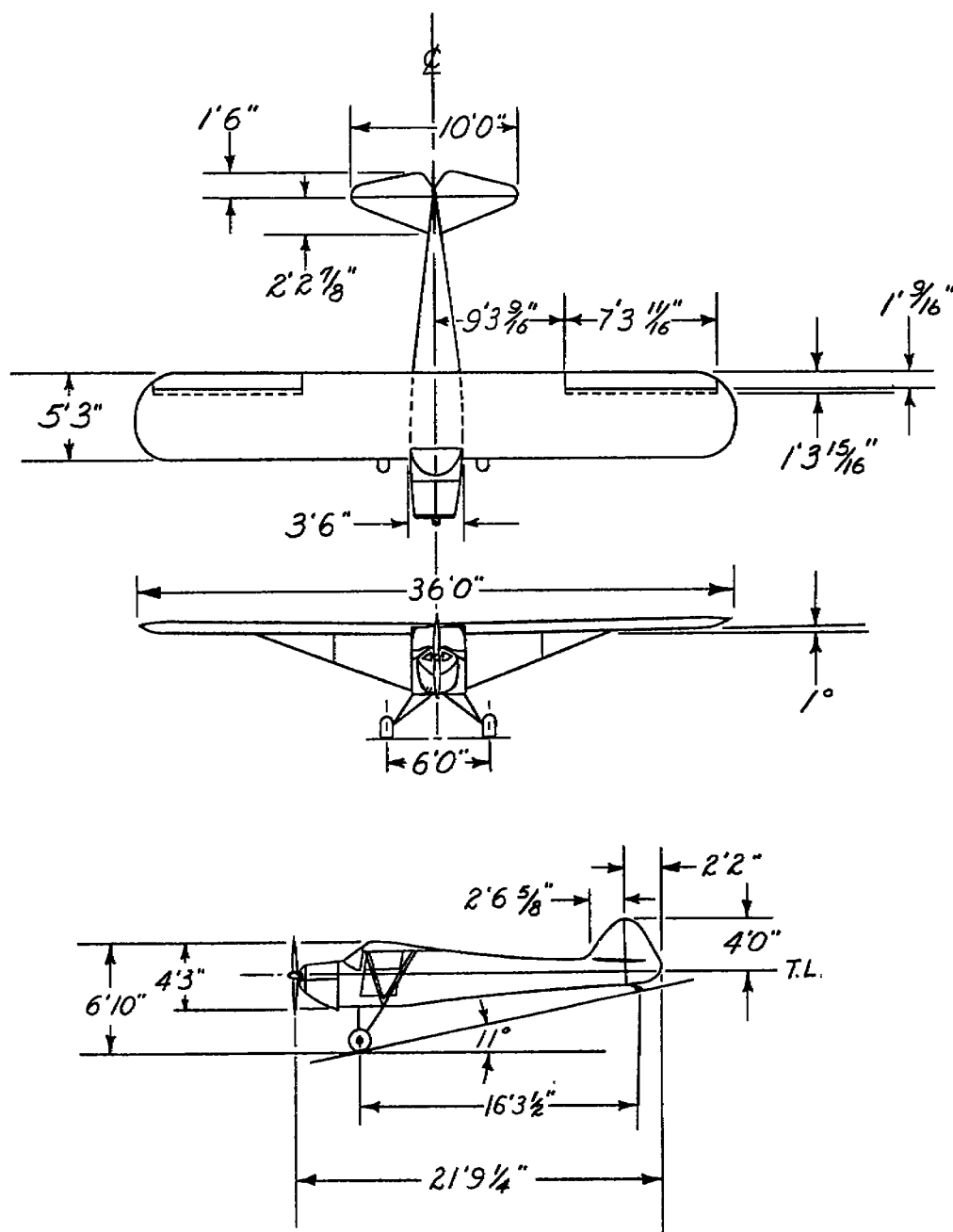
Figure 32.- Three-view drawing of Taylorcraft.
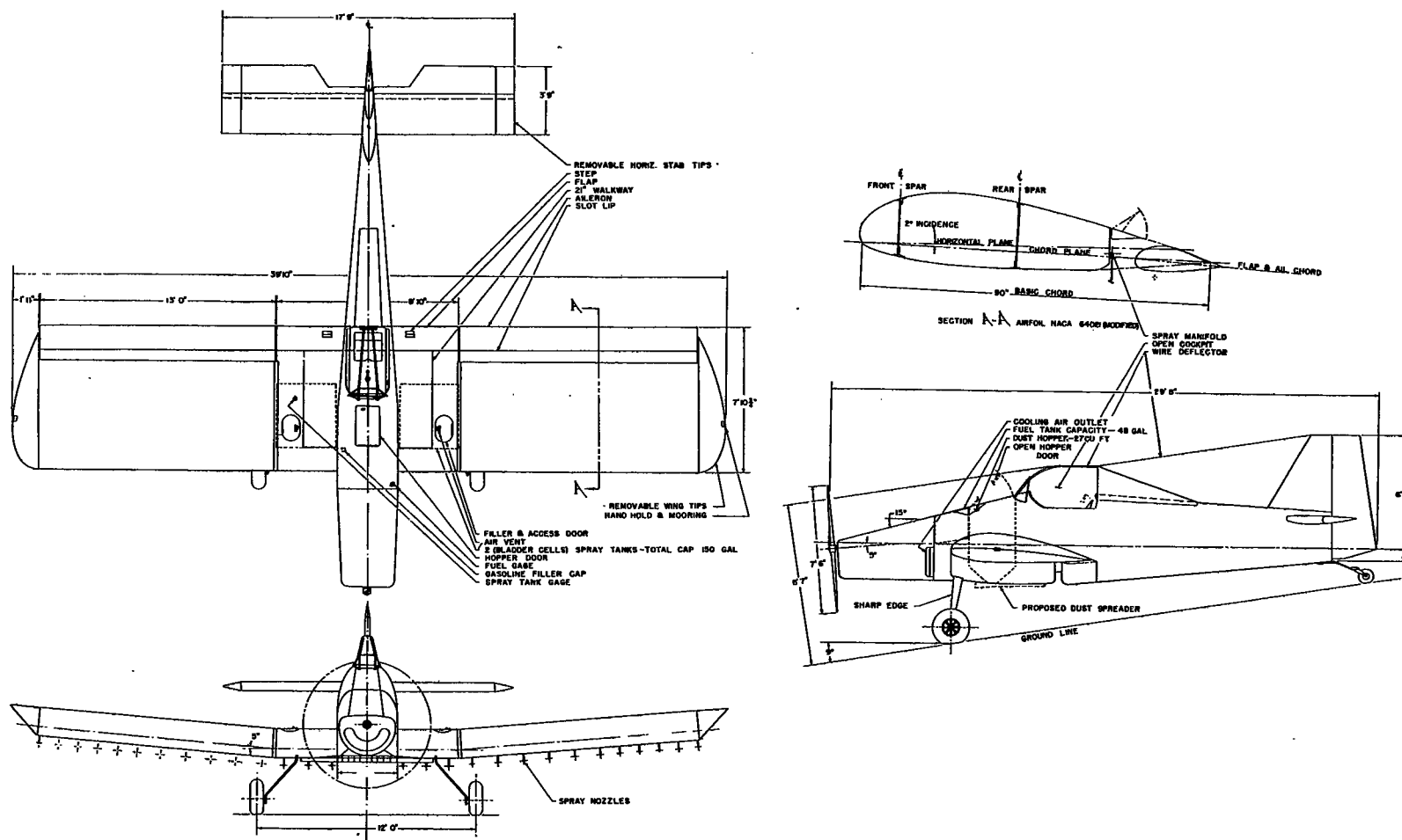
Figure 33.- Three-view drawing of AG-1 airplane.
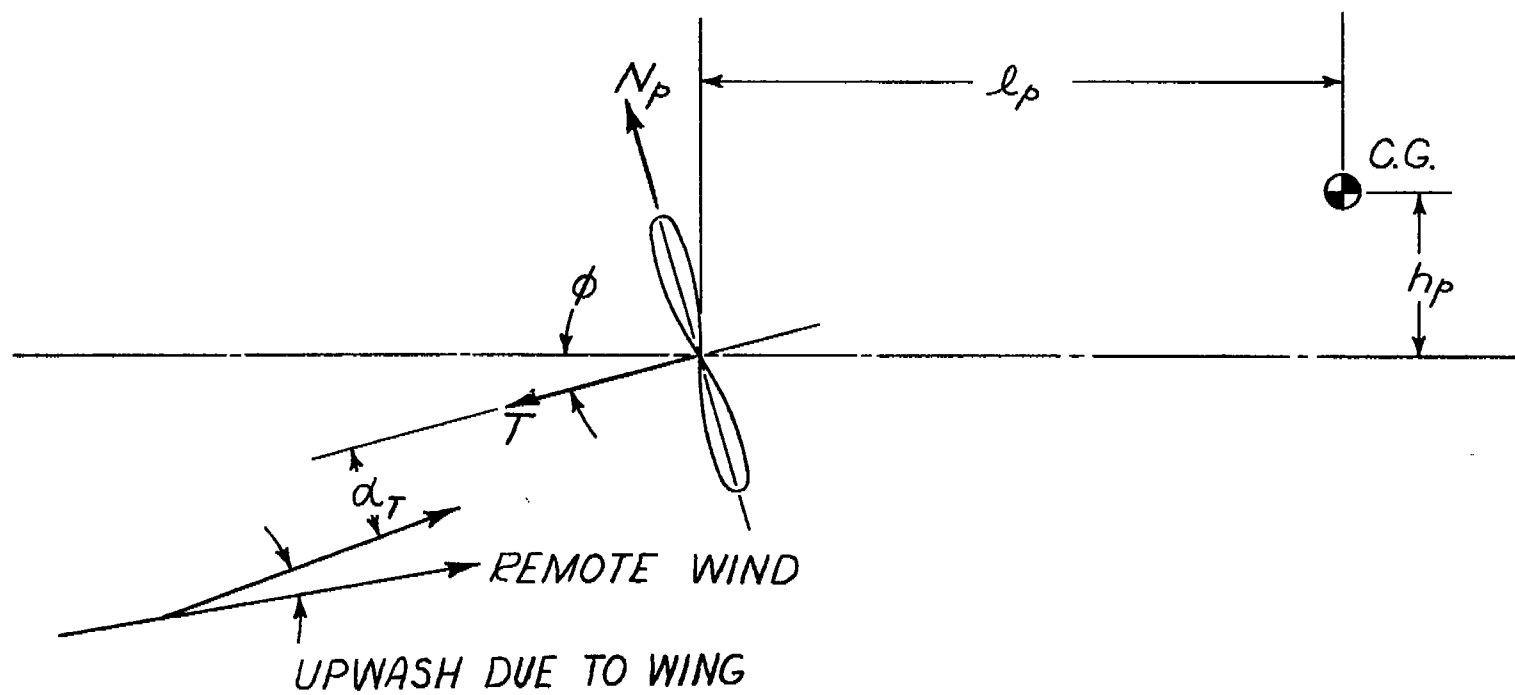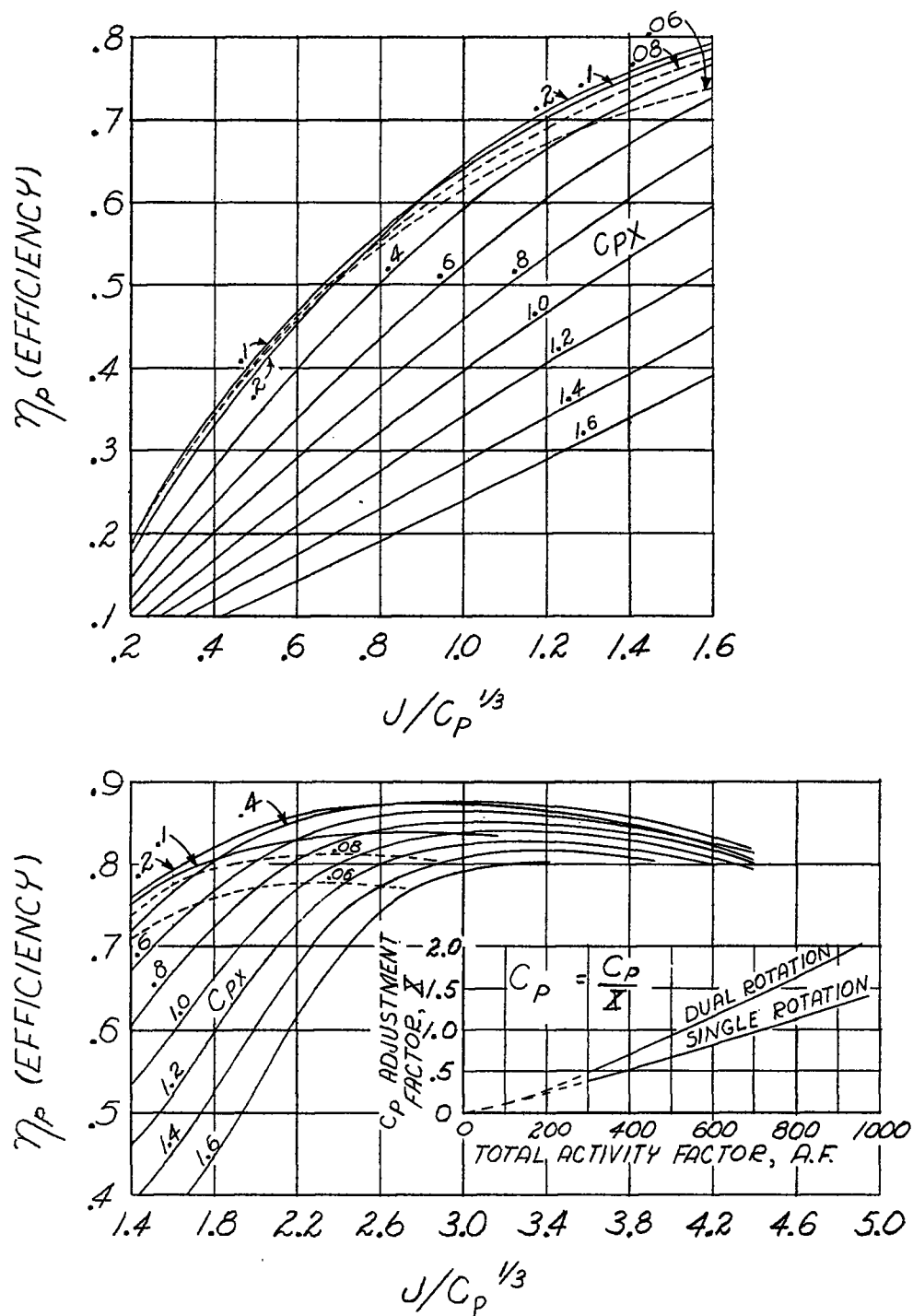
Figure 34.- Notation for direct power effects.

Figure 35.- General propeller chart. (Reprinted from ref. 6 with permission of John Wiley & Sons, Inc.)
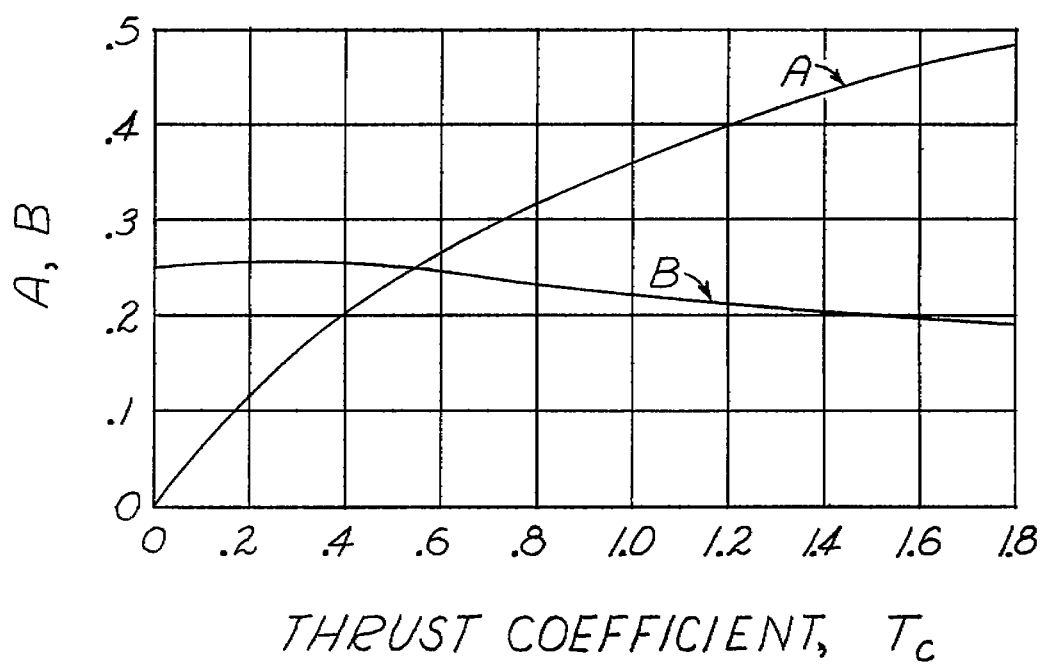
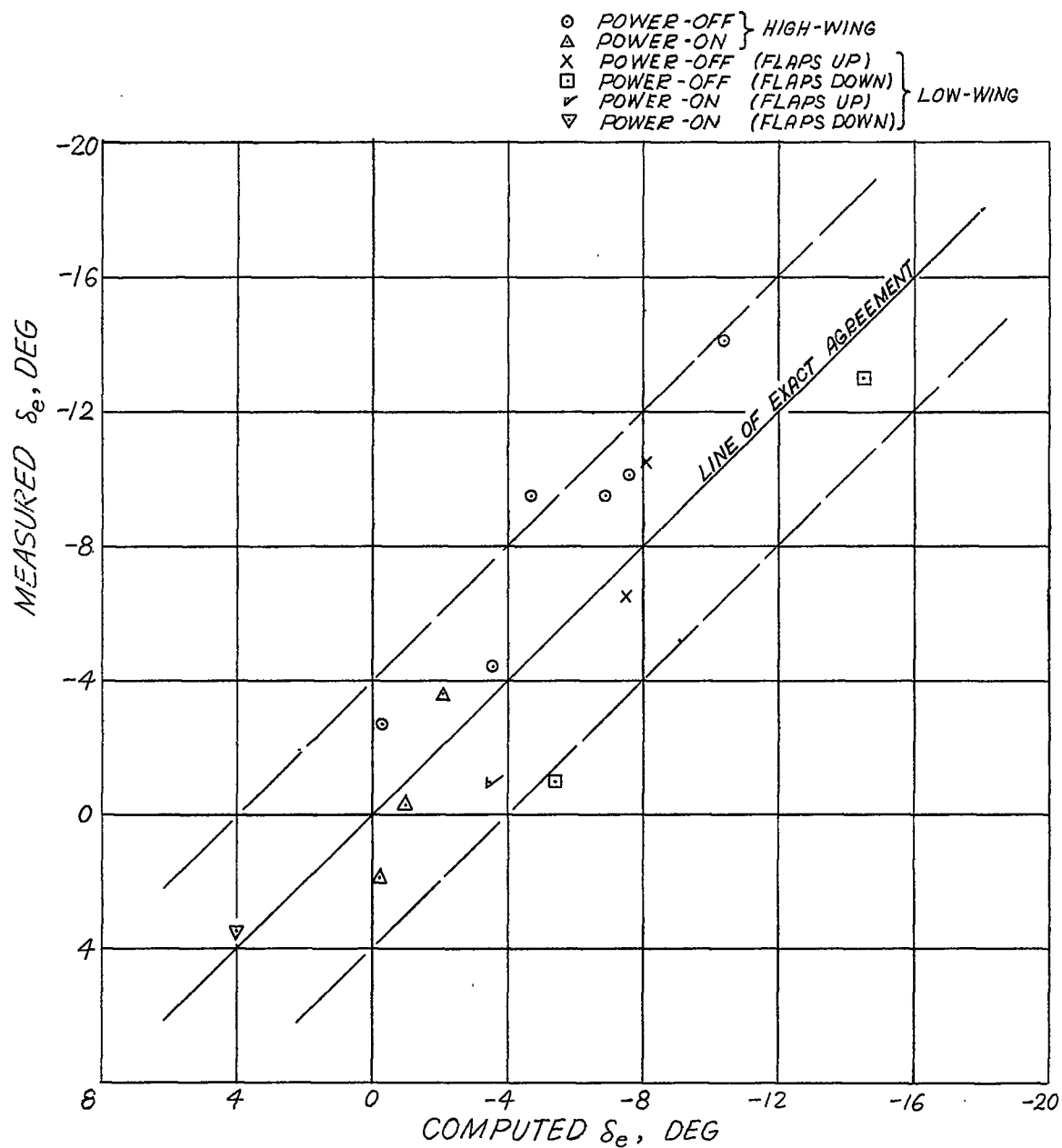Figure 36.- Propeller downwash factors (ref. 10).

Figure 37.- Comparison between computed and flight values of
elevator deflection required to trim.